Flavio Ragni

NEURAL MECHANISMS OF VISUAL MENTAL IMAGERY IN THE HEALTHY AND DAMAGED BRAIN

PhD thesis

University of Trento – Center for Mind/Brain Sciences (CIMeC)

The studies described in this thesis were carried out

at the Center for Mind/Brain Sciences of the

University of Trento, Italy.

Printed By

Proofreading
Megan Varano

University of Trento

Center for Mind/Brain Sciences (CIMeC)

Doctoral School in Cognitive and Brain Sciences

Cycle XXXI | 2015-2018

PhD Thesis

NEURAL MECHANISMS OF VISUAL MENTAL IMAGERY IN THE HEALTHY AND DAMAGED BRAIN

Doctoral Student: **Flavio Ragni**

Center for Mind/Brain Sciences, University of Trento, Italy

Advisor: **Prof. Angelika Lingnau**

Center for Mind/Brain Sciences, University of Trento, Italy

Contents

Chapter 1.

Introduction and Background

1.1 Overview

What is the color of your best friend's eyes? Will the new piece of furniture you intend to buy fit in your living room? To answer these questions, you would probably proceed by visualizing the aforementioned scenarios and exploring them with your "mind's eye." This process is commonly referred as visual mental imagery and refers to the ability to generate a vivid image of an external object in the absence of any physical stimulation. This cognitive ability, although trivial at first glance, has a profound impact on our daily life and is involved in many forms of complex reasoning and problem solving.

In this chapter, I will briefly introduce the two most relevant models of visual mental imagery (i.e. "propositional" and "depictive" theories) and discuss the claims they posit about the organization of the brain. I will then review the heterogeneous body of literature about the neural correlates of visual mental imagery with a particular focus on the debate revolving around the involvement of early visual areas. Indeed, a large number of behavioral (Shepard & Metzler, 1971; Hayes, 1973; Kosslyn, 1973) neurostimulation (Kosslyn et al., 1999; Cattaneo et al, 2009) and neuroimaging studies (Amedi et al., 2005; Klein et al., 2000; Ishai et al., 2002; Slotnick et al., 2005) highlighted that, under certain conditions, visual imagery relies on the same brain areas involved in the perception of external objects - in particular the primary visual cortex. In the third section, I will describe other brain areas involved in visual imagery, constituting the so called "visual imagery network." I will then review the more recent literature investigating the representational content of

different brain areas using multivariate pattern analysis (MVPA) during imagery tasks. In the fifth section, I will introduce hemianopia, a neuropsychological deficit characterized by the loss of vision in one hemifield due to post-chiasmatic lesions. This clinical population has been shown to retain the ability to imagine stimuli in the affected portion of the visual field (Bridge et al., 2012), despite the impossibility to process visual inputs. I will describe the phenomenology of this neuropsychological deficit and its etiology. Lastly, I will consider the possibility of using visual mental imagery as a rehabilitation tool. I will consider the techniques designed thus far to compensate for this deficit and, in the last section, I will delineate the theoretical and functional bases that would support the implementation of visual mental imagery as a tool to reinstate visual awareness in hemianopic patients.

1.2 Visual mental imagery: theories and methods

Interest in the study of visual mental imagery can be traced back to the 18th century. The first systematic dissertation on this topic comes from the Scottish philosopher David Hume, who was first in recognizing the importance of imagery processes (or ideas) for human reasoning and also highlighting their phenomenological similarity with real percepts. In particular, according to the philosopher, mental images and real percepts "differ only in degree, and not in nature" (Hume, 1739), stating that mental images are a fainted version of perceived stimuli. However, in the early years of cognitive psychology (i.e. beginning of 20th century), visual imagery was progressively neglected. In a scientific community heavily influenced by Behaviorism, a psychological approach emphasizing scientific and objective methods of investigation, an inherently private and subjective cognitive ability such as mental imagery was branded as unproductive and therefore not worthy of study.

In the 1960s, the Cognitive Revolution brought the focus of psychology back to the study of internal events (Miller, 2003). This paradigm shift allowed visual imagery to regain credit and mental representations started to be considered central and vital to psychological theorizing. The interest in this cognitive ability progressively increased - rising in the 1970s in what the scientific community defined the "imagery debate." The focus of the dispute was about understanding whether or not mental images are a qualitative

independent form of mental representations, both structurally and functionally. It is undoubtable that, when we imagine a place or a familiar face, what we experience from the phenomenological point of view is, in fact, an image; however, what exactly does this tell us about the nature, i.e. the format, of the representations used to generate them?

Two opposing classes of theories emerged. The first one, referred as "propositional theory," states that mental imagery, such as all other cognitive processes, relies on "propositional representations" (Pylyshyn, 1973, 2002, 2003; Anderson and Bower, 1973). These representations are very similar to the ones used in language and specify the semantic relations between concepts. For example, we can create a mental representation of our cat as a network of interconnected concepts related to it (e.g. "fluffy," "ginger," "affectionate," etc.). According to Pylyshyn, the use of the term "mental image" is misleading as it implies having a pictorial copy of the external world. This would be highly inefficient in terms of storage capacity needed to retain all the information transmitted by the retina. Most importantly, it would postulate the existence of a second processing system (i.e. homunculus) needed to interpret the information projected on the "mind's eye." Thus, hypothesizing the existence of two different formats of representation (i.e. pictorial and propositional) would unnecessarily increase the complexity of the mental organization.

Kosslyn (1980; 1994) proposed a different view, namely the "depictive theory" of mental imagery. Propositional representations are indeed fundamental, as proved by the fact that we use these form of mental constructs in everyday life. However, the author proposed the existence of at least one other type of format which uses a spatial medium to represent information. According to this theory, mental images are depictive representations of external objects. This, in turn, implies the existence of a homeomorphic relation between mental images and percepts, where the spatial relations between the parts composing the mental image have a one-to-one correspondence to the spatial relations among the parts of the external stimulus themselves.

This model was then formalized by Farah (1984) and described as a functional system made by several "information-bearing structures" and "information-manipulating processes." There are essentially two structures composing this model: a long-term visual memory component and the visual buffer. The former stores information about object's appearance that are not conscious, and can be accessed and manipulated

by one of the processes specified by the theory. The second, and probably most important, is the medium where mental images are depicted and gain their similarity with real percepts. The information-manipulation processes allow the individual to perform operations on the contents of the visual buffer. The “generation process” allows the top-down generation of mental images in the visual buffer from long-term memory representations. The “inspection process” allows the individual to scan such representations. Finally, the “manipulation process” operates the representations by rotation or translation.

The first attempts to study visual mental imagery came from behavioral paradigms, which at first explicitly focused on its relations and degree of similarity with perception. The first example is the so-called “Perky effect” (Perky, 1910). In this experiment, the author asked the participant to imagine a colored object while fixating on what seemed a blank screen. In reality, faint images were being projected on it during visual imagery just above the normal threshold of visibility. All the subjects participating in the experiment reported to have produced vivid mental images but none of them noticed the actual presence of a visual stimulus on the screen. This was taken as a first proof of the phenomenological similarity between imagery and perception, and of the mutual influence these two modalities could have on each other. In another classic experiment, Shepard and Metzler (1971) asked participants to judge if a test figure was the same or a mirror-reversed version of a probe image. Before the presentation, the test figure was rotated to one of several possible orientations. What the authors found is that the time required for the participant to make this identity judgment increased proportionally with the amount of rotation. This result is consistent with the idea that subjects rotated the test image to the standard orientation before deciding, showing that imagined entities obey the same physical rules as real world objects. Similar parallelisms between imagery and perception have been obtained for effects of image size. If asked to retain a stimulus (lowercase letter) and decide if a test stimulus was the same or different, decision times increased if the test letter was smaller than the original (Hayes, 1973). Moreover, if asked to visualize a previously memorized image and “focus” on a part of it to find if a property was present, decision times increased as a function of the scanning distance (Kosslyn, 1973).

Taken together, results from these pioneering behavioral studies indicated that perception of external stimuli and top-down generation of mental images share common properties, and potentially common neural

substrates as well. In the following paragraph, I am going to describe the neural correlates of visual mental imagery, considering evidence from lesions and neurophysiological studies.

1.3 Neural correlates of visual mental imagery

The model proposed by Farah does not simply posit a series of processes and structures necessary for the experience of visual mental imagery, but also makes an explicit prediction about the cortical regions involved. In particular, the strongest claim is that to give to visual mental images their quasi-pictorial format, the visual buffer must be implemented in retinotopically organized early visual areas, in particular V1 (Kosslyn, 1994). If this was the case, and so if there was a structural overlap between areas supporting perception and visual imagery, there should be cases where a specific impairment in the visual domain is also paralleled in the imagery domain. Indeed, in her review, Farah (1988) reported a number of examples of associations between perceptual and imagination deficits in the neuropsychological literature, as measured by performances in different tests commonly requiring visual imagery to be performed correctly. Patients with acquired color blindness, for example, showed an inability to report the color of common objects from memory (Riddoch and Humphreys, 1987). Analogous associations were found with respect to object recognition, with patients affected from visual agnosia showing difficulties in describing the appearance of familiar objects from memory and object localization (Levine, Warach, and Farah, 1985). Neglect patients represent another source of evidence. After right parietal lobe damage, the misrepresentation of the left half of space was also present for imagined objects or scenes (Bisiach and Luzzatti, 1978). However, clinical studies showing a double dissociation between imagery and perception deficits questioned the anatomo-functional equivalence between the two cognitive domains.

One of the first accounts of visual imagery deficit in the absence of perceptual impairments comes from Riddoch (1990), who described the case of a patient impaired in both generating mental images and performing transformations on them. A computed tomography (CT) scan highlighted a left-parietal lesion in absence of any apparent occipital damage. More recently, Moro et al. (2008) made analogous observations in two case studies. Both patients did not show any signs of agnosia, memory or language selective deficits,

but presented a severely impaired ability in using visual imagery, as assessed by a wide range of tests including imagery of objects, shapes and colors, as well as drawing from memory. Also in this case, early visual cortex (V1) was intact in both patients. The opposite pattern of deficit was also described by Behrman et al. (1994). They reported the case of patient CK, who presented preserved visual mental imagery in spite of a severe visual object recognition deficit. Similarly, Bridge et al. (2012) described the rare case of patient SBR, who in spite of a bilateral lesion restricted to the gray matter of the calcarine sulcus, was able to perform visual mental imagery of different stimuli, showing a pattern of cortical activation very similar to individual sighted subjects. However, standard campimetry on this patient revealed a possibly incomplete visual field defect with areas of preserved vision, which could have contributed to the observed results. De Gelder et al. (2014) described the case study of patient TN with completely afunctional V1, as confirmed by extensive visual perimetry testing. When asked to imagine different stimuli, both with an emotional (e.g. angry person) and neutral valence, the patient showed a bilateral fronto-parietal activation comparable with healthy participants. This common pattern of activation between normal sighted participants and patient TN suggests that V1 might not be necessary to perform visual imagery.

Together, the results from neuropsychological studies suggest that perception and visual mental imagery share overlapping but not necessarily identical neural systems. In particular, they challenge one of Kosslyn's main assumptions, which is the use of a single visual buffer common to both cognitive processes. Damage to the occipital lobe, in fact, can lead to perceptual deficits but it seems neither necessary nor sufficient to produce deficits in the ability to perform visual mental imagery.

However, results from transcranial brain stimulation studies implied a closer connection between areas suggested to be involved in the processing of perceptual information and visual mental imagery. Delivery of repetitive transcranial magnetic stimulation (rTMS) over early visual cortex impaired the subject's performance when they were asked to judge properties of imagined stimuli (Kosslyn et al., 1999). In another study, Cattaneo (Cattaneo et al., 2009) showed that single-pulse TMS stimulation on early visual cortex (V1) could improve performance in a visual imagery task. Analogous results were found by Sparing et al. (2002), who showed that performing a visual imagery task increased visual cortex excitability, as indexed by a decrease of minimum TMS intensity necessary to induce phosphenes (commonly referred as phosphene

threshold, PT). All in all, behavioral, neuropsychological, and neurophysiological studies do not provide a homogeneous account of the neural mechanisms subtending visual mental imagery. Overall, the role of early visual areas in mental imagery is still debated. The studies described in the following section aimed to address this issue using neuroimaging techniques.

1.4 Neuroimaging studies

To rule out the possibility that early visual cortex involvement in imagery is epiphenomenal, researchers adopted different techniques which allowed them to explore brain activation during visual mental imagery. In particular, positron emission tomography (PET) first and functional magnetic resonance (fMRI) after, were used to investigate the involvement of early visual cortex in visual mental imagery.

One of the first PET studies showing activation in retinotopically organized visual areas, was performed by Kosslyn et al. (1993), who showed activation of area BA17 during visual mental imagery in three different experiments. In the first experiment, they presented participants with a grid and asked them either to observe a letter or to imagine its presence (*Figure 1.1*). The task consisted in judging if an X mark displayed within one of the squares composing the grid fell on the imagined or perceived stimulus, or outside of it. Results showed that visual imagery of letters elicited an increase of regional blood flow in area BA17 and that this activation was higher than in the perception condition. These results were replicated manipulating the size of the imagined stimuli. Not only was early visual cortex activated during the imagery task but the activation also reflected spatial properties of imagined stimuli. Letters imagined at smaller visual angle activated more posterior parts of area BA 17, whereas bigger letters in more anterior parts, followed a retinotopical organization. Analogous findings were reported by another PET study (Kosslyn et al., 1995) in which participants were required to imagine objects of different sizes and subsequently make a spatial comparison judgment. Here as well, early visual cortex (BA 17) showed a regional blood flow increase during visual imagery, and the topography of this activation was coherent with the size of the imagined stimuli. Crucially, this occipital locus of activation was present for both visual imagery of high and low-resolution

gratings (Thompson et al., 2001), indicating a recruitment of early visual cortex independent from the amount of details present in the mental representation.

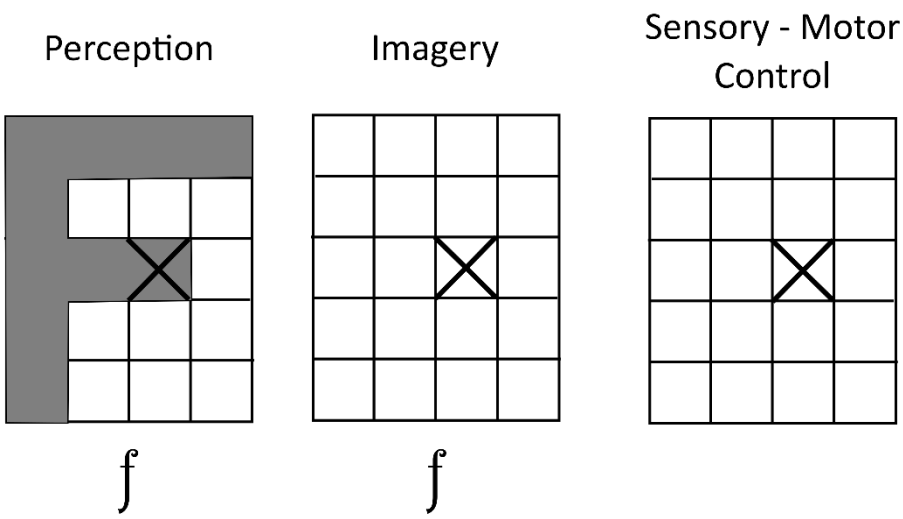

Figure 1.1. Task overview of Experiment 1 (Kosslyn et al., 1993). Participants had to either imagine or observe a letter (e.g. letter "f") on an empty grid and judge whether a cross fell on or off the letter. Adapted from Kosslyn et al. (1993).

The advent of fMRI and the benefits of its higher spatial resolution compared with PET allowed further examination of the involvement of early visual cortex during visual mental imagery. In their event-related fMRI study, Klein et al. (2000) asked participants first to imagine an animal and then to judge either a concrete (e.g. a visible detail of the body) or an abstract characteristic (e.g. behavioral tendencies) of the generated mental image. Activation of calcarine cortex was reported and was present across both conditions, indicating that the simple act of generating a visual mental image involved the activation of early visual areas, independently of the level of detail required to perform the task. This activation seems to be independent from the type of memory that mediates the generation of mental images. In their study, Ishai et al. (2002) asked subjects to imagine faces of famous people, using as prompt either specific pictures they saw shortly before (short-term memory condition) or relying on their own pictorial representation of the celebrity (long-term memory condition). Both short and long-term memory conditions induced an activation of early visual cortex, with a stronger recruitment in the first condition compared to the second.

However, similarly to the behavioral, neurophysiological and neuropsychological studies described above, neuroimaging studies revealed contradictory results. A consistent number of fMRI and PET studies failed to report early visual cortex activation during visual mental imagery, questioning its functional role. For example, in their PET study Mellet et al. (1996) asked participants to construct visual mental images of three-dimensional objects - assembling cubes together following auditory instructions. They found activity in superior occipital, parietal, and frontal regions, but no activation in primary visual areas nor in nearby cortices. Similar results were also found using spatial navigation tasks (Mellet, Bricogne, et al., 2000).

In an fMRI study, Ishai et al. (2000) compared activations evoked by perception and imagery of different stimulus categories (i.e. houses, faces, and chairs). Visual imagery of different stimulus categories led to activation in subsets of the same inferotemporal category-selective regions recruited during perception, accompanied by an increase of the blood oxygenation level dependent (BOLD) signal in parietal and prefrontal areas. No signs of recruitment in the calcarine cortex were reported. In another study, Formisano et al. (2002) adopted the "mental clock task." They presented subjects with pairs of auditory cues consisting of different hours of the day (e.g. "nine thirty," "eight o'clock"), and asked to visualize them on an analogic clock. The task was to judge on which of the clock faces the hands formed a greater angle (e.g. "eight o'clock"). By means of a time-resolved univariate analysis, the authors investigated brain areas involved in mental imagery and the dynamics of their sequential activation during the task. The results indicated an early activation in auditory cortices after the presentation of the auditory cue, followed by the recruitment of fronto-parietal areas involved in mental image generation. No activation of early visual areas was reported.

How can one account for the huge variability reported in the literature relative to the involvement of early visual areas? In their meta-analysis including 42 studies using PET, fMRI or single-photon emission computed tomography (SPECT), Kosslyn and Thompson (2003) identified three criteria that could predict visual cortex activation in visual imagery studies. The first one is represented by the requirement of inspect "high-resolution" details of a mental representation (e.g. indicate which of two imagined faces has the biggest nose). This operation would require participants to actually "place the detail" in the depictive representation and this in turn would lead to activation in retinotopically organized visual areas. Secondly, early visual cortex seems to be activated for tasks that require shape-based processing (e.g. mentally rotating an object), as

opposed to spatial processing (e.g. visualizing the usual routes from home to work). Spatial representations, such as the ones used during mental navigation, are stored in retinotopically organized visual areas of posterior parietal cortex (Sereno et al, 2001; Sack et al., 2012) and thus would not require to be reconstructed in early visual areas. Finally, the likelihood to find activation in V1 increases when techniques that are more sensitive are employed. In particular, not only fMRI studies can guarantee a higher spatial resolution with respect to PET studies, but also they allow researchers to perform single-subject analyses, considering potential individual differences in early visual cortex recruitment between participants. Whereas the involvement of V1 is still a matter of debate that has not been solved with neuroimaging studies, several studies highlighted the recruitment of a broader network of areas outside the occipital cortex during imagery tasks. These areas have been traditionally considered to be involved in perceptual, memory, and executive functions, and might be involved in visual mental imagery as well. In the following paragraph, I am going to describe these regions constituting the imagery network.

1.5 Beyond visual cortex: the visual imagery network

Visual mental imagery recruits a huge network of brain areas that are involved in different aspects of the generation and maintenance of mental images. In particular, several studies highlighted a recruitment of inferotemporal regions (i.e. FFA, PPA, LOC) during imagery tasks that traditionally have been considered to process different stimulus categories during perception. The fusiform face area (FFA; Kanwisher et al., 1997) exhibits a stronger response when subjects are presented with picture of faces compared to other classes of stimuli, such as familiar objects or places (Haxby et al., 1991, 1999). Conversely, the parahippocampal place area (PPA; Epstein & Kanwisher, 1998), conversely, shows a preferential activation for visual stimuli depicting indoor or outdoor scenes. Finally, the lateral occipital complex (LOC; Grill-Spector et al., 2001) is involved in recognition of both familiar and unfamiliar objects. Interestingly, these brain regions are recruited when imagining the same stimulus categories. O'Craven and Kanwisher (2000) asked participants to generate vivid mental images of famous faces and places while they measured brain activity with fMRI. Results showed that

brain regions activated during visual imagery of the two stimulus categories were strikingly similar to those recruited during perception. In particular, visual imagery of faces and places activated portions of FFA and PPA respectively, though with a lower magnitude of the BOLD signal with respect to perception of the same stimulus categories (*Figure 1.2*). Ishai et al. (2000) reported similar results showing that visual imagery of faces, places, and chair was able to induce content-related activation in a subset of inferotemporal regions showing the same category-selective response during perception. These results indicate that inferotemporal cortices store a sensory representation of external entities, and that these representations are reactivated during visual mental imagery.

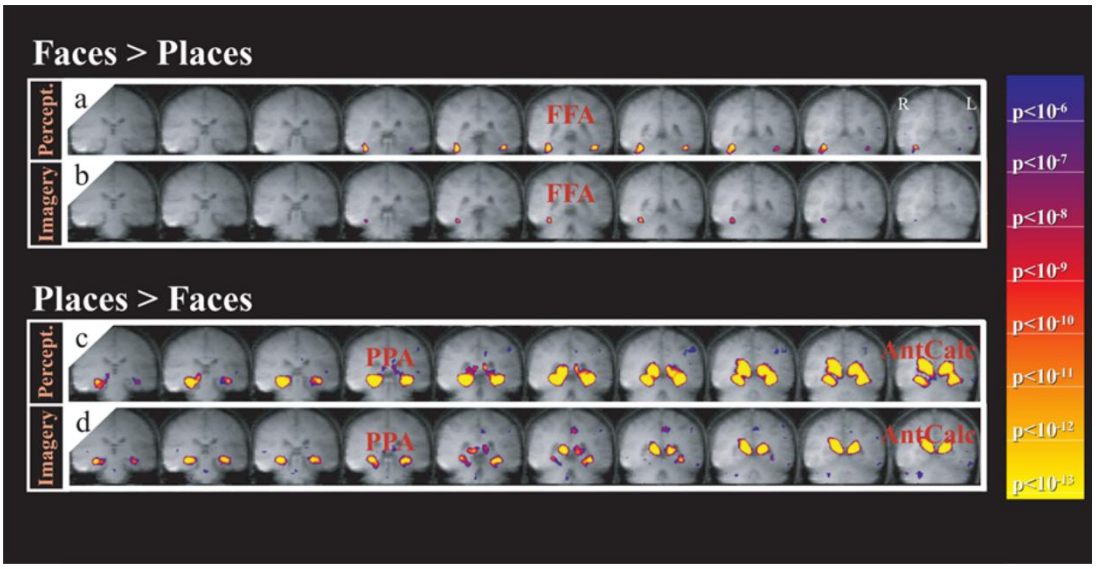

Figure 1.2. Results from O'Craven and Kanwisher (2000). Imagery of faces and places activated portions of FFA and PPA, respectively. Adapted from O'Craven and Kanwisher (2000).

Within the parietal lobe, the areas that are involved in visual imagery are the superior parietal lobe (SPL) and the intraparietal sulcus (IPS). These brain regions have been traditionally considered to be involved in attentional processes and working memory (Wojciulik & Kanwisher, 1999; Kastner & Ungerleider, 2000). Several fMRI studies reported activation of parietal areas during visual mental imagery (Knauff et al., 2000; Formisano et al., 2002; Mechelli et al., 2004), indicating their functional role in providing attentional resources necessary to generate and maintain mental images active for a delayed period of time. These findings were later confirmed by Slotnick et al. (2005). In their study, they compared brain activation while subjects performed a standard double-wedged retinotopic mapping and an analogous “imagery” version,

where only the outer arcs of the stimulus were visible and participants had to mentally reproduce it. Results showed, in addition to topographically organized activity in striate and extrastriate cortices, a sustained activation of the superior parietal lobe throughout the imagery delay, highlighting the involvement of SPL in providing attentional resources during the entire imagery task.

Moreover, recent studies from Sack et al. (2002; 2008; 2012) revealed that parietal regions are also recruited when participants are required to judge the spatial relations between different parts of a mental image (e.g. mentally constructing an abstract geometric figure following auditory instructions, and then comparing it to a target stimulus). According to the authors, in analogy with perception, this type of "spatial" mental imagery would be processed in a dorsal route including parietal and premotor cortices, as opposed to a ventral route involving category selective regions in inferotemporal cortex, responsible for representing the *content* of visual imagery (*Figure 1.3*). In this model, information coming from these two complementary pathways would be integrated in a coherent representation by the third and last portion of the visual imagery network, i.e. prefrontal regions.

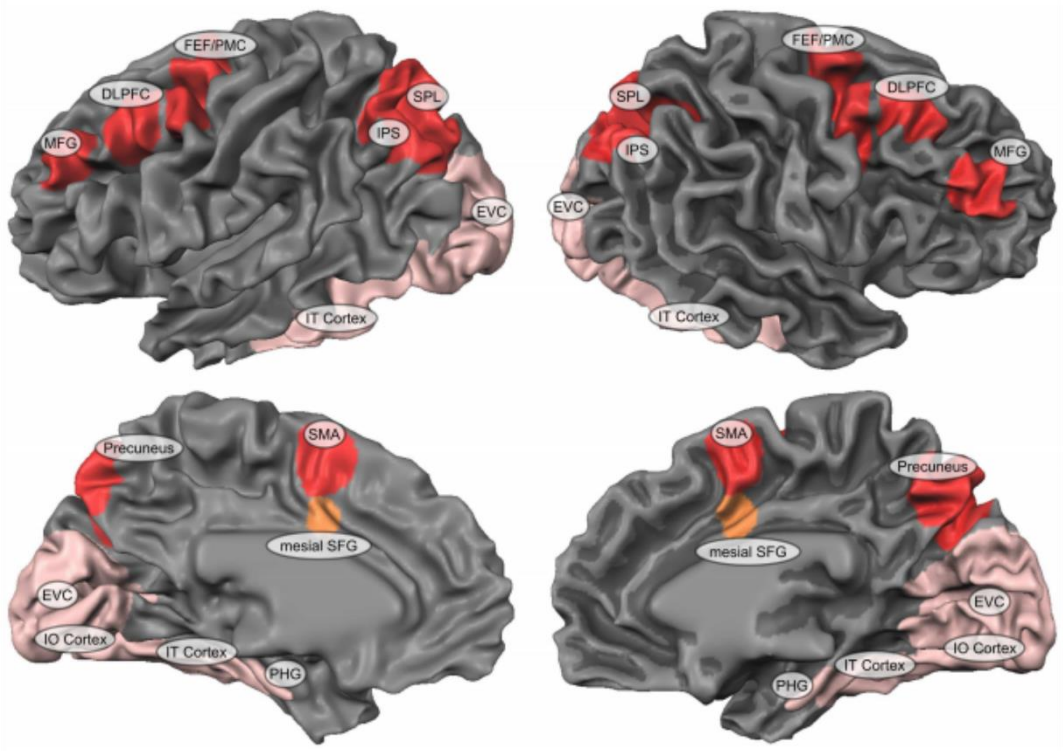

Figure 1.3. The visual imagery network as proposed by Sack et al (2012). Medial and lateral view of brain regions composing the dynamic visual imagery network model. The "dorsal" fronto-parietal pathway (red) is responsible for spatial aspects of visual mental imagery, whereas the "ventral" occipito-temporal pathway (pink) represents the content of mental images. Adapted from Sack et al. (2012).

In a study combining fMRI and electroencephalography (EEG), de Borst et al. (2012) asked participants to learn complex visual scenes (e.g. pictures depicting the interior of different rooms). An auditory cue instructed participants on which scene they had to imagine. The task was to judge, after a delay ranging from 5 to 7 seconds, whether a fragment of a scene presented visually was a mirror reversed version of the previously learned scene. They found early activation of prefrontal regions (i.e. mesial superior frontal gyrus, right middle frontal gyrus and prefrontal cortex) during visual imagery, followed by recruitment of temporal and parietal nodes of the visual imagery network. In particular, the activity in mesial SFG seemed crucial to the retrieval and integration of visuo-spatial information, and was correlated with behavioral performance in the task. Taken together, these results indicated a crucial role of frontal regions in integrating information coming from occipito-temporal (i.e. detailed representations of mental images) and parietal regions (i.e. spatial configuration of mental images) in one coherent mental representation.

To understand how the regions involved in the visual imagery network orchestrate the processes necessary to perform visual mental imagery, several studies focused on investigating the patterns of functional connectivity occurring between parietal, prefrontal and inferotemporal areas. Mechelli et al. (2004) investigated effective connectivity between different brain areas while subjects performed visual perception or mental imagery. In a block design, participants were asked either to passively look at black and white images of houses, faces and chairs, or to generate vivid mental images from long-term memory of the same categories. Dynamic causal modeling (DCM) analysis was performed to assess content related activation in both conditions. Results indicated that during perception, as expected, activation in category-selective regions was bottom-up modulated by an increase of selective connectivity from early visual cortex. In contrast, when subjects were asked to generate mental representations of the same stimuli in absence of an external retinal input, activation in the same areas was mediated by top-down mechanisms, originating in parietal and prefrontal cortices and running through inferotemporal cortex (*Figure 1.4*). In particular, the authors suggested that superior parietal cortex could host a general attention mechanism, providing the attentional resources necessary to keep the mental representation active and to perform operations on it, independently of its content. Prefrontal cortex, on the other hand, would be involved in the retrieval of sensory representations, stored in ventral occipito-temporal cortex, providing information about the content of visual mental imagery.

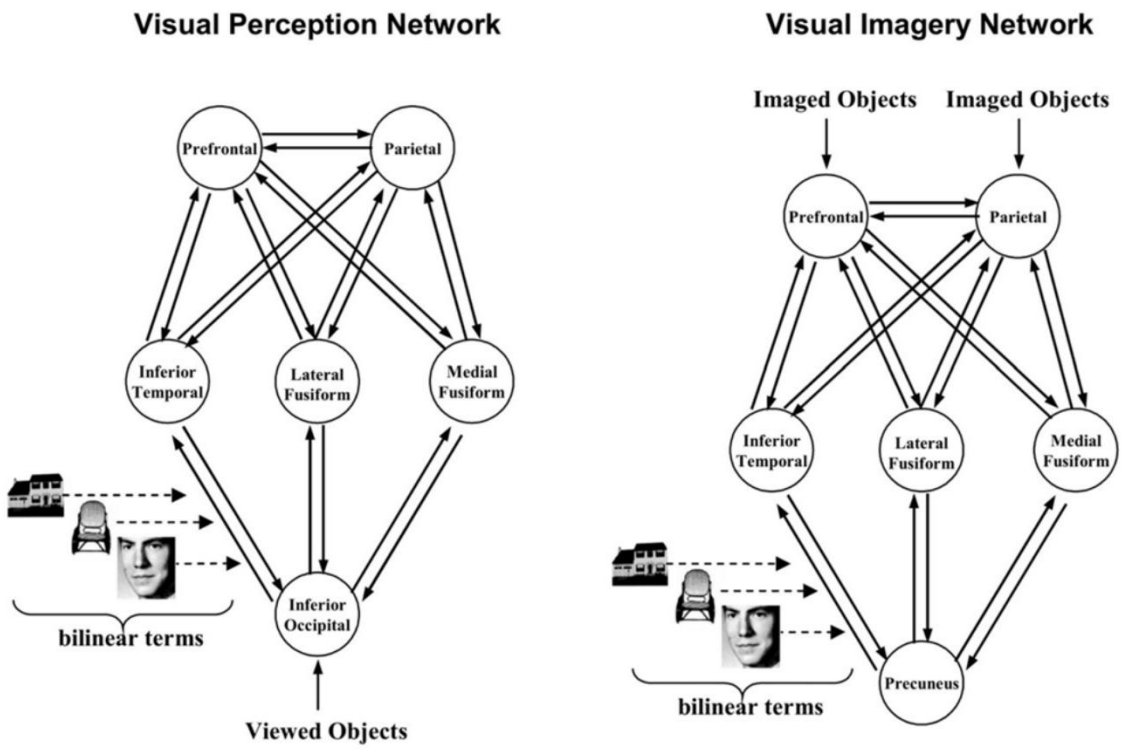

Figure 1.4. Visual perception (left) and visual imagery (right) network proposed by Mechelli et al. (2004) for the DCM analysis. During visual perception, a bottom-up flow of information from low-level visual areas in inferior occipital cortex, to category-selective areas in inferior temporal cortex and parietal and prefrontal region is assumed. During visual mental imagery, conversely, an opposite flow of information is assumed. Modulation from prefrontal areas reaches category-selective temporal regions, responsible for retrieving sensory representations of imagined stimuli. The same top-down modulation exerts an influence also over parietal cortices, responsible for providing the attentional mechanisms needed to keep the mental image active for a delayed period of time. Adapted from Mechelli et al. (2004).

Similar findings were obtained by Dijkstra et al. (2017), who directly compared the directionality of neural signal flow during visual perception and imagery using DCM. Results showed that during perception, the increase in bottom-up connectivity (from visual to higher-level brain areas) due to the sensory input was accompanied by an increase of top-down coupling from the inferior frontal gyrus (IFG) to occipital cortex. Conversely during imagery, in the absence of bottom-up stimulation, the same top-down modulation was detected, with a much stronger increase with respect to perception. The authors hypothesized that this coupling between prefrontal and occipital regions reflects a top-down attentional mechanism common to both visual perception and mental imagery, responsible for enhancing visual representations in early visual areas. Dentico et al. (2014) directly compared the directionality of neural signal flow during a visual

perception and imagery tasks. Exploiting the high temporal resolution of high-density electroencephalography (hd-EEG), the author identified a reverse of neural signal flow between parietal and occipital cortices during visual imagery as compared to perception. Interestingly, no statistically significant differences in frontal connectivity with parietal or occipital regions were detected.

Overall, neuroimaging studies agreed in describing a top-down modulation during visual mental imagery that involves prefrontal, parietal, and visual areas. This reverse flow of information highlights that imagery is a high-level process relying on similar neural substrates as those involved during perception. However, this description is based on results coming from univariate analyses of fMRI data, which proceed by assessing differences in activation at the single voxel level or averaging across entire brain regions. By measuring differences in the BOLD response between different conditions or stimuli, univariate analyses allow researchers to understand which regions are recruited during the execution of tasks involving different cognitive functions. Despite providing precious information, this functional mapping approach has one important weakness. By averaging the activation across multiple voxels in the brain, it does not consider relevant information that might be contained in the relationship between multiple voxels within a brain region (i.e. also referred as spatial pattern of information). To this aim, in recent years Multivariate Pattern Analysis (MVPA) of fMRI data was developed. By training and testing a machine learning classifier on distributed patterns of activation across multiple voxels, MVPA allows the researcher to understand which brain regions encode (i.e. contain a neural representation of) different conditions, providing a new way to look at brain imaging data. This entails at least two elements of novelty compared to traditional mass-univariate approaches. First, examining the information encoded across multiple voxels allows researchers to infer the representational content of different brain areas while subjects perform different tasks. Second, by considering pattern of voxels exhibiting weak but consistent differences between conditions, MVPA can provide higher sensitivity in discriminating between different conditions of interest with respect to traditional univariate analyses (Oosterhof et al., 2016). This new approach to fMRI data allowed researchers to investigate neural representations underlying imagined stimuli, and exploring their similarities to those

elicited by perception of real stimuli, providing new evidence about the organization of imagery within the brain.

1.6 Neural representations during visual mental imagery

During the last two decades, MVPA techniques gained increased popularity in the neuroscientific field. This groundbreaking new approach allowed researches to overcome several limitations of univariate analyses and to explore subtle differences in patterns of activation elicited by different conditions. Despite its increasing popularity, the MVPA literature on visual mental imagery is still scarce.

The first MVPA study exploring the representational content of early visual areas was performed by Stokes et al. (2009). In a block design, participants were asked to imagine or observe two different simple letters (i.e. the letter "X" and the letter "O"). A linear classifier was trained to discriminate between patterns of neural activity associated with imagining or viewing the two stimulus exemplars. Results revealed that the identity of the imagined stimuli can be decoded in high-level visual areas (i.e. LOC). Moreover, the cross-condition decoding (i.e. classifier trained on imagery trials, tested on perception trials and vice versa) revealed shared representations between imagery and perception in LOC. Similar results were later found using more complex stimulus categories. For example, Lee et al. (2012) asked participants to imagine or observe pictures of 10 different real-world objects, differing widely in their orientation, shape, and color. The authors found that areas throughout the ventral visual stream (i.e. V2, V3, V4, LO and pFs) encoded the identity of both perceived and imagined complex stimulus categories. Following studies used MVPA to investigate imagery representations in other category selective regions of inferotemporal cortex (i.e. FFA and PPA), finding significant encoding for imagined faces and places, respectively (Reddy et al., 2010; Cichy et al., 2011). Taken together, MVPA results confirmed that visual mental imagery not only recruits the same brain areas involved in perception, as already stated by previous investigations adopting different methodologies (i.e. univariate, behavioral, neurophysiological), but that they also share common neural patterns of activation.

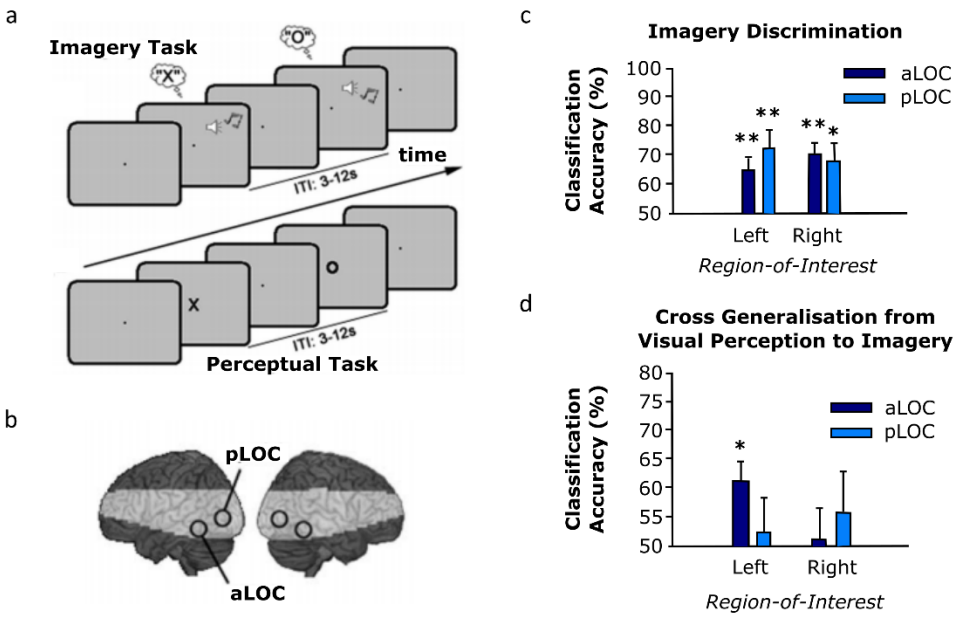

Figure 1.5. Results from Stokes et al. (2009). a) Experimental design. During the imagery condition (upper panel), participants either had to imagine a letter "X" or a letter "O" in the center of the screen, following instructions delivered via auditory cues. In the perception condition (lower panel), participants were instructed to observe the same two letters ("X" or "O"). b) MVP analysis was performed in two regions of interest (aLOC ad pLOC) in both hemispheres. c) Results from the decoding analysis during the imagery condition. In both hemispheres, the identity of the imagined stimulus could be decoded from patterns of activation in both aLOC and pLOC. d) Results from the cross-generalization decoding. A classifier was trained on patterns of activation from the perception condition and tested on the imagery condition. Results indicate shared representations between imagined and perceived stimuli in the left aLOC. Adapted from Stokes et al. (2009).

Compared to univariate studies, the MVPA literature focused mainly on high-level extrastriate visual areas, neglecting to investigate the representational content of early visual cortex. The only study specifically considering V1 was conducted by Albers et al. (2013). In a delayed match-to-sample task, participants were asked to imagine (visual imagery) or to keep in memory (visual working memory) the identity of gabor patches with different orientations. Results indicated that the orientation of the imagined stimuli was encoded in early visual areas, comprising regions from V1 to V3. As previously shown in high-level visual areas, cross-condition classification with visual perception was possible, indicating that similar neural codes are used by both bottom-up stimulation (i.e. perception) and top-down internal generation (i.e. imagery) of the same stimuli.

Overall, MVPA studies showed that visual mental images are represented in both high (i.e. LOC, FFA, PPA) and low level (i.e. V1, V2, V3) visual areas, which has been traditionally considered to process external stimuli during real perception. Moreover, in category selective inferotemporal cortices (i.e. LOC, FFA, PPA) representations of imagined stimuli are shared with those elicited by bottom-up visual stimulation, indicating common patterns of neural activity for both processes. On the other hand, the degree of complexity of the stimuli represented in primary visual cortex is less clear. The only study targeting specifically V1 (Albers et al., 2013), in fact, found significant decoding employing relatively simple stimuli (i.e. gabor patches with different orientations). This result is in line with the traditional functional specialization attributed to early visual cortex, which contains neurons selectively tuned to respond to low-level features of perceived stimuli (Hubel, 1995; Ward, 2010). However, recent studies highlighted the importance of top-down influences from higher-level visual areas on early visual cortex (Muckli & Petro, 2013). Vetter et al. (2014), for example, were able to decode the identity of real and imagined sounds from patterns of activity in V1. The authors hypothesized this encoding of category-specific information in early visual cortex might be mediated by top-down feedback from multisensory brain areas such as pSTS and the precuneus. To date, it is yet not clear what the exact role is of non-retinal influences on early visual areas, and more specifically what type of information about complex stimulus categories can be processed within V1. MVPA seems to be a reliable tool to investigate the neural representations of imagined stimuli, that could be implemented in future studies to better investigate the role of V1 during visual mental imagery.

In the previous paragraphs, we described the neural bases of visual mental imagery and how different areas constituting the visual imagery network interact in the healthy brain. The literature highlighted that several brain regions involved in processing perceived stimuli are also recruited during internal generation of visual mental imagery. Nevertheless, these two cognitive functions rely on an opposite flow of information: a bottom-up flow from low-level to high-level regions during perception, and a top-down flow from high-level to low-level areas during imagery. As previously reported, neuropsychological studies described cases of double dissociations between perception and imagery, showing that, despite relying on similar brain areas, these two processes are partially independent. Based on these observations, researchers hypothesized a potential role of visual imagery as a rehabilitative tool in the treatment of perceptual deficits. In particular, a specific class of neuropsychological patients was considered (i.e. hemianopic patients), showing impairments in visual perception following damages to retrochiasmatic visual pathways. In the following paragraphs we are going to give an overview about the nature and symptoms of this condition, and we will discuss the potential implementation of visual imagery in rehabilitation paradigms.

1.7 Hemianopia

Hemianopia is a visual field defect, characterized by the abolition of one half of the visual field due to lesions affecting the optic chiasm or more posterior visual pathways. Hemianopic deficits can be divided in two different categories depending on which portion of the visual field has been lost. In heteronymous hemianopia, the loss of vision affects the two internal or external portions of the visual field; in homonymous hemianopia, the visual field defect covers one entire hemifield. If the hemianopic deficit is not complete, and thus only a portion (or quadrant) of the visual field is affected, the deficit is referred to as quadrantanopia.

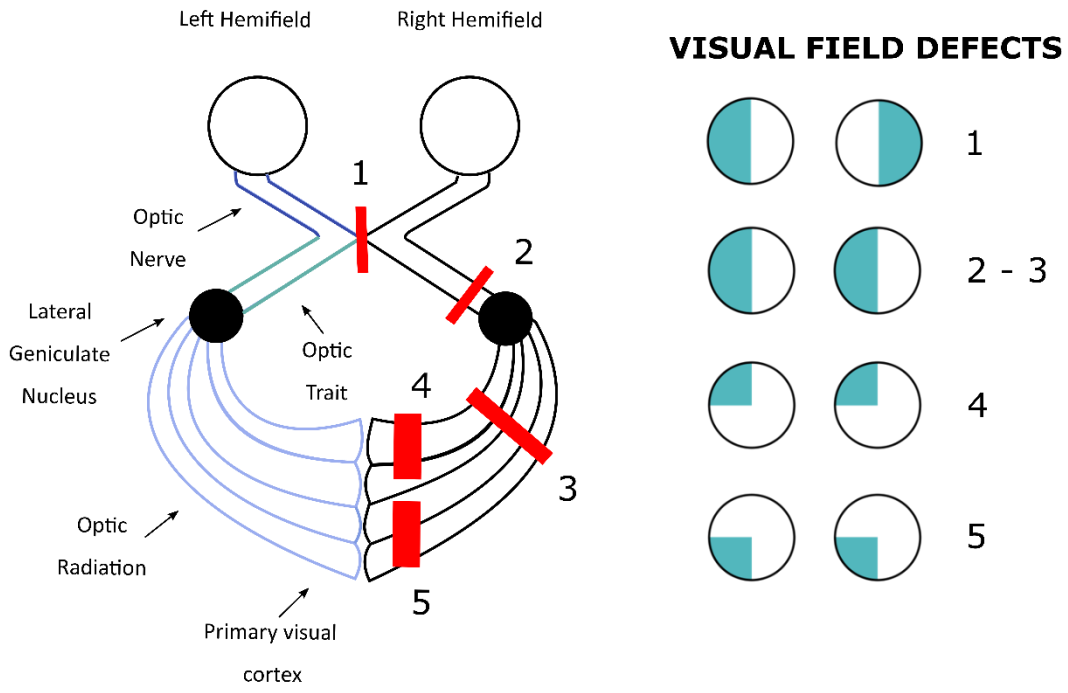

Figure 1.6. Visual field defects. Schematic representation of the geniculo-striate visual pathway (left). Visual information is transmitted from the retina through the optic nerve (blue), the optic tract (light green), the lateral geniculate nucleus (black) and the optic radiation (purple) towards primary visual cortex. Lesions affecting one of these components result in different visual field defects (right). Lesions to the optic chiasm can cause heteronymous hemianopia (i.e. loss of sight in the two peripheral portions of the visual field; 1); lesions affecting the optic tract or interrupting optic radiations completely results in homonymous hemianopia (i.e. loss of vision in one entire hemifield; 2 - 3); lesions affecting only partially optic radiations cause quadrantanopia (i.e. loss of vision in a portion – or quadrant – of the visual field; 4 – 5).

Homonymous hemianopia is one of the most frequent visual field deficits and usually follows a lesion affecting the lateral geniculate nucleus (LGN), optic radiations or the primary visual cortex. The etiology of hemianopic deficits is very heterogeneous. According to the literature, in about 70% of cases it is due to arterial infarctions, in 15% of cases to tumors, and in 5% to hemorrhages (Pambakian & Kennard, 1997). These lesions are localized mainly in the occipital lobe (45%), followed by optic radiations (32%), optic traits (10%), and lateral geniculate nucleus (1.3%) (Goodwin, 2014).

Spontaneous recovery of visual functions in hemianopic patients is possible and usually takes place in the days immediately following the insult. Within the first 48 hours, spontaneous recovery is maximal and is

correlated with the extent of cerebral damage; after 10-12 weeks, any form of further recovery is negligible. Up to 50% of patients show spontaneous forms of recovery of various degrees, but only 10% of them will recover their full field (Pambakian and Kennard, 1997).

Hemianopic deficit has a dramatic impact on patients' daily life activities. The inability to perceive stimuli in the blind portion of the visual field can cause severe impairments in spatial navigation, as well as difficulties in reading and driving. In turn, all these impairments highly increase the risk of incurring in domestic injuries, with significant repercussions on emotional and social well-being (Vu et al., 2004).

Considering the profound impact hemianopia has on patients' quality of life, and the low chances of a spontaneous recovery, research and development of potential rehabilitation techniques have a fundamental role. To date, rehabilitation techniques can be divided into three different groups: the adoption of optical devices, visual-scan training, and visual stimulation of the blind field.

The use of optical devices was first proposed by Peli (2000). The core idea underlying this approach is to compensate the loss of vision by shifting images of objects from the blind hemifield to the sighted one. This relocation of the blind hemifield is obtained by means of prism segments placed monocularly on spectacle lenses, above and below the gaze line of the contralesional hemifield. The efficacy of this approach in expanding the upper and lower visual fields of patients after a treatment period was reported by different studies (Giorgi et al., 2009; O'Neill et al., 2011), and had a good impact on everyday life activities, such as avoiding obstacles or navigating in crowded environments.

The second group of rehabilitation techniques consists in teaching hemianopic patients behavioral strategies aimed at reducing deficits associated with the loss of vision in a portion of the visual field. Pambakian et al. (2004) created a new rehabilitation technique based on a visual search paradigm, designed to train patients to improve eye-movement efficiency in the blind field. By means of a portable system, participants were trained in a 3-month program to perform a wide variety of visual search tasks, consisting of finding a target stimulus amongst distractors as rapidly as possible. Results showed positive effects in the adoption of this treatment. Patients exhibited a significant reduction in the time required to accomplish the visual search, and these improvements were maintained beyond the training phase of the study. The visual search

paradigm also improved performance on daily life activities, but did not lead to an enlargement of the visual field.

Regarding the rehabilitation paradigms based on visual stimulation of the blind field, one of the most famous and controversial is the so-called "Visual Restoration Therapy" (VRT) proposed by Sabel (Sabel et al. 2011). This technique is based on the assumption that, after post-chiasmatic lesions, the blind portion of the visual field is not a homogeneous region of absolute blindness, but could present "areas of residual vision (ARVs)," located at the borders of the sighted visual field. In these ARVs, damage due to the lesion is not complete and this, in turn, could cause the presence of neurons retaining their functional abilities but processing stimuli at a suboptimal level. The idea behind VRT is to induce plastic mechanisms of recovery in these transition zones at the border of the visual field defect, employing a form of massive visual stimulation by means of repetitive flashing lights. This could induce neurons near the damaged site to form new synapses with other functional neurons and help compensate the visual field loss.

In the last few decades, research and development of rehabilitation techniques has grown substantially. However, there is not yet a general consensus about the efficacy of the aforementioned techniques due to the variability of clinical outcomes and the scarce functional benefits in real-life situations (Pouget et al., 2012). Peripheral prisms, for example, require a consistent amount of training to be correctly employed, which can be stressful and frustrating for patients. Furthermore, the superimposition of part of the affected hemifield on the sighted visual field can create peripheral diplopia (i.e. double vision), which in turn can reduce patients' compliance in adopting optical devices as a long term solution (Bowers et al., 2008). The clinical outcomes of the VRT as a rehabilitation technique are to date controversial. The field expansion following a six-month treatment reported by the authors was detected by means of a form of high resolution perimetry (HRP) developed ad-hoc. However, this technique does not permit satisfactory monitoring of fixations and such improvements were not observed with conventional campimetry (Pouget et al., 2012).

Given the limitations of the previously described techniques, research and development of new approaches to the rehabilitation of visual field defects is a matter of primary importance. In particular, in the present thesis we propose a novel approach contemplating the use of visual mental imagery as a tool to reinstate perceptual awareness in the damaged brain. As highlighted in the previous paragraphs, the act of generating

an internal image of an external object involves a network of areas largely overlapping with those involved during actual perception. We thus suggest the use of visual mental imagery to "access" the deafferented or lesioned portion of early visual cortex in patients suffering from homonymous hemianopia. In the following paragraph, I will consider the potential application of such imagery–based treatment, suggesting a form of intervention aimed to potentiate brain activity within preserved visual areas.

1.8 Visual mental imagery and hemianopia: preserved functions in the damaged brain

Despite the loss of vision in the contralesional part of the visual field, hemianopic patients can retain some residual abilities. In particular, a growing number of studies have shown that hemianopic patients are still able to generate visual images in the affected part of the visual field. Marzi et al. (2006) described the case of patient CA, a 35-year-old woman affected by right homonymous hemianopia due to damage of the optic radiations caused by an intraparenchimal bleeding. In their study, they asked the patient to imagine a small stimulus, represented by a luminous square subtending 1° of visual angle, in four different spatial locations, at 2° and 8° eccentricity from the center of the screen, in the upper and lower hemifield. After an acoustic tone, the subject had to imagine the stimulus in a specific spatial location and press a button once she reached a vivid mental image; reaction times were recorded. Results showed that, similarly to healthy participants, the patient showed an eccentricity-related effect in the sighted hemifield: time required to generate a vivid mental image was shorter for small eccentricities (2°) compared to higher eccentricities (8°). This finding is in perfect agreement with results obtained during perception of real stimuli: due to some proprieties of early visual cortex, such as the density of ganglion cells and the cortical magnification factor (Chelazzi et al., 1988; Kitterle, 1986), visual stimuli are detected faster when presented close to the center of the visual field (i.e. small eccentricity) with respect to the periphery (i.e. high eccentricity). The presence of an analogous eccentricity effect for internally generated representations of the same stimuli was interpreted by the authors as proof of the involvement of retinotopically-organized visual areas in visual imagery.

Interestingly, in the blind hemifield of patient CA this eccentricity effect was completely absent. This would indicate that V1 deafferentation consequent to the interruption of optic radiations disrupted the retinotopic representation but did not abolish the ability to perform visual mental imagery.

The results reported above suggest that visual imagery is possible in patients affected by homonymous hemianopia and that visual imagery in these patients maintains some features (e.g. eccentricity related effects) comparable to healthy subjects. Gbadamosi and Zangemeister (2001) focused on scanpaths patterns during the visualization of mental images. When perceiving a visual stimulus, individuals alternate saccades and fixations to explore it; this pattern of eye movements can be described as the so called "scanpath." Interestingly, normal-sighted participants performed eye movements during imagery as well. These scanpaths are characterized by a smaller number of saccades and fixations compared to those performed during perception. These different temporal and spatial characteristics indicate that there is no need for full-scale eye movements to visualize and inspect a visual mental image, but it is sufficient to perform a reduced version of them. Interestingly, the same pattern of eye-movements is preserved in patients with homonymous visual field defect. In spite of their perceptual deficit, they seem to reinstate the same top-down visual strategies during the production of a mental prototype of an external stimulus.

The preserved visual imagery abilities in patients affected by lesion to cortical visual pathways, and the striking phenomenological and functional similarities with healthy individuals, could allow us to hypothesize the implementation of a new rehabilitative technique. The idea behind this hypothesis is that, by using the top-down flow of information during imagery, we would be able to induce activation within preserved regions of V1 processing the affected hemifield. The recruitment of early visual areas would potentially induce plastic mechanisms of change that would reinstate perceptual awareness, increasing the size of the perceived visual field. If this revealed to be true, we hypothesize the possibility to create rehabilitative paradigms based on visual mental imagery that could be implemented as future clinical interventions.

1.9 Thesis summary

In light of the literature described in the previous sections, two main broad research questions can be derived and we will address them in the following chapters. The first one is relative to the representational content of different brain areas involved in visual mental imagery. In particular: a) what type of information is encoded in V1 during visual mental imagery?, b) is this information shared with perception?, c) are there any other brain regions within the imagery network representing the same information? Moreover, considering the potential use of visual mental imagery as a rehabilitative tool in patients suffering from visual field defects, we might investigate d) if it is possible to recruit specific portions of early visual cortex by means of visual mental imagery.

In this thesis, we are going to explore these questions adopting an fMRI approach. In Study 1 (Chapter 2), we will try to understand the degree of complexity of the information encoded in primary visual cortex, its similarities and differences with representations of perceived stimuli, and how this information is encoded in areas outside early visual cortex. We found significant encoding of complex stimulus categories in early visual areas, as well as in inferotemporal and parietal cortices. Moreover, in agreement with previous studies, we found that a subset of these regions showed shared representations with perception.

In Study 2 (Chapter 3), we are going to explore whether it is possible to selectively recruit individual quadrants within the visual field using visual mental imagery. We tested a group of healthy individuals and patients suffering from homonymous hemianopia in a visual imagery paradigm. Results indicated that healthy individuals are able to recruit early visual cortex by means of top-down mechanisms, while for patients there is a huge interindividual variability that allowed a reliable recruitment limited to the healthy hemisphere.

Finally, we will discuss the main results according to the current literature, trying to clarify the complex mechanisms supporting visual imagery and suggesting possible additional studies.

Chapter 2.

Decoding imagined stimuli from different categories

Flavio Ragni[1], Raffaele Tucciarelli[2], Patrik Andersson[3], and Angelika Lingnau[1,2*]

[1]Center for Mind/Brain Science (CIMeC), University of Trento, 38068 Rovereto (TN), Italy

[2]Deparment of Psychology, Royal Holloway University of London, TW20 0EX, Egham (London) UK

[3]Department of Clinical Neuroscience, Karolinska Institutet, 17177, Sweden

2.1 Abstract

In the absence of inputs from the external world, individuals are still able to internally generate vivid images of external stimuli. This cognitive process is known as visual mental imagery and involves a network of prefrontal, parietal and inferotemporal regions, and early visual cortex. Previous studies using MVPA found representation of complex imagined stimulus categories in extrastriate visual areas (LOC, PPA, FFA), but not in V1. Here we asked whether complex stimuli can be decoded in early visual areas during visual mental imagery, using stimulus categories not used in previous MVPA studies. In a delayed spatial judgment task, we asked participants to imagine or perceive lowercase letters, simple shapes, and objects. To examine whether it was possible to discriminate between neural patterns in the perception and imagery condition, we performed a ROI-based and whole-brain searchlight-based MVPA analysis. We were able to decode the three stimulus categories in early visual (V1, V2), parietal (SPL, IPL, aIPS) and inferotemporal (LOC) areas. In a subset of these areas, we also obtained significant cross-decoding across visual imagery and perception. Our results provide evidence for distinct roles of parietal and inferotemporal regions during visual imagery, with the former processing the spatial layout of imagined stimuli and the latter the content of imagined stimulus categories. In the absence of bottom-up visual input, we hypothesize early visual cortex can access both types of information via feedback connections.

2.2 Introduction

As human beings, we strongly rely on visual perception to process information coming from the external world. At the same time, we are able to create a mental representation of a percept in the absence of visual input, as the well-known example of having to think of a pink elephant when being instructed not to do so demonstrates. This ability, often referred as "seeing with the mind's eye," is called "visual mental imagery." During perception, information is processed along a pathway from the retina over the optic nerve, the optic chiasm and the lateral geniculate nucleus to the early visual cortex (V1) for basic visual processing and to parietal and inferotemporal cortices responsible for higher level visual processing (Ungerleider & Haxby, 1994). By contrast, during visual imagery, a top-down organization has been suggested in which sensory representations of external stimuli, e.g. objects in inferotemporal areas, are reenacted by means of signals coming from prefrontal areas (Mechelli et al., 2004; Dijkstra et al., 2017). The same top-down modulation also exerts an influence over parietal areas involved in attentional mechanisms and in the representation of the spatial configuration of imagined stimuli (Sack et al., 2012). According to depictive theories of visual imagery (Kosslyn, 1981; 2005), this top-down modulation ultimately leads to a recruitment of V1, serving as a "dynamic blackboard" (Bullier, 2001) where mental images acquire their resemblance to actual percepts.

A number of PET (Kosslyn et al., 1993) and fMRI studies (Amedi et al., 2005; Klein et al., 2000; Ishai et al., 2002; Slotnick et al., 2005) demonstrated a recruitment of V1 in visual imagery tasks. By contrast, a number of studies failed to observe any reliable recruitment of V1 (Ishai et al., 2000; Formisano et al., 2002; Sack et al., 2002) or found a deactivation of V1 (Mellet et al., 2000. For a review see Kosslyn & Thompson, 2003), which led to a lack of a general consensus regarding the role of V1 during visual imagery.

The advent of MVP analysis (Haxby, 2001; Kriegeskorte et al., 2006) allowed the examination of the representational content of V1 during visual imagery tasks. Albers et al. (2013) asked participants to imagine gratings with different orientations over a delayed period of time. Decoding of the representational pattern associated with each stimulus was possible within V1, despite overall low levels of neural activity in early visual areas. Other studies investigated whether more complex imagined stimulus categories, such as letters (Stokes et al., 2009), faces and scenes (Reddy et al., 2010; Cichy et al., 2011) and common objects (Lee et al.,

2012) could be encoded in V1. All these studies showed significant decoding for all tested categories in extrastriate visual areas but not in primary visual cortex. At the same time, V1 is known to encode more complex stimulus features than previously thought, such as complex sounds of different semantic categories (Vetter et al., 2014), most likely due to top-down modulations.

In light of these conflicting results, we aimed to elucidate whether complex stimuli can be decoded in early visual cortex during visual imagery using stimulus categories not used in previous MVPA studies. To this aim, we asked participants to either visually imagine ('imagery' task) or perceive ('perception' task) lowercase letters, simple shapes, and objects. Performance was measured using a delayed spatial judgement task. To examine whether it is possible to distinguish between neural patterns during the imagery and the perception condition in early visual cortex, we used region-of-interest (ROI)-based and a whole-brain MVPA searchlight analysis (Kriegeskorte et al. 2006). To anticipate our results, we were able to distinguish between the three stimulus categories in early visual (V1 and V2), parietal (SPL, IPL and aIPS) and inferotemporal (LOC) areas, in line with the view that complex stimulus information is passed all the way down to early visual cortex even in the absence of retinal stimulation.

2.3 Behavioral pilot study: stimulus selection

For the fMRI study, we decided to adopt a delayed spatial judgment task similar to that employed by Kosslyn and colleagues (Kosslyn et al., 1993; see paragraph *1.4 Neuroimaging studies*). However, we introduced a number of significant changes. First, we decided to test a higher number of stimulus categories with respect to the original study. Second, to make the spatial judgment task more challenging and thus induce a stronger mental imagery, we eliminated the reference grid during the imagery delay. These modifications required an extensive behavioral testing prior the execution of the fMRI task. To determine which stimulus categories are best suited to be used in the fMRI task, we performed a behavioral study outside the scanner. This study was based on the eccentricity effect (Chelazzi et al., 1988). Participants are faster to detect stimuli presented closer to fixation in comparison to stimuli presented further away from fixation. This effect is assumed to be based on cortical magnification (Kitterle, 1986; Marzi & Di Stefano, 1981). Marzi et al. (2006) demonstrated that a similar eccentricity effect can be obtained for imagined stimuli and interpreted this observation as a sign of the involvement of retinotopically organized early visual cortex. Following this logic, we reasoned that stimuli which show a reliable eccentricity effect should be good candidates to be chosen for our fMRI study.

Participants. Fourteen healthy volunteers (10 females, mean age 24.6) participated in the study. All participants had normal or corrected-to-normal vision and had no history of neurological or psychiatric disease. Before taking part in the study, all participants gave their written informed consent. Due to difficulties in maintaining their gaze at fixation during the task in at least two out of 4 experimental runs (see section Data analysis, eye-tracking data), three participants were excluded. Two additional participants were excluded due to a high number of missed responses (15% and 69%), leading to a final sample of nine participants (5 females, mean age 25.2 ± 4.7). The study was approved by the Ethics Committee for research involving human participants at the University of Trento, Italy.

Stimuli. We asked participants to imagine six different stimulus categories (checkerboards, gratings, simple shapes, lowercase letters, objects and invented shapes), each one composed of four different stimulus

exemplars (*Figure 2.1*). Checkerboards, gratings, invented shapes, lowercase letters, and simple shapes were created in Inkscape (Harrington et al., 2004). Objects were selected from the 260 standardized pictures composing the Snodgrass database (Snodgrass & Vanderwart, 1980) and then edited in Inkscape to match their background color across categories. To prevent afterimages during visual presentation of the stimuli, we created a visual mask, common for all stimulus exemplars. The mask was created using a custom-written MATLAB script. Each stimulus was converted to grayscale, eliminating hue and saturation information. Values for each pixel were then averaged across all stimuli, resulting in a sample picture. As the last step, the spatial position of pixels in this sample picture were shuffled, resulting in a black and white visual mask.

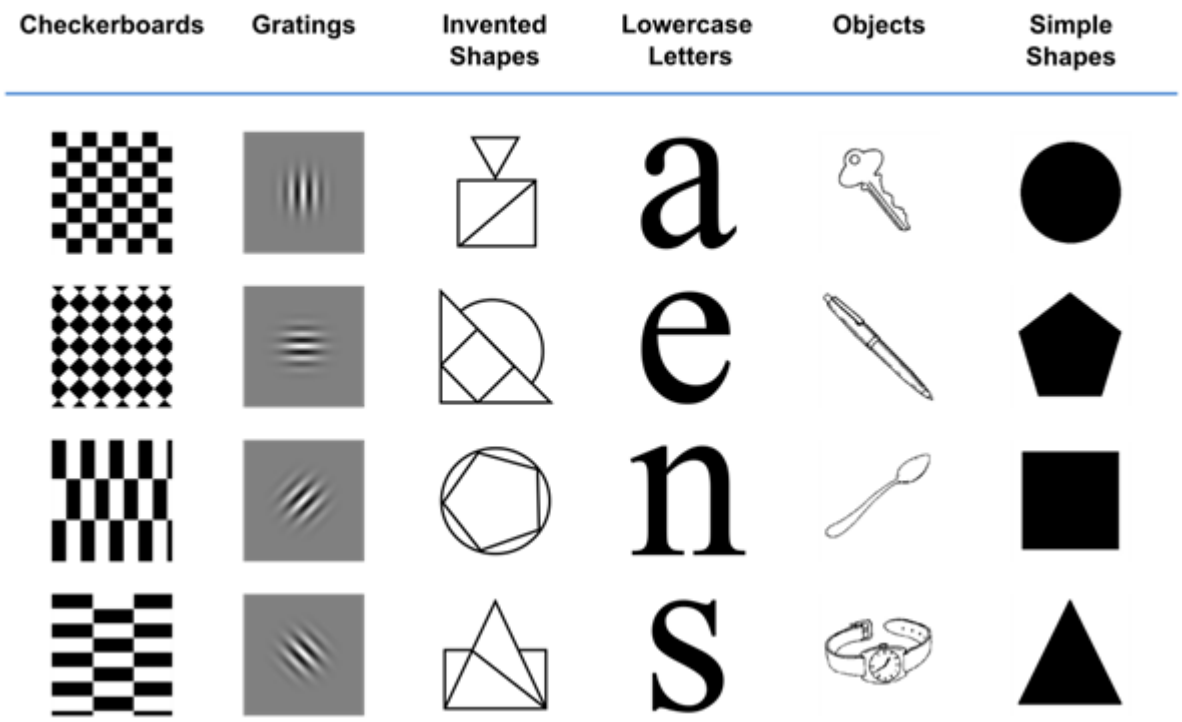

Figure 2.1. Behavioral pilot study: stimulus exemplars. Full set of stimulus exemplars used in the behavioral pilot study. For each stimulus category (checkerboards, gratings, invented shapes, lowercase letters, objects, and simple shapes), 4 stimulus exemplars were selected.

Experimental design. The experiment was divided in two sessions to be performed on two consecutive days. Each session comprised two runs (24 blocks each), each lasting approximately 20 minutes. The entire experiment comprised a total of 960 trials (40 trials for each combination of spatial position (4) and stimulus exemplar (6)). On each day, participants saw all the stimuli twice, in a randomized order. Participants were

instructed to perform visual imagery in four different spatial locations, either 2° or 8° of visual angle (relative to the central fixation point) to the left or right side of the screen. To keep the size of the imagined stimuli constant, participants were asked to performed visual imagery within placeholders positioned at the aforementioned locations and comprising 2° of visual angle (*Figure 2.2a*). All four placeholders were presented on the screen throughout the trial. Each block started with the presentation of the stimulus exemplar to be imagined (1s) at the center of the screen, followed by a mask (1s). An auditory cue ("far left", "far right", "near left", "near right"; 400 ms) instructed participants at which location they had to imagine the stimulus. Participants were asked to indicate by button press when they reached a vivid mental image. If no response was provided, the program automatically passed to the next trial after six seconds (see *Figure 2.2b*). After 10 trials, a new block started and the stimulus to be imagined changed. At the end of the experiment, we obtained subjective ratings of the vividness of visual imagery and the perceived difficulty in generating the imagined stimuli from each participant. We recorded reaction times and monitored eye-movements using a video-based eye tracking system (Eyelink 1000, SR Research).

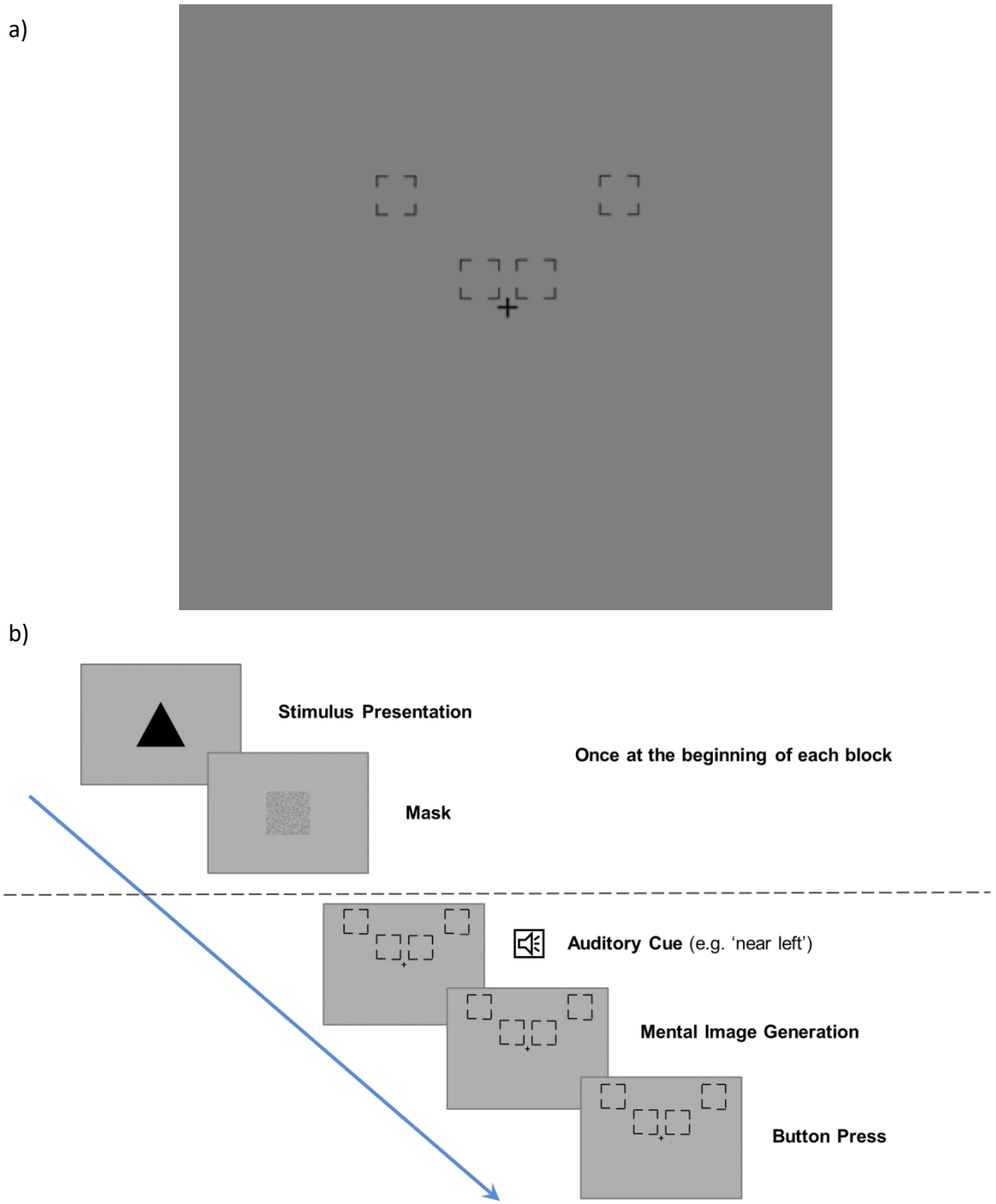

Figure 2.2. Behavioral pilot study. a) Placeholder position. During each block, participants had to imagine the selected stimulus in four different spatial locations, either 2° or 8° from central fixation cross, on the left or the right side of the screen. To keep the size of the mental image constant, imagery was performed within one of four placeholders positioned at the aforementioned locations, comprising 2° visual angle each. b) Trial structure. Each block started with the presentation of a stimulus exemplar, followed by a mask. An auditory cue instructed participants at which location they had to imagine the stimulus. Participants had to indicate by button press when they reached a vivid mental image.

Data analysis. For each participant, we averaged reaction times (RTs) for each spatial position (2° and 8° eccentricity) and side (left or right) separately for each stimulus category. We then performed a repeated-measures ANOVA, with eccentricity (2 levels), side (2 levels), and stimulus category (6 levels) as factors. Moreover, to assess differences in vividness and difficulty while generating mental images between the six selected stimulus categories, we performed two additional repeated-measures ANOVAs (factors: vividness rating and stimulus category (6 levels) for vividness ratings; difficulty ratings and stimulus categories (6 levels) for difficulty ratings).

To assess the ability of our participants in maintaining their gaze at fixation, we examined their gaze position throughout each run with respect to the central fixation cross.

Results. Participants were faster to indicate that they experienced a vivid mental image when they were asked to perform visual imagery nearer to fixation (2°; mean RT = 2669.3 ± 333 ms) in comparison to further away from fixation (8°; mean RT = 2973.5 ± 417.8 ms) in line with previous studies (Marzi et al., 2006). This observation is supported by the corresponding repeated-measures ANOVA [main effect eccentricity: $F(1, 8) = 16.8$, $p = 0.003$]. Degrees of freedom were adjusted by the Greenhouse-Geisser procedure when appropriate (corresponding p-values denoted as p_{GG}). Reaction times differed between stimulus categories [main effect of category: $F(2.3, 26.1) = 10.46$, $p_{GG} = 0.001$; mean checkerboards: 3005.6 ± 133.5 ms; mean gratings: 2828.7 ± 133 ms; mean lowercase letters: 2827.3 ± 112.9 ms; mean objects: 2774.2 ± 125.7 ms; mean invented shapes: 3020.5 ± 154.8 ms; mean simple shapes: 2575.5 ± 114.6 ms]. The eccentricity effect was not modulated by stimulus category [interaction categories*eccentricity: $F(2.42, 19.40) = 0.553$, $p_{GG} = 0.616$], suggesting that the eccentricity effect was present for all six examined stimulus categories.

For two categories (i.e. checkerboards and invented shapes), we found a stronger eccentricity effect when imagery was performed on the left side of the screen; whereas for the remaining ones (i.e. gratings, lowercase letters, simple shapes and objects), the pattern was the opposite [interaction side*eccentricity*category: $F(5.55) = 2.63$, $p=0.034$; see *Figure 2.3*]. None of the other interactions were significant [interaction category*side: $F(2.29, 18.38) = 1.2$, $p = 0.328$; interaction side*eccentricity: $F(1, 8) = 0.340$, $p = 0.576$].

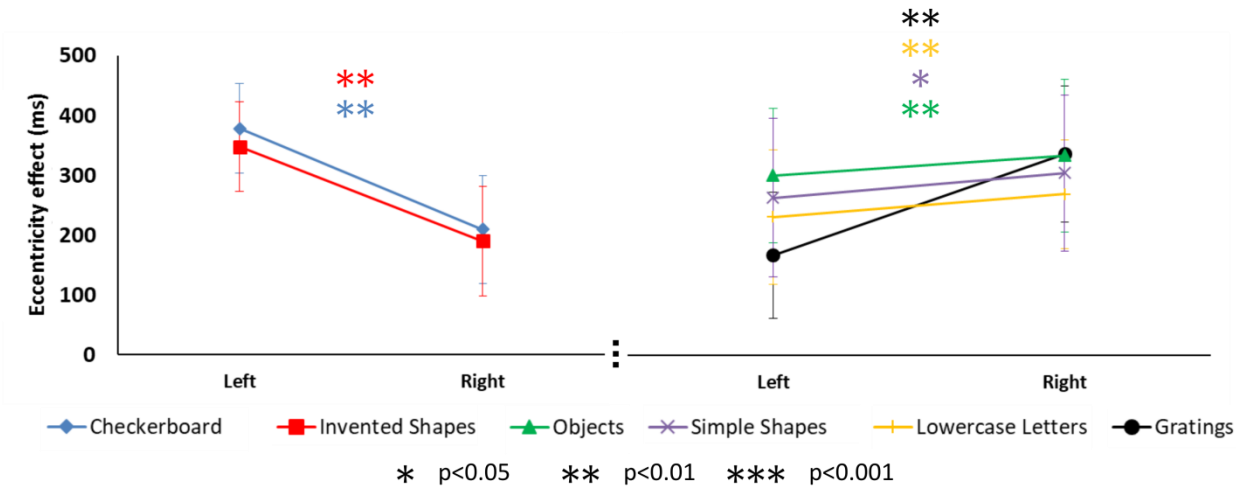

Figure 2.3. Magnitude of the eccentricity effect (RT for stimuli presented at 8 deg – RT for stimuli presented at 2 deg visual angle) as a function of stimulus position (left, right), separately for the six stimulus categories. As can be seen, the eccentricity effect was larger for stimuli presented on the left side of the screen for checkerboards and invented shapes, whereas the opposite pattern was obtained for gratings, lower case letters, simple shapes, and objects. Error bars: standard error of the mean (S.E.M.).

A repeated-measures ANOVA of the vividness and difficulty ratings revealed that both ratings were modulated by stimulus category [main effect of stimulus category for vividness rating: $F(5, 40) = 6.45$, $p = 0.003$; main effect of stimulus category for difficulty ratings: $F(5, 40) = 8.157$, $p < 0.001$; see *Figure 2.4a*].

We thus decided to select lowercase letters, objects and simple shapes for the fMRI study.

To test whether the eccentricity effect differed between the four stimulus exemplars constituting each category, we performed an additional ANOVA for each stimulus category [Lowercase letters: repeated-measures ANOVA, factors: eccentricity, side, stimulus exemplars. Interaction eccentricity*stimulus exemplar: $F(3, 24) = 1.69$, $p = 0.195$; Objects: repeated-measures ANOVA, factors: eccentricity, side, stimulus exemplars. Interaction stimulus exemplars*eccentricity: $F(3, 24) = 1.137$, $p = 0.354$. Simple Shapes: repeated-measures ANOVA, factors: eccentricity, side, stimulus exemplars. Interaction stimulus exemplars*eccentricity: $F(3, 24) = 0.846$, $p = 0.482$]. Due to this lack of difference in the magnitude of the eccentricity effects between stimulus exemplars, we selected stimuli within each category that differed widely for low-level visual features, such as orientation or shape (i.e. circle and triangle for simple shapes; pen and watch for objects; letter “e” and “n” for lowercase letters. *Figure 2.4b*).

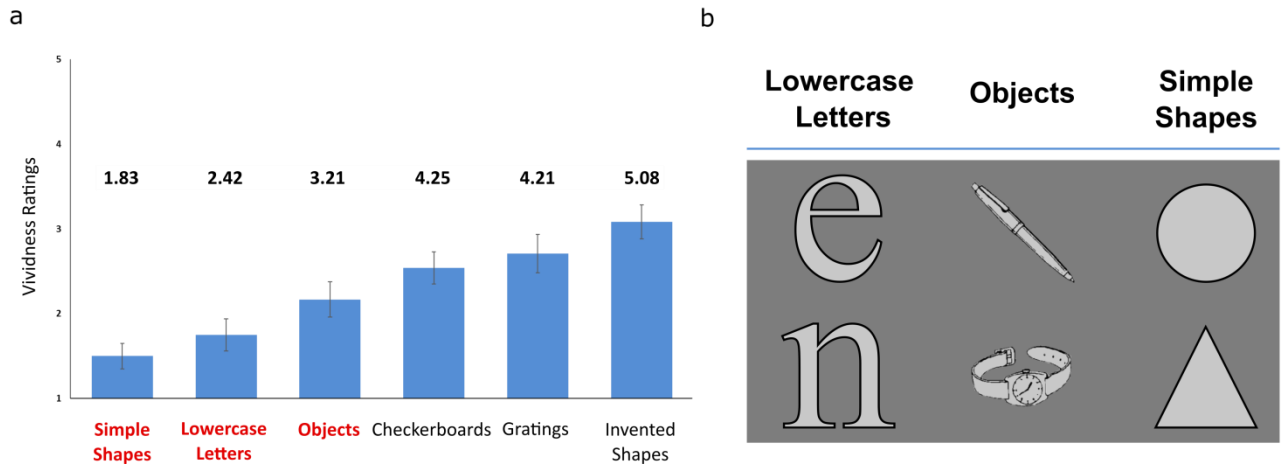

Figure 2.4. a) Individual ratings of difficulty (black numbers) and vividness (blue bars) of mental imagery for each stimulus category. Stimulus categories highlighted in red are those selected for the fMRI study. Vividness scale: 1. Perfectly clear and as vivid as normal vision; 2. Clear and reasonably vivid; 3. Moderately clear and vivid; 4. Vague and dim; 5. No image at all. Difficulty scale: 1. Easiest category to imagine – 6. Hardest category to imagine. b) Stimulus categories and exemplars used for the fMRI experiment. For each stimulus category (i.e. lowercase letters, objects and simple shapes), we selected two stimulus exemplars on the basis of the behavioral pilot experiment described above.

2.4 Materials & Methods

2.4.1 Participants

Twenty-nine healthy volunteers participated in the study. All participants had normal or corrected-to-normal vision and had no history of neurological or psychiatric disease. Before taking part in the study, all participants gave their written informed consent. Due to technical problems during data acquisition, data from three participants had to be excluded from the study. Moreover, due to poor performance in the behavioral task (see section *Data analysis, behavioral data*), five additional participants were excluded, leading to a final sample of twenty-one subjects (11 males, 10 females, mean age 26.1 ± 3.8). The study was approved by the Ethics Committee for research involving human participants at the University of Trento, Italy.

2.4.2 Setup

Visual stimuli were back-projected to a screen via a liquid crystal projector (OC EMP 7900, Epson Nagano, Japan; frame rate: 60 Hz; screen resolution: 1280x1024 pixels). Participants laid horizontally in the scanner in a conventional fMRI configuration, and viewed the screen binocularly through a rectangular mirror (17.8°x13.4° of visual angle) positioned on the head coil. The auditory cue was delivered by means of MR-compatible headphones (SereneSound, Resonance Technology, Inc.). Button presses were collected via an MR-compatible response button (Lumina LP 400, Cambridge Research Systems). Stimulus presentation, response collection, and synchronization with the scanner were controlled using "ASF" (Schwarzbach, 2011), based on MATLAB (MathWorks, Natick, MA, U.S.A.) and the Psychtoolbox-3 for Windows (Brainard, 1997).

2.4.3 Stimuli

Based on the results of the behavioral pilot study (see *Behavioral pilot study: stimuli selection* for details), we selected three stimulus categories (i.e. lowercase letters, objects and simple shapes) for the fMRI study, each one composed of two stimulus exemplars (i.e. "e" and "n" for lowercase letters, pen and watch for objects, circle and triangle for simple shapes).

To ensure that participants actively engaged in the visual mental imagery task throughout the fMRI experiment, we designed a delayed spatial judgment paradigm in which participants had to judge the position of a black dot with respect to a stimulus they just imagined (see *Experimental design*, *Imagery task* for details). To this purpose, we created a set of 20 non-overlapping dots for each individual stimulus exemplar. Half of these dots were positioned inside the area delimited by the external boundaries of the silhouette ("match" dots) and the other half outside it ("no match" dots; *Figure 2.5*). Each dot comprised 0.5° of visual angle. To prevent afterimages following the visual presentation of the stimuli, we created visual masks consisting of a phase-scrambled image of each stimulus exemplar by means of a Fourier transformation implemented in Matlab. To this purpose, original stimuli were imported in Matlab and converted to intensity images, with values ranging from 0 (black) to 1 (full intensity or white). Separately for each RGB component, a fast Fourier transform was applied. We then added a random phase to the phase angle of the transformed

component, and applied an inverse Fourier transform to the modified image to revert it to its original dimensionality. With this procedure, we obtained a total of six masks, one for each individual stimulus exemplar (see *Figure 2.5*).

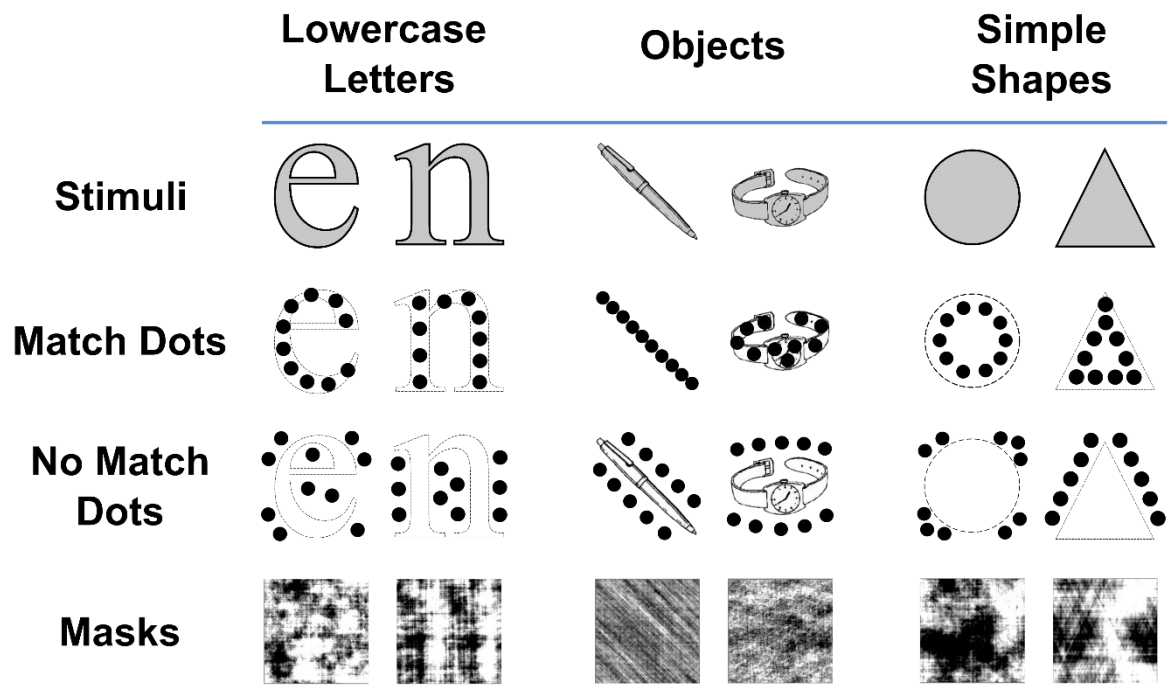

Figure 2.5. Stimulus exemplars. First row: there were two exemplars for each of the three stimulus categories (Lowercase Letters, Objects, Simple Shapes). Second row: Matching dot positions for each stimulus exemplar. Third row: Non-matching dot positions for each stimulus exemplars. Fourth row: Fourier-scrambled masks for each of the stimulus exemplars (see text for details).

2.4.4 Behavioral pilot study: fMRI task

To ensure that participants were able to perform a spatial judgment task on imagined stimuli and that both "match" and "no match" dots had comparable difficulty levels across stimulus categories, we performed a short behavioral pilot experiment. N=6 participants completed 5 runs of the imagery task outside the scanner (see *Experimental design*, *Imagery task* for details).

Results showed that all participants were able to perform the task above chance [mean accuracy: 72.1% ± 4.9%], both for matching and for non-matching dots [mean accuracy match dots: 70.6% ± 10%; mean accuracy No Match dots: 74.4% ± 8.3%]. No significant difference in accuracy was found between matching and non-matching dots [repeated measures ANOVA; factors: dot type, stimulus category. Main effect of dot

type: F(1, 5) = 0.356, p = 0.577]. The spatial judgment task proved to be more difficult for visual imagery of Lowercase letters [mean accuracy: 61.7% ± 8.7%] in comparison to visual imagery of Objects [mean accuracy: 77.1% ± 8.8%] and Simple shapes [mean accuracy: 78.8% ± 7.5%; repeated measures ANOVA; factors: dot type, stimulus category; main effect of stimulus category: F(2, 10) = 7.766, p = 0.009]. No interaction between stimulus category and dot position was found [repeated measures ANOVA; factors: dot type, stimulus category; interaction dot type*stimulus category: F(2, 10) = 0.618, p = 0.558].

2.4.5 Experimental design

To examine patterns of brain activation during visual mental imagery and the similarity with visual perception, we used an experimental design made by blocks of trials of the same type (i.e. stimulus categories) and each one of those was made by multiple events/trials. In this "mixed design (see Petersen et al., 2012)," the stimulus category was blocked while the stimulus exemplar was randomized within each block. To avoid possible learning effects due to previous visual presentation of the stimuli to be imagined, participants performed the imagery condition in runs 1-5, and the perception condition in runs 6-10. Each participant completed a single experimental session, consisting of a short familiarization with the task outside the scanner (~20 minutes), a structural scan (~5 minutes) and 10 experimental runs (~6 minutes each). Each functional run started and ended with 10 seconds of rest, and contained 6 blocks (two for each stimulus category), interleaved by fixation blocks of 10 seconds each. Each block (43 seconds) consisted of 4 trials (2 Match and 2 No Match), for a total of 240 trials for each participant (40 trials for each factorial combination of task (2) and stimulus category (3)). The order of the blocks within each run and the exemplar to be imagined in each trial was randomized. The spatial position of the stimulus exemplars within each category in the instruction phase (i.e. left or right with respect to the fixation cross) was counterbalanced across runs, following an ABAB design for half of the participants and BABA for the other half.

Imagery condition. Each block of the imagery condition started with the presentation of the two exemplars of one of the three categories - one on the left and one on the right side of the screen (*Figure 2.6*), for 1.5 seconds. To prevent after-images, stimulus presentation was followed by the appearance of two masks (1.5s) at the same spatial location. Each trial was preceded by an inter-trial interval (ITI) of 1 second, consisting of

the presentation of a central fixation cross and a superimposed placeholder. The placeholder comprised 6° of visual angle, and served as a reference for the spatial position and size of the mental image. An auditory cue (i.e. “left” or “right”, 500ms) instructed participants which of the two previously presented stimuli to imagine in the current trial. After the auditory cue, participants were instructed to imagine the stimulus previously shown at the location indicated by the auditory cue within the placeholder for a total of 7 seconds. During this time window, participants were instructed to try and generate the most vivid mental image they could, keeping the same size and spatial location of the original stimuli inside the placeholder. Next, the fixation cross and placeholder disappeared, and a black dot (1/2° visual angle) appeared for 2 seconds within the area previously contained within the placeholder. Participants were asked to judge whether the dot fell within ("match" trials) or outside ("no match" trials) the outline of the stimulus they had just imagined. Participants were instructed to provide the most accurate answer they could, favoring accuracy over speed. The offset of the black dot was followed by the next trial. Participants were asked to indicate their response by button press with the index and middle finger of the right hand within 2 seconds during which the dot remained on the screen.

Perception condition. The perception condition was similar to the imagery condition (*Figure 2.6*) except for the following ways. After the presentation of the auditory cue, participants were presented with the line drawing of the stimulus corresponding to the auditory instruction within the placeholder for 0.5 seconds, followed by a mask (1.5s), and a fixation cross with a superimposed placeholder (4s). This was followed by the presentation of a black dot (2s). Participants had to judge whether the dot fell on the perceived stimulus (“match” trials) or outside it (“no match” trials) by pressing the buttons with the index and middle fingers of the right hand.

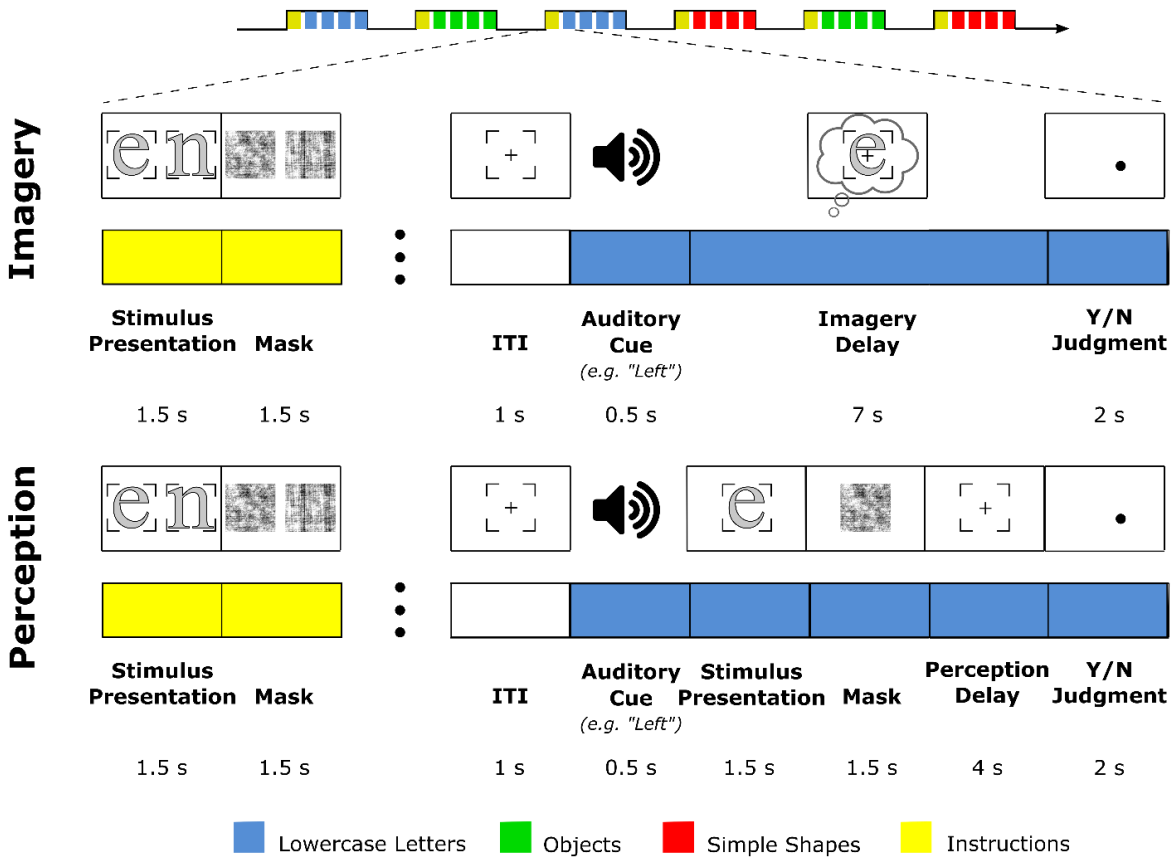

Figure 2.6. Task overview. Top panel: imagery condition. Participants were asked to imagine three different stimulus categories in a block design. Each block consisted of four runs and started with the presentation of the two stimulus exemplars pertaining to one of the three categories, one on the left and one on the right side of the screen, followed by a mask to prevent afterimages. Each trial started with a central fixation cross and a superimposed placeholder (1s). Next, participants were presented with an auditory cue ('left,' 'right') that indicated which of the two previously presented stimuli to imagine in the center of the placeholder, for 7 seconds. Throughout the imagery delay, only the fixation cross and the placeholder were present on the screen. Next, placeholder and fixation cross disappeared, and a black dot appeared on the screen (2s); participants had to judge whether the dot fell within or outside of the boundaries of the imagined stimulus. This was followed by the next trial. After a block of four trials, there was a fixation period of 10 seconds. Bottom panel: perception condition. The perception condition was identical to the imagery condition, except for the following. After the auditory cue, participants were presented with the visual stimulus corresponding to the instruction and the superimposed placeholder (1.5s) and a mask (1.5s). This was followed by the central fixation cross and the placeholder (4s), and the presentation of the black dot (2s). Participants had to judge whether the dot fell within or outside of the boundaries of the perceived stimulus.

To examine general visual imagery abilities, we asked each participant to fill out the Vividness of Visual Imagery Questionnaire (VVIQ; Marks, 1973) at the end of the session. This questionnaire aims to assess

individual variability in the strength and vividness of mental images by providing a set of scenarios to be imagined (e.g. *"think of some relative or friend whom you frequently see (but who is not with you at present) and consider carefully the picture that comes before your mind's eye"*). For each of the scenarios, participants have to rate the vividness of the mental image they are able to generate on a 5-point Likert scale (answer alternatives: 1. *Perfectly clear and as vivid as normal vision*; 2. *Clear and reasonably vivid*; 3. *Moderately clear and vivid*; 4. *Vague and dim*; 5. *No image at all),* both with eyes open and with both eyes closed. In addition, for each stimulus exemplar, we also collected ratings of vividness (answer alternatives: 1. *Perfectly clear and as vivid as normal vision*; 2. *Clear and reasonably vivid*; 3. *Moderately clear and vivid*; 4. *Vague and dim*; 5. *No image at all)* and of the difficulty in generating the mental image during the task (answer scale: 1. *Easiest stimulus to imagine* – 6. *Hardest stimulus to imagine*).

2.4.6 Data acquisition

Data were collected using a 4T Bruker MedSpec Biospin MR scanner equipped with an eight-channel birdcage head coil. Functional data were acquired using an EPI sequence (TE/TR = 28.0/2000.0, flip angle = 73°, matrix size = 64x64, 30 interleaved slices, in-slice resolution 3 mm). The slices were axial, slightly tilted to be approximately parallel to the calcarine sulcus in order to optimize brain coverage. One-hundred and seventy-one volumes were acquired for each functional run.

To be able to coregister the low-resolution functional images to a high-resolution anatomical scan, we acquired a T1-weighted anatomical scan (magnetization-prepared rapid-acquisition gradient echo; TR: 2700 ms; voxel resolution: 1 x 1 x 1 mm; TE: 4.18 ms; FA: 7°; FOV: 256 x 224 mm; 176 slices; generalized autocalibrating partially parallel acquisition with an acceleration factor of 2; inversion time: 1020 ms).

2.4.7 Data analysis

Behavioral analyses. For each participant, accuracy was assessed computing the percentage of correct answers separately for the imagery and perception condition and for the three stimulus categories.

Moreover, we compared the accuracy for “Match” and “No Match” trials. Due to a technical fault, accuracy was not recorded for one run of the perception condition in one participant. We performed a repeated measure ANOVA, with condition (2 levels) and stimulus categories (3 levels) as factors.

fMRI data analysis

Preprocessing. Data were preprocessed and analyzed using FSL 5.1 (FMRIB’s Software Library, https://fsl.fmrib.ox.ac.uk/fsl) in combination with custom software written in Matlab. To avoid T1 saturation, we discarded the first 4 volumes of each run. Preprocessing included motion correction to the mean image, followed by slice timing correction (ascending interleaved even-odd order), spatial smoothing (Gaussian kernel FWHM = 5 mm), and high-pass temporal filtering (t > 0.01 Hz) to remove frequency artefacts. Each functional scan was registered to its corresponding coplanar high-resolution image with rigid body transformations and to the MNI152 standard brain using nonlinear transformation (12 degrees of freedom).

Univariate RFX-GLM analysis. To examine the BOLD response during the two conditions (imagery, perception), we performed a random effects (RFX) general linear model (GLM) analysis (N=21). Separately for each of the two conditions (imagery, perception), we created predictors for each stimulus category, resulting in a total of three predictors for each experimental run. Predictors for the imagery condition were time-locked to the onset of the imagery delay (duration: 6s); predictors for the perception condition were time-locked to the appearance of the stimulus (duration: 3s). In addition, predictors for the presentation of the auditory cue (time-locked to the onset of the instructing cue), button presses (time-locked to the appearance of the black dot), presentation of the two stimulus exemplars pertaining to the target category at the beginning of each block, and subsequent mask presentation were added to the model as nuisance regressors. This lead to a total of six predictors for each experimental run. Each predictor was convolved with the canonical hemodynamic response function (HRF). Parameters from 3D motion correction were not included in the model in light of the potential deleterious impact they could have on GLM sensitivity in block designs (e.g. Johnstone et al., 2006).

To understand whether imagery of different stimulus categories induced activation in different brain regions, we created three main functional contrasts for each pairwise comparison between categories (i.e. Lowercase Letters vs Simple Shapes, Lowercase Letters vs Objects, Simple Shapes vs Objects).

Results from the Univariate RFX-GLM analysis were FWE cluster-corrected using Gaussian Random Field theory (GRF; Worsley et al., 1996), and then projected on an inflated brain in BrainVoyager QX 2.8.0 (BrainInnovation). Brain areas were labeled by means of the Juelich Histological Atlas (Eickhoff et al., 2007), as implemented in FSL 5.1.

ROI definition. ROIs were defined using standard masks provided by the Juelich Histological Atlas (Eickhoff et al., 2007). To obtain non-overlapping ROIs, we applied a threshold of 0.5 to the probabilistic maps and binarized these maps using FSLmaths. For each participant, we selected the 250 voxels showing the highest *t* values during both the perception and the imagery condition.

This selection consisted in four steps: first, for each participant, we averaged the t-values across the five experimental runs for each voxel, separately for the imagery and perception conditions. Next, we normalized the average t-value of each voxel in the imagery and perception conditions separately using the following formula (feature scaling):

$$N = \frac{(mean_{voxel\ n} - min_{cond})}{(max_{cond} - min_{cond})}$$

Where $mean_{voxel\ n}$ represents the mean value of the n^{th} voxel across the five experimental runs of the selected condition (perception or imagery), min_{cond} the lowest value across all voxels in the selected condition, and max_{cond} is the highest value across all voxels in the selected condition.

In this step, the t-value expressed in each voxel is rescaled with respect to the maximum and minimum value in the imagery and perception conditions separately. The output of this normalization is two vectors, one for each experimental condition, with values for each voxel ranging between 0 and 1. This allowed us to refer

the recruitment of each voxel in each of the two conditions to a common scale despite the overall difference in magnitude of the strength of the activation between imagery and perception in visual areas.

Third, in order to select voxels showing the highest activation both in imagery and perception conditions, we transformed our data using the following index:

$$I = (mean_{PER} \times max_{PER}) + (mean_{IMG} \times max_{IMG})$$

where $mean_{PER}$ represents the normalized mean (across the five runs) value of a single voxel in the perception condition, $mean_{IMG}$ is the normalized mean value of a single voxel in the imagery condition, max_{PER} is the maximum normalized *t* value of a voxel within the perception condition, and max_{IMG} the highest normalized *t* value of a voxel within the imagery condition. Finally, we selected the 250 voxels showing the highest *I* values (see *Figure 2.7*).

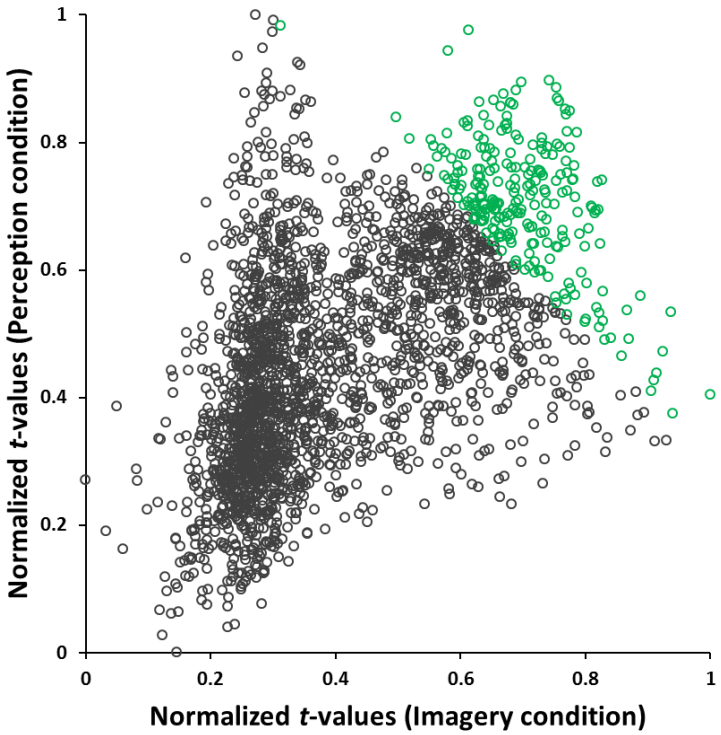

Figure 2.7. Example voxel selection for the V1 ROI in one representative participant. In green are the 250 voxels showing the highest normalized t-value (see text for details) both in the perception and imagery condition.

We repeated these steps for all ROIs (V1 and V2). To examine classification accuracy in areas not expected to be involved in the imagery process, we included a control ROI encompassing the ventral bilateral striatum, defined using the Juelich Histological Atlas.

Multivariate pattern classification (MVP) analysis. We ran both an ROI- and searchlight-based analysis (Haxby, 2001; Oosterhof et al., 2016; Kriegeskorte et al. 2006) using a regularized linear discriminant analysis (LDA) classifier. The purpose of the ROI-based MVP analysis was to test whether it was possible to decode imagined and perceived stimulus categories in early visual areas, defined as described in the previous section. For the MVP analysis, we used a different design matrix. Specifically, we created predictors for each individual block in the perception and imagery conditions, separately for each stimulus category. This resulted in 6 predictors for each experimental run (2 for lowercase letters, 2 for objects and 2 for simple shapes). In addition, we added nuisance regressors modeling the auditory cue (time-locked to the onset of the instructing cue), button presses (time-locked to the appearance of the dot), and one additional regressor comprising the presentation of the two stimulus exemplars and the subsequent masks at the beginning of each block, for a total of 9 predictors.

We used *t*-values rather than β weights as input for the classifier. Since *t*-values are computed by dividing the beta estimates by its standard error estimate, they have been argued to be better suited for decoding since this suppresses the contribution of noisy voxels (Misaki et al., 2010). Classification accuracies were computed using a leave-one-run-out cross-validation method (i.e., patterns from N-1 runs served as the training set, whereas the pattern from the remaining run served as the testing dataset). Moreover, to examine the similarity between the neural pattern of representation between imagined and perceived stimuli, we performed cross-condition decoding. The classifier was trained to discriminate between the three stimulus categories in one condition (e.g. perception) and tested on its ability to discriminate the same categories in the other condition (e.g. imagery), and vice versa. Results from the two cross-condition classifications were averaged, resulting in one accuracy score for each ROI. To assess the significance of the decoding accuracy, the individual accuracy scores of our participants were entered into a two-tailed one-sample t-test across participants, against chance decoding (33.3%), separately for each ROI. Statistical results

were corrected for multiple comparisons (number of ROIs x number of tests) using the false discovery rate (FDR) method (Benjamini and Yekutieli, 2001). An analogous ROI-based MVP analysis was also performed between stimulus exemplars (for additional information, see *Appendix, Supplementary materials: chapter 2*). To examine which additional areas potentially represent imagined and perceived stimulus categories, we performed a whole brain searchlight-based MVP analysis (Kriegeskorte et al. 2006; Oosterhof et al., 2016). Decoding procedures were very similar to the ROI-based MVPA, except that the spherical searchlight (~100 voxels per sphere) approach was applied to each voxel in the brain. Decoding accuracies from each searchlight were assigned to the central voxel. To identify voxels where classification accuracy was greater than chance (33.3%), we performed a one-tailed one-sample t-test across individual cortical maps, separately for the imagery condition, the perception condition, and cross-condition decoding. Statistical *t* maps were corrected for multiple comparisons using the FDR method (Benjamini and Yekutieli, 2001). For visualization purposes, we projected group maps on a segmented and inflated MNI aligned brain (Colin Holmes' 27-scan average brain image, as implemented in NeuroElf, v 1.1) in BrainVoyager QX 2.8.0 (BrainInnovation), separately for the perception, imagery and cross-decoding condition. Brain areas were labeled by means of the Juelich Histological Atlas, as implemented in FSL 5.1.

Correlation between the blood oxygenation level dependent (BOLD) signal and behavioral performance. In order to understand the contribution of different brain areas to behavioral performance during visual imagery, we explored the relation between the amplitude of the BOLD signal and accuracy in the imagery task, as well as the relation between the amplitude of the BOLD signal and individual vividness ratings. To this aim, we selected four ROIs as revealed by the uni- and/or multivariate analyses, namely, primary visual cortex (V1), superior parietal lobe (SPL), anterior intra-parietal sulcus (aIPS) and lateral occipital complex (LOC). With respect to V1, we used the same ROIs defined for the MVPA analysis (see *ROI definition* for more details). For SPL and aIPS, ROIs were defined based on the univariate contrast imagery>baseline (see *Univariate RFX-GLM analysis* for more details). Instead, LOC was defined based on the group accuracy map resulting from the MVPA searchlight-based analysis on the imagery condition (see *Multivariate pattern classification (MVP) analysis* for more details). For all the considered regions, we extracted the average BOLD

amplitude expressed as % BOLD signal change during the imagery delay (relatively to baseline) using the Featquery tool in FSL 5.1. We then computed the linear correlation (Pearson correlation coefficient) between the average activation extracted from the 4 ROIs and 2 behavioral indices: the accuracy in the imagery condition, expressed as the percentage of correct answers, and individual ability to generate vivid mental images as assessed by the VVIQ questionnaire. The VVIQ score is expressed as average between the score of visual imagery performed with eyes open and eyes closed, as done in previous studies (Amedi et al., 2005). The analysis was performed using SPSS 20.

Low-level features differences between stimulus categories. To understand whether the stimulus categories we employed for the current study (i.e. lowercase letters, objects and simple shapes) differed with respect to low-level visual features, we computed image statistics for each stimulus exemplar. To this aim, we employed the GIST descriptor toolbox (Oliva & Torralba, 2001; http://people.csail.mit.edu/torralba/code/spatialenvelope/). The image of each stimulus exemplar was passed through a series of Gabor filters across 8 orientations and 4 spatial frequencies, resulting in 6 vectors of 512 values representing the spatial frequencies and orientations present at different positions across the image of each individual stimulus. To obtain a measure of low-level features representing each stimulus category, we averaged GIST descriptors across all images within each category. The group descriptors were windowed on a 4x4 grid for representation purposes. We then computed the square Euclidean distance between the amount of low-level features of each stimulus category and the remaining two using the following formula:

$$D = sum((gist1 - gist2).\hat{}2)$$

Where *gist1* is the GIST descriptor of the first category and *gist2* the GIST descriptor for the second category.

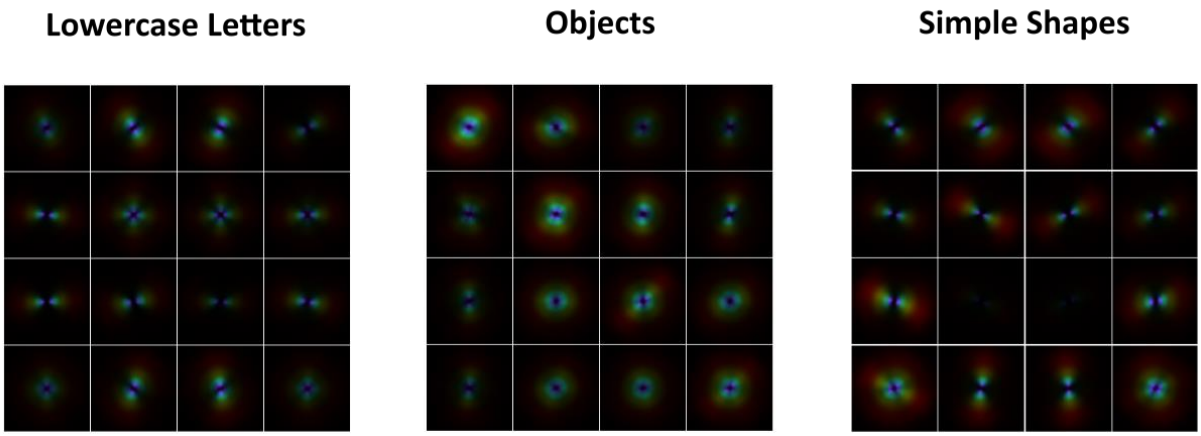

Figure 2.8. Average image properties for each stimulus category. Average GIST descriptors representing low-level features were computed averaging single-stimulus GIST images (for more details see Material and Methods). Results are presented on a 4x4 grid for visualization purposes.

2.5 Results

2.5.1 Behavioral results

Accuracy in the behavioral task was computed individually for each participant as percentage of correct answers (i.e. correct spatial localization of a Match dot as positioned on the imagined/perceived stimulus; correct spatial localization of a No Match dot as positioned outside the imagined/perceived stimulus), separately for the perception and imagery conditions. Since we instructed participants to favor accuracy over speed in the completion of the task, reaction times were not included in this analysis.

Figure 2.9 shows the accuracy in the spatial judgement task as a function of condition (imagery, perception) and stimulus category (lowercase letters, objects, simple shapes). Not surprisingly, we found a higher accuracy in the spatial judgement task for the perception condition [mean: 69,71% ± 18.6%] in comparison to the imagery condition [mean: 63.55% ± 13.4%] in all three categories.

These observations are supported by the corresponding statistics, using a repeated measures ANOVA with the factors task and stimulus categories. Accuracy differed between the two tasks [main effect of task [$F(1, 20) = 39.48$, $p<0.001$] and between stimulus categories [main effect of stimulus category: $F(2, 40) = 12.14$, $p<0.001$]. As also seen in *Figure 2.9* the effect of stimulus category on accuracy interacted with the task [interaction stimulus category*task, $F(2, 40) = 10.57$, $p<0.001$], which is likely due to the fact that accuracy for imagery of lower case letters was lower than for imagery of objects and simple shapes.

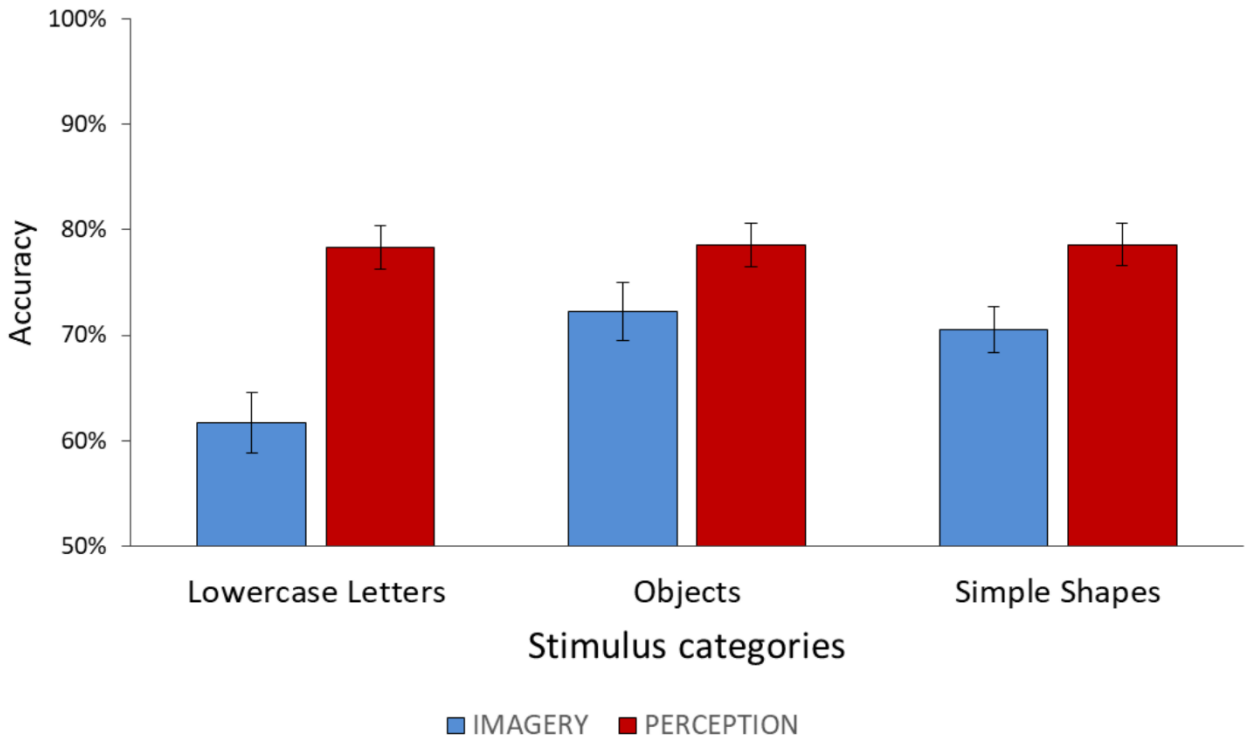

Figure 2.9. Mean accuracy (N=21) in the spatial judgement task during the imagery and perception condition as a function of stimulus category. Error bars: standard error of the mean (S.E.M.).

2.5.2 Univariate Analysis

Perception condition. As can be seen in *Figure 2.10* showing the RFX GLM contrast [perception > baseline], the perception condition led to a widespread recruitment of striate and extrastriate visual areas. In addition to left and right primary visual cortex (V1), we found bilateral recruitment of areas V2, V3, V4 and V5. Moreover, we also found a bilateral recruitment of the lateral occipital complex (LO), known to be involved in the processing of shape and objects (Kourtzi and Kanwisher, 2000; Grill-Spector et al., 2001).

Additionally, this contrast recruited a network of parietal (bilateral superior parietal lobule (SPL), left and right aIPS, bilateral primary somatosensory cortex (S1) and frontal (left dorsal (PMd) and ventral premotor cortex (PMv) regions (for a summary of cluster coordinates see *Appendix, Supplementary material: Chapter 2*).

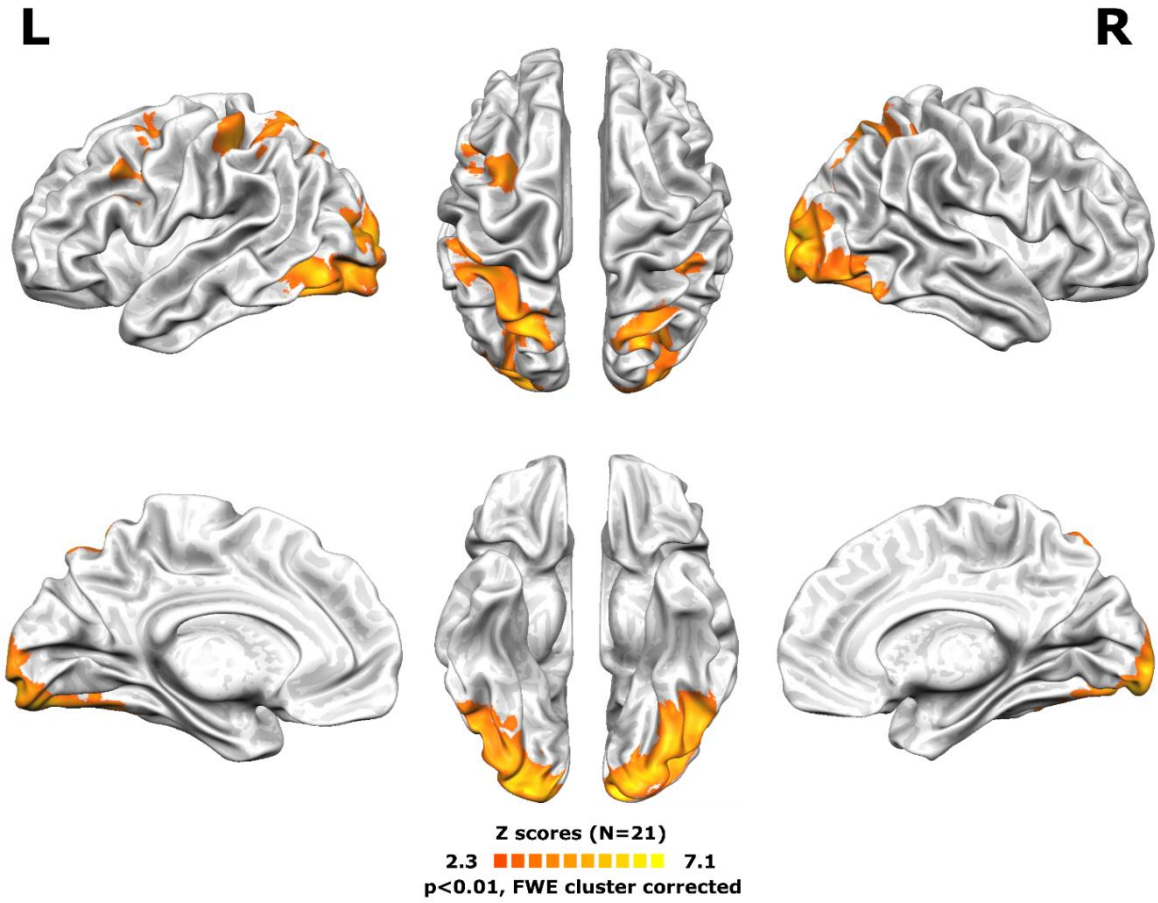

Figure 2.10. Results of the univariate RFX GLM contrast (N = 21 participants) perception > baseline. The group statistical map was FWE cluster-corrected using GRF theory and projected on an inflated surface mesh.

Imagery condition. *Figure 2.11* shows the RFX GLM contrast [imagery > baseline]. We found a selective recruitment of the left hemisphere, involving the superior parietal lobe (SPL), the aIPS, the left primary somatosensory cortex (S1) and the PMd (for a summary of cluster coordinates see *Appendix, Supplementary material: Chapter 2*).

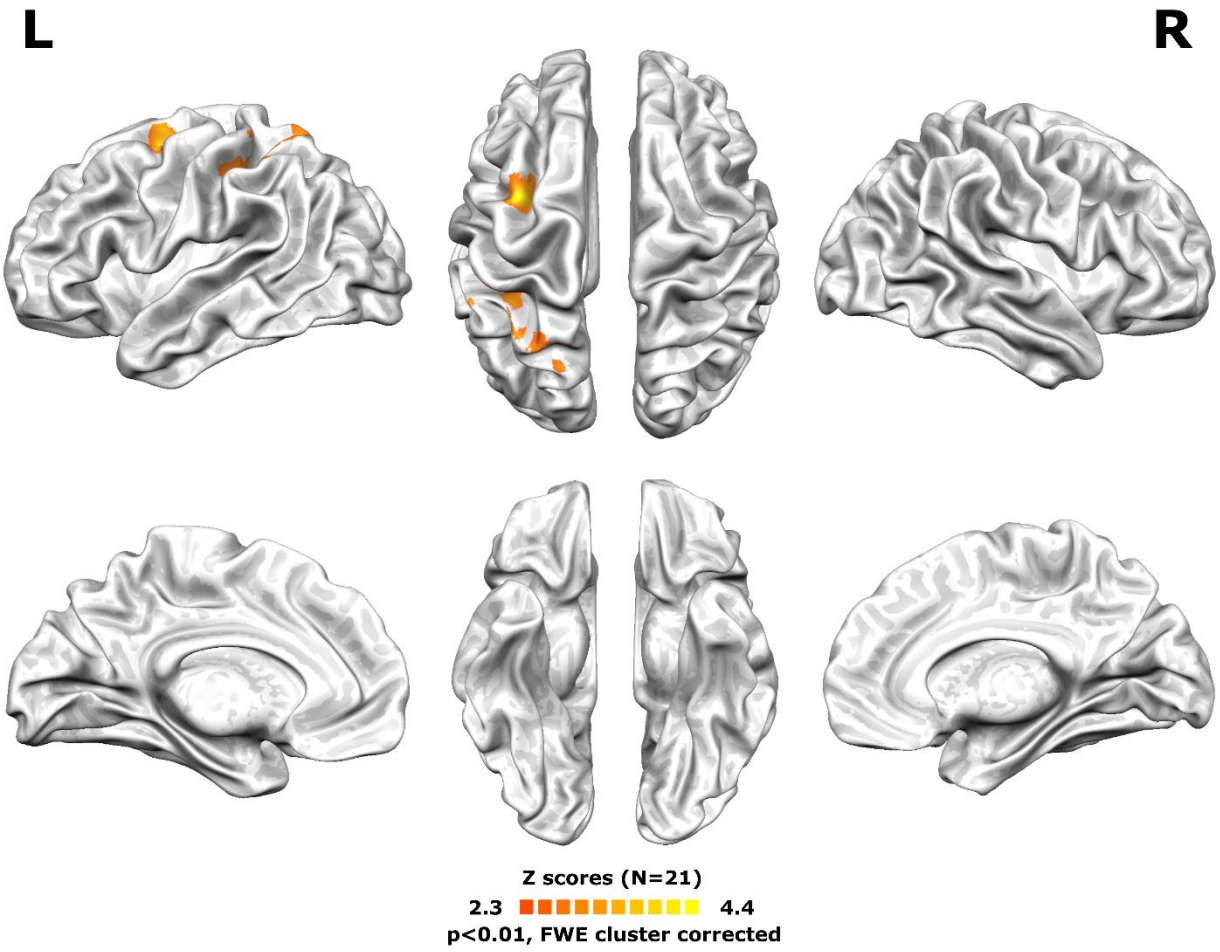

Figure 2.11. Results of the univariate RFX GLM contrast (N = 21 participants) imagery > baseline. The group statistical map was FWE cluster-corrected using GRF theory and projected on an inflated surface mesh.

Univariate differences in activation between categories. The analysis of differences in univariate recruitment between imagined stimulus categories (see *Figure 2.12*) revealed significant differences between Lowercase Letters and Objects. In particular, Lowercase Letters induced higher recruitment of small clusters of bilateral V1, V2, higher level visual areas (right LOC) and a portion of left inferior temporal cortex that might be close to the visual word form area (VWFA, Yeatman et al., 2013). We also found higher recruitment of the right SPL, bilateral S1 and bilateral PMd. Univariate activation between Lowercase Letters and Simple Shapes, and between Simple Shapes and Object did not revealed any significant differences (for a summary of cluster coordinates see *Appendix, Supplementary material: Chapter 2*).

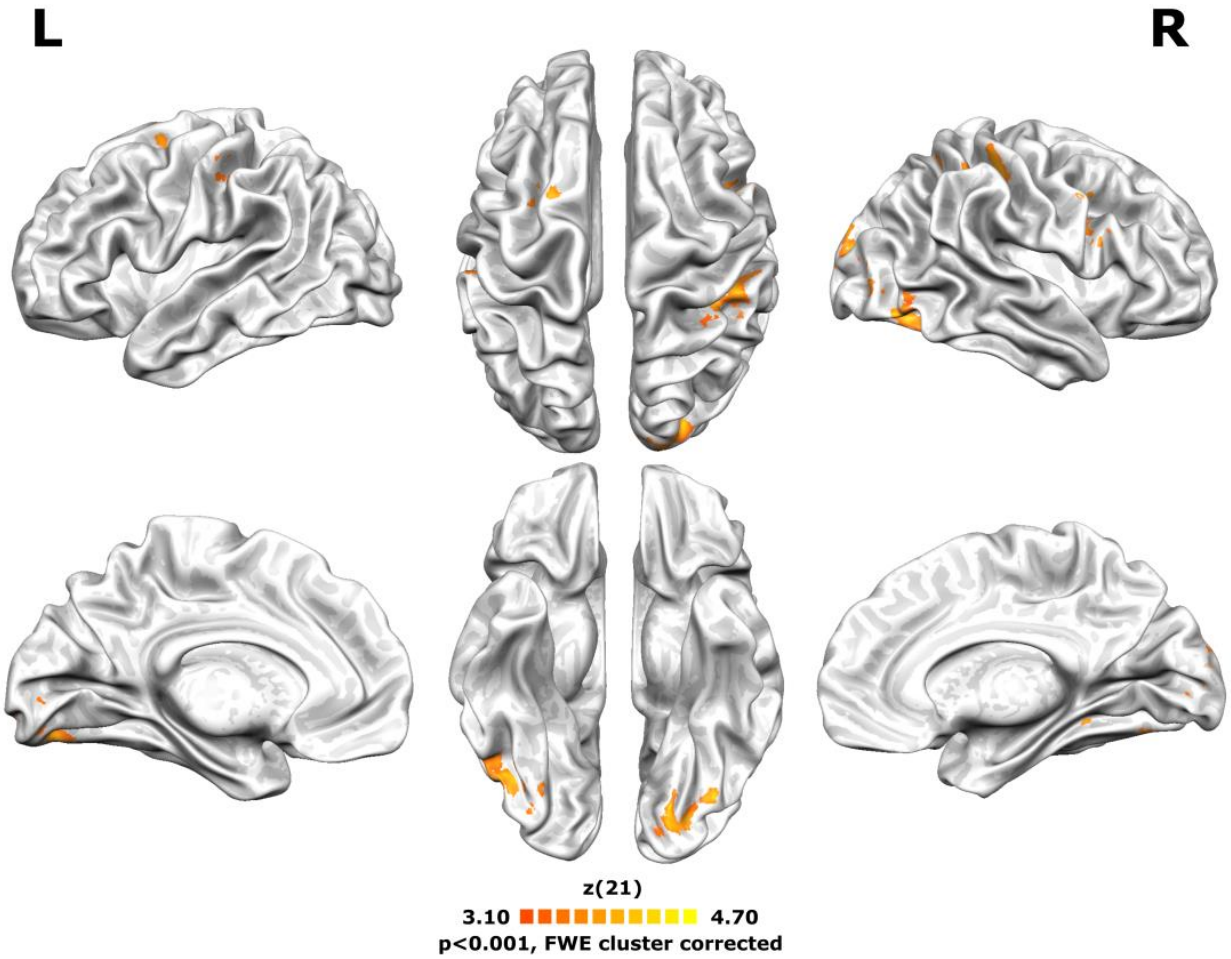

Figure 2.12. Results of the univariate RFX GLM contrast (N = 21 participants) lowercase letters > objects for the imagery condition. Differences in univariate activation were found in lower-level visual areas (V1 and V2), higher-level visual areas (right LOC, WVFA) and parietal (left SPL) areas. The group activation map was FWE cluster-corrected using GRF theory and projected on an inflated surface mesh.

2.5.3 Multivariate pattern analysis

ROI-based MVP analysis. In the ROI-based MVPA, we tested whether the three stimulus categories could be decoded on the basis of patterns of brain activity obtained during perception and visual imagery of the same stimuli. We found significant above chance classification accuracy for perceived stimulus categories in both V1 (mean accuracy: 49.52% ± 12.8%; two-tailed one-sample *t* test: $t_{(20)}$= 5.780, p<0.001) and in V2 (mean accuracy: 52.38% ± 12.8%; two-tailed one-sample *t* test: $t_{(20)}$= 6.827, p<0.001). Within the same ROIs, we were also able to decode the imagined stimulus categories (V1: mean accuracy 38.41% ± 9.7%; two-tailed one-sample *t* test: $t_{(20)}$= 2.401, p=0.026. V2: mean accuracy 40% ± 9.2%; two-tailed one-sample *t* test: $t_{(20)}$= 3.325, p=0.003). In the control region, i.e. ventral bilateral striatum, classification accuracy was at chance both in the perception condition (mean accuracy 34.1% ± 11%; two-tailed one-sample *t* test: $t_{(20)}$= 0.331, p=0.74) and in the imagery condition (mean accuracy 32.7% ± 9.8%; two-tailed one-sample *t* test: $t_{(20)}$= -0.298, p=0.76) (see *Figure 2.13*).

Cross-condition MVPA. In the cross-condition MVPA, we aimed to investigate the similarity between the representation of imagined and perceived stimuli in early visual areas. In particular, we examined whether it is possible to train a classifier to successfully distinguish between the three stimulus categories based on the patterns of activation elicited by visual stimuli (perception condition), and then test the classifier on patterns of activation elicited by visual imagery (imagery condition) of the same stimuli (and vice versa). As can be seen in *Figure 2.13*, the results indicate above chance cross-classification accuracy in V1 (mean accuracy 36.27% ± 4.7%; two-tailed one-sample *t* test: $t_{(20)}$= 2.893, p=0.009), but not in V2 (mean accuracy 35.63% ± 5.6%; two-tailed one-sample *t* test: $t_{(20)}$= 1.895, p=0.07). Classification accuracy did not reach significance in the ventral bilateral striatum (mean accuracy 35.48% ± 6.5%; two-tailed one-sample *t* test: $t_{(20)}$= 1.516, p=0.14).

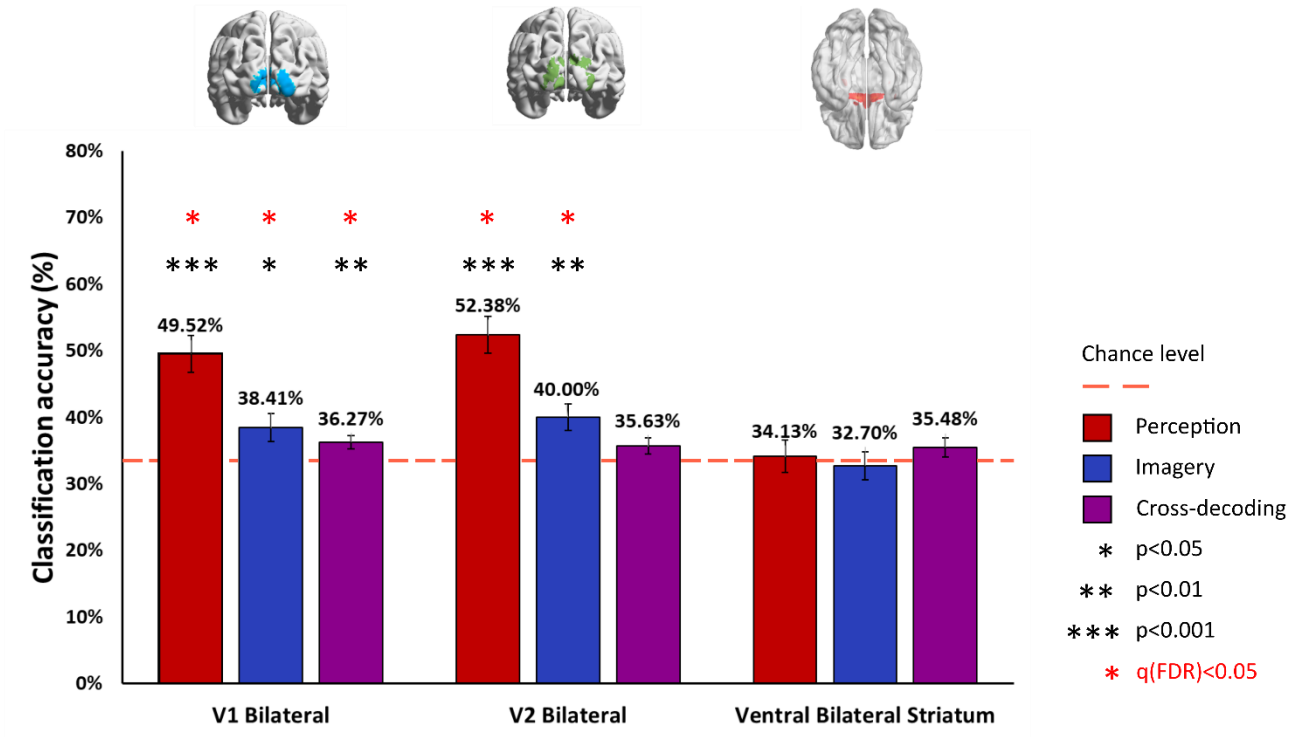

Figure 2.13. Results of the ROI-based MVP analysis. Mean decoding accuracy as a function of stimulus category, separately for V1, V2, and a control ROI (ventral bilateral striatum). Blue bars, perception condition. Red bars, imagery condition. Purple bars, cross-decoding condition. Statistical significance was assessed by means of a one-sample t-test against chance (33.3%). Results were corrected for multiple comparisons using a false discovery rate (FDR) < 0.05. Significance levels: one black asterisk, p<0.05; two black asterisks, p<0.01; three black asterisks, p<0.001; one red asterisk, q(FDR)<0.05. Error bars: standard error of the mean (S.E.M.).

2.5.4 Searchlight-based MVPA

Perception condition. To identify additional areas that can distinguish between the three stimulus categories, we performed a whole-brain searchlight-based MVPA. *Figure 2.14* shows the group *t* map for the decoding of stimulus categories in the perception condition. As can be seen, this analysis revealed significant decoding in early visual areas (V1, V2, V3, V4 and V5 bilaterally), in the left and right lateral occipital complex (L-LOC), and in the left S1. Moreover, we also obtained significant above-chance classification accuracy in the superior (SPL) and inferior (IPL) parietal lobule bilaterally, and in the left aIPS (for a summary of cluster coordinates see *Appendix, Supplementary material: Chapter 2*).

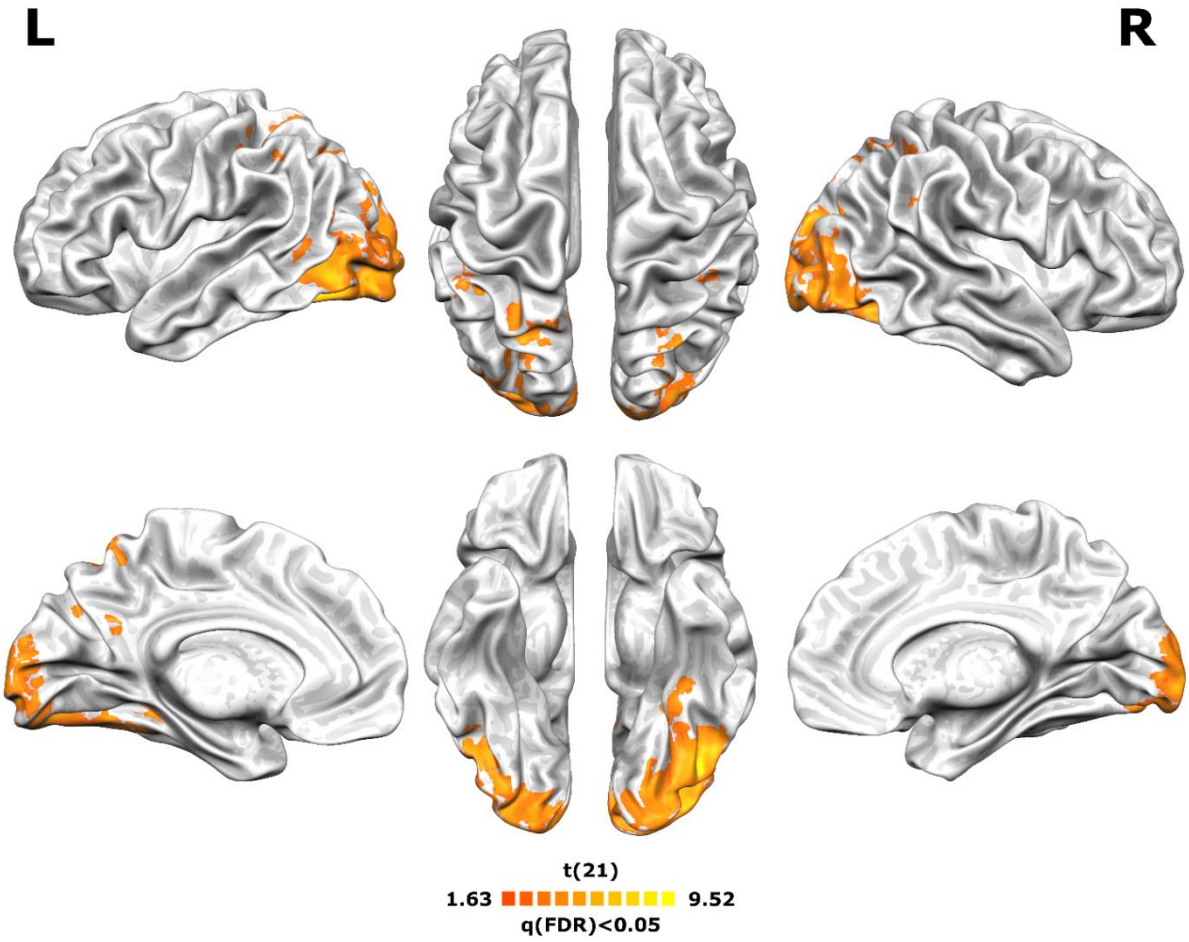

Figure 2.14. Results of the searchlight-based MVPA for the perception condition (see methods for details). The spherical searchlight comprised 100 voxels. The group t map was corrected for multiple comparisons using a q(FDR)<0.05 and projected on an inflated surface.

Imagery condition. *Figure 2.15* illustrates the group *t* map for the searchlight-based MVPA of the imagery condition. We found significant clusters in early visual areas (left V1 and bilateral V2), in the left and right LOC, SPL, aIPS, and left IPL. Moreover, we also found significant above chance classification accuracy in S1 in both hemispheres and in the left PMd. LOC coordinates are within the range of those indicated in previous studies (Grill-Spector et al., 1999; 2001; Pourtois et al., 2009; for a summary of cluster coordinates see *Appendix, Supplementary material: Chapter 2*).

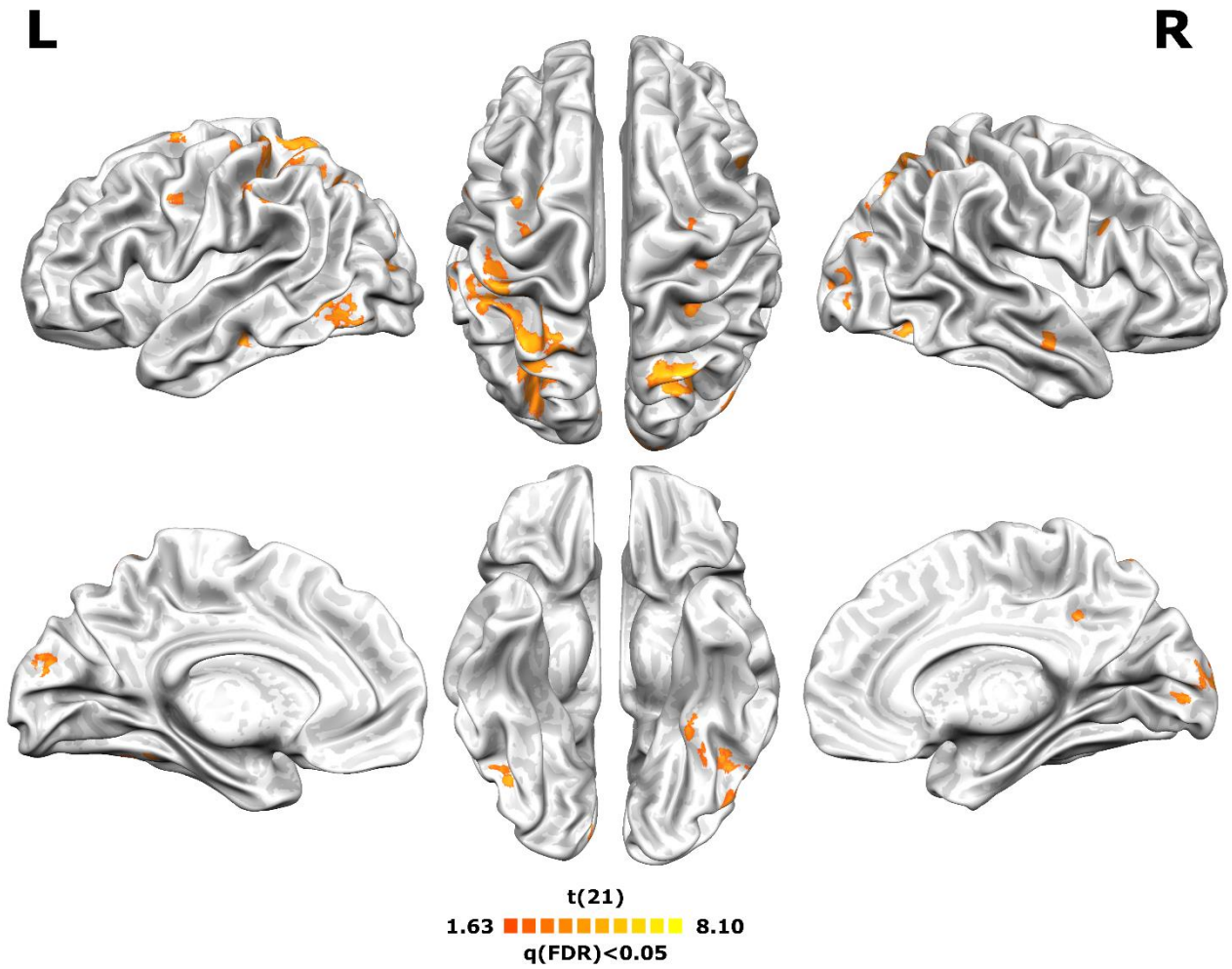

Figure 2.15. Results of the searchlight-based MVPA for the imagery condition (see text for details). The spherical searchlight comprised 100 voxels. The group t map was corrected for multiple comparisons using a q(FDR)<0.05 and projected on an inflated surface.

Cross-decoding. *Figure 2.16* illustrates the group *t* map for the cross-condition decoding. Significant clusters were found in right V2, left LOC, left IPS, left aIPS, bilateral SPL and left S1 (for a summary of cluster coordinates see *Appendix, Supplementary material: Chapter 2*).

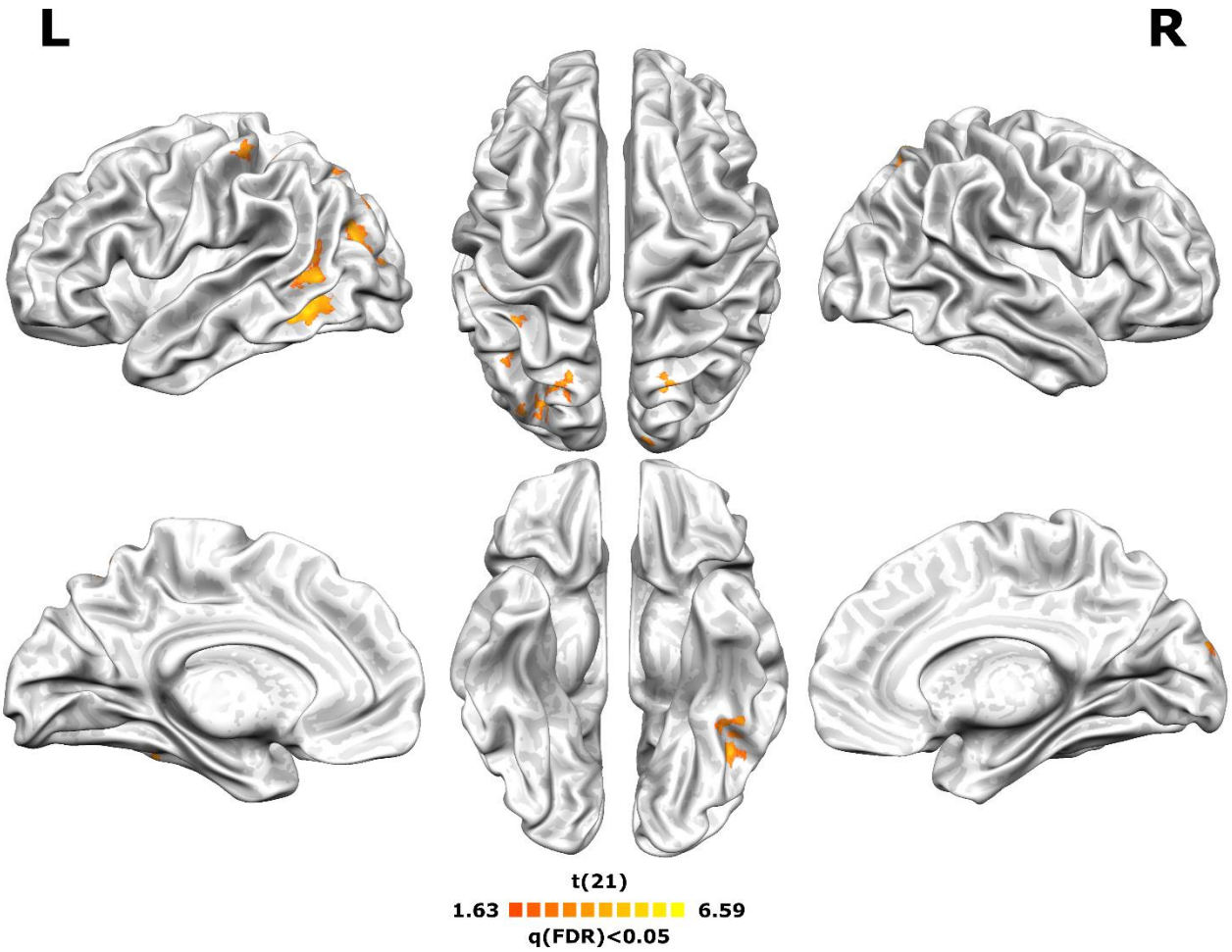

Figure 2.16. Results of the searchlight-based MVPA for cross-condition decoding. The spherical searchlight comprised 100 voxels. The group t map was corrected for multiple comparisons using a q(FDR)<0.05 and projected on an inflated surface.

2.5.5 Low-level features differences between stimulus categories.

Table 2.1 reports distances in low-level features between each stimulus category. Lowercase Letters and Simple Shapes seems to be the most similar stimulus categories (Lowercase Letters vs. Simple Shapes: D = 0.4061), whereas stimuli pertaining to Objects differs from both Lowercase Letters (Object vs. Lowercase Letters: D = 0.6177) and Simple Shapes (Object vs. Simple Shapes: D = 0.5743).

	Spatial Frequency Distance (D)
Lowercase Letters vs. Objects	0.6177
Lowercase Letters vs. Simple Shapes	0.4061
Objects vs. Simple Shapes	0.5743

Table 2.1. Spatial frequency distance between stimulus categories. Table summarizing the distance in spatial frequencies between lowercase letters, objects and simple shapes (see Material and Methods). As can be seen, objects seems to be the stimulus category differing the most from the others in terms of low-level features.

2.5.6 Correlation between BOLD activity and behavioral measures

We obtained a moderate positive correlation between the amplitude of the BOLD and accuracy in the imagery condition in the SPL (r=0.619, p=0.003) and in the aIPS (r=-0.595, p=0.004; *Figure 2.17*, left column). By contrast, we obtained no systematic relationship between the amplitude of the BOLD signal and behavioral performance in primary visual cortex (r=0.171, p=0.459) or LOC (r=0.357, p=0.113).

Regarding the correlation between cortical activity during the imagery condition, expressed as % of BOLD signal change, and the subjective vividness ratings for visual mental imagery, the analysis performed did not highlight any significant correlation in the considered ROIs (V1, r=0.384, p=0.085; SPL, r=-0.49, p=0.832; r=-0.72, p=0.758; aIPS, r=-0.72, p=0.758; LOC, r=0.04, p=0.863; *Figure 2.17*, right column).

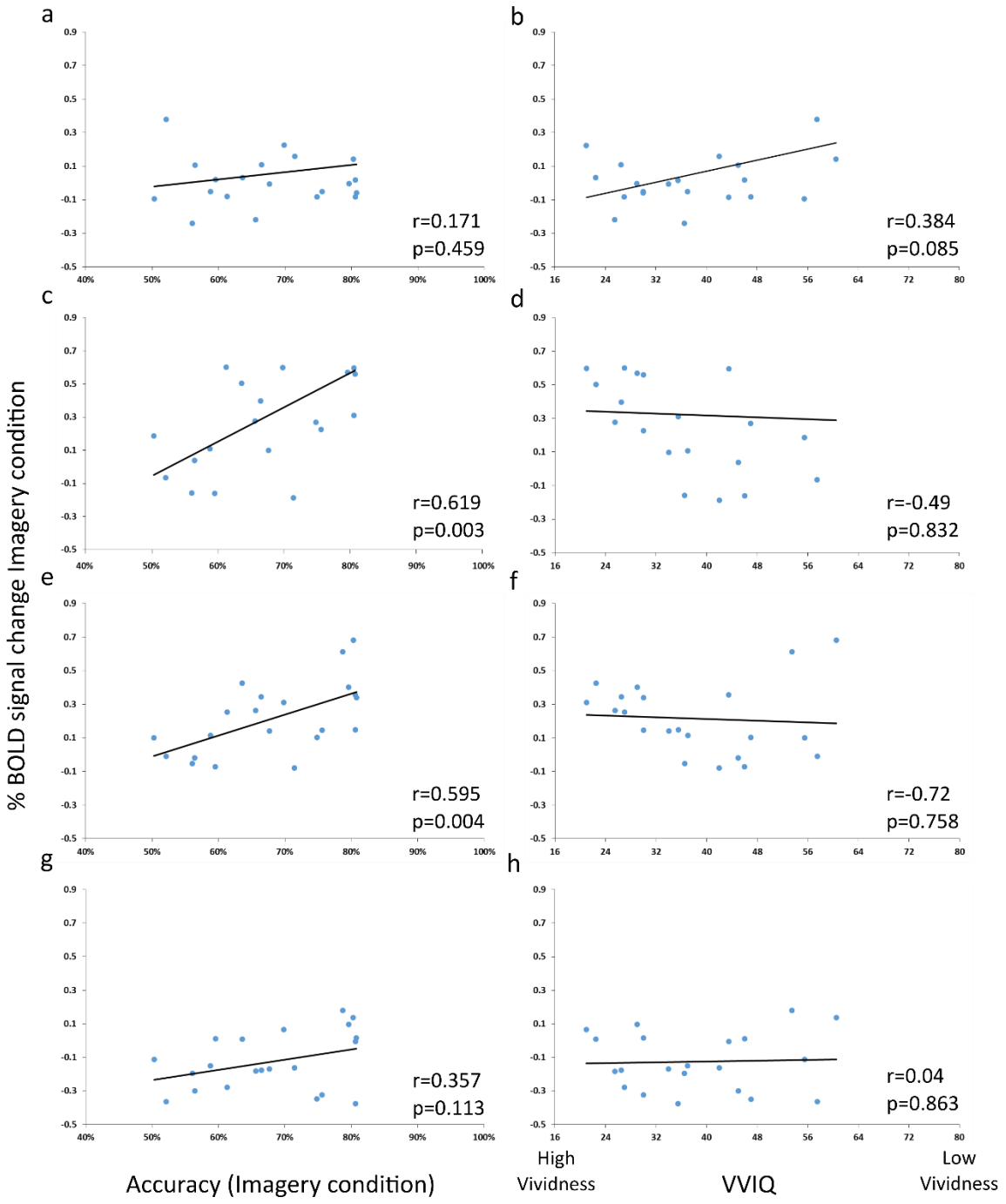

Figure 2.17. Correlation between amplitude of the BOLD signal and behavioral measures. Correlation between mean activation in V1 expressed as % of BOLD signal change and accuracy during the imagery condition (a), and vividness of mental imagery as assessed by the VVIQ (b). The same analysis was repeated for mean activation in SPL (c, d), aIPS (e, f) and LOC (g, h).

2.6 Discussion

To explore whether complex stimulus categories can be encoded in early visual cortex during visual mental imagery, we used a multivariate pattern analysis approach. We found that neural activity patterns in early visual (V1, V2), parietal (SPL, IPL and aIPS), infero-temporal (LOC) and prefrontal (PMd) areas could reliably predict which of the three stimulus categories was imagined by our participants. Moreover, in parietal and infero-temporal regions, we found shared representation across visual mental imagery and visual perception of the same stimuli. In the following, we will discuss these results in more detail.

2.6.1 The role of early visual cortex during visual imagery

In the absence of a reliable univariate recruitment of early visual cortex, we were able to decode the imagined stimulus category on the basis of patterns of activation in V1 and V2. The absence of a reliable recruitment of early visual cortex during visual imagery is in line with emerging literature suggesting a high variability in the univariate recruitment of V1 (e.g. Ishai et al., 2000; Formisano et al., 2002; Yomogida et al., 2004).

Our decoding results in early visual cortex are in line with the results of Albers et al. (2013), who demonstrated decoding of relatively simple stimuli (i.e. gratings with different orientations) in early visual cortex (V1 to V4). By contrast, other studies using letters (Stokes et al., 2009) and different common object categories (Reddy et al., 2010; Cichy et al., 2011; Lee et al., 2012) found a representation of complex stimuli in extrastriate visual areas and category selective inferotemporal cortices (PPA, FFA, LOC, EBA) but not in V1. Together, these results suggest that the degree to which it is possible to decode the content of imagined stimuli in early visual cortex might depend on the type of stimulus and/or the task, with a preference for low level stimuli such as the ones used by Albers et al. (2013) and the ones used in the current study.

We suggest that, in the absence of bottom-up visual stimulation, early visual cortex receives information about imagined stimulus categories from frontal and parietal brain regions via top-down feedback, at least for relatively simple stimulus categories such as gratings, letters, simple shapes, and simple objects. In line with this view, Vetter et al. (2014) were able to decode the identity of real and imagined sounds from patterns

of activity in V1, which is likely to have been mediated by top-down feedback from multisensory brain areas such as pSTS and the precuneus. One possible alternative explanation is that what the machine learning classifier is decoding is not higher-level categorical information pertaining to the adopted experimental stimuli, but information about low-level features or orientation differing from category to category. In fact, our analysis of low-level features between stimulus categories (see *Material and Methods*) clearly indicated the presence of moderate differences between lowercase letters, objects and simple shapes. If this alternative explanation was true, we would expect to find significant decoding only in low-level visual areas (i.e. V1 and V2) which contain neurons selectively tuned to respond to orientations and spatial frequencies (Hubel, 1995). The presence of a significant above chance decoding accuracy in category selective visual areas (i.e. LOC), however, indicates that higher-level categorical information are also reactivated during visual mental imagery. It is thus likely to hypothesize that early visual cortex, along with low-level features differences between different stimulus categories, could also represent higher-level information coming from other nodes of the visual imagery network. Further research is required to determine the degree of complexity of stimuli that can be represented in early visual cortex during imagery.

2.6.2 The role of parietal and premotor cortex during visual imagery

We found a univariate recruitment of parietal (SPL, aIPS) and premotor (PMd) cortex. Likewise, we were able to decode imagined stimulus category in SPL, IPL, S1, and PMd.

The recruitment of parietal regions during visual mental imagery is in line with previous studies (Knauff et al., 2000; Formisano et al., 2002; Ganis et al., 2004). In both regions, we found a positive correlation between neural activity and behavioral performance, suggesting a critical role of both regions in participants' ability to discriminate the position of a dot with respect to an imagined stimulus.

Recent studies showed parietal regions (i.e. SPL and aIPS) to be involved during mental imagery of different hand actions (Oosterhof et al., 2012) and during the encoding of the identity of artificial stimuli during visual working memory (Christophel et al., 2012; 2014). Premotor cortex can host distinct representations of both

identity and spatial position of stimuli in a visual working memory task during the retention delay (Naughtin et al., 2014).

Previous studies examining the differential patterns of connectivity between perception of real stimuli and visual mental imagery found a reversed flow of information between these two cognitive processes. In particular, they highlighted how information can be transmitted from prefrontal (Mechelli et al., 2004; Dijkstra et al., 2017) and parietal (Dentico et al., 2014) to occipital nodes of the visual imagery network. These findings suggest that the same top-down mechanism might underlie the results of the current study as well.

2.6.3 The role of the LOC in visual imagery

In the absence of a univariate recruitment, we were able to decode the imagined stimulus category in the LOC, a brain area known to be involved in object recognition (Grill-Spector et al., 2001). Its involvement in visual mental imagery of different object categories has been reported in previous studies (Stokes et al., 2009; Cichy et al., 2011; Lee et al., 2012).

2.6.4 Shared neural representation for imagined and perceived stimuli

Our ROI and searchlight based MVPA revealed shared representations for imagery and perception in bilateral V1, in a portion of the right V2, and in bilateral LOC. These observations are in line with the results by Albers et al. (2013), demonstrating cross-decoding for imagery and perception in V1. Likewise, several studies revealed shared representations for imagery and perception in high-level visual areas (including LOC) (Stokes et al., 2009; Reddy et al., 2010; Lee et al., 2012).

Moreover, we found shared representations for imagined and perceived stimuli in a network of parietal areas, comprising bilateral SPL, left aIPS and left IPL, known to play a role in tasks with a strong spatial component (Mellet et al., 1996; Trojano et al., 2000; Sack et al., 2002). We hypothesize that the shared representations for imagery and perception observed in the current study are due to the fact that the task required participants to judge the position of the cue with respect to a visible stimulus or with respect to a

stimulus that had to be imagined, forcing them to process the spatial configuration of the perceived and imagined stimulus. It is likely that different tasks requiring judgment of different aspects of the stimulus, such as its shape or its weight or size in the real world, will reveal a different set of areas in comparison to those found in the current study.

Together, our results are in line with the existence of two distinct pathways engaged during visual mental imagery (Sack et al., 2012). In analogy with perception, a ventral occipito-temporal imagery network, involving category-selective regions in inferior temporal cortex, is assumed to represent the content of mental images; whereas the dorsal spatial network, encompassing parietal and premotor cortices, are involved in the encoding of the spatial configuration of imagined stimuli. Information from these two pathways are assumed to be integrated by frontal regions, allowing the creation of a coherent mental representation during visual mental imagery (Sack et al., 2012). In the absence of a reliable recruitment of frontal regions or the decoding of stimulus categories in frontal regions, the current study did not provide any support of this latter point.

2.6.5 Conclusions

In line with previous studies (Sack et al., 2012), our results provide evidence for distinct roles of parietal, premotor, and temporal regions during visual imagery, with parietal and premotor regions processing the spatial layout of imagined stimuli, and temporal regions decoding the content of imagined stimulus categories. We hypothesize that, in the absence of bottom-up information, early visual cortex has access to both types of information via feedback connections.

In the previous chapter, we investigated the representational content of different brain areas constituting the visual imagery network during the internal generation of mental representations. Participants were tested in a delayed spatial-judgment task, and asked to imagine stimuli pertaining to three possible categories (i.e. lowercase letters, simple shapes and objects). Using a combination of ROI-based and searchlight-based MVPA analyses, we found significant encoding for imagined categories in parietal and premotor cortices, responsible for processing the spatial layout of mental images and temporal regions, processing the content of imagined stimuli. Moreover, the same categorical information about imagined stimuli was decoded from patterns of activity in early visual cortices, indicating a potential role of low-level visual areas in processing more abstract information during visual mental imagery.

In the second part of this thesis, we are going to explore the possibility to exploit the top-down modulation occurring during visual mental imagery to recruit specific portions of early visual cortex. By testing both normal-sighted participants and patients suffering from homonymous hemianopia, we aim to assess the feasibility of this approach in modulating the activity on low-level visual areas. If this is revealed to be true, it would be possible to hypothesize the creation of rehabilitative paradigms based on visual mental imagery. In fact, by top-down recruiting silenced but preserved portions of early visual cortices in patients suffering from homonymous hemianopia, it would be possible to induce plastic mechanisms of change in the damaged brain, with the hope to reinstate perceptual awareness.

Chapter 3.

Quadrant-selective top-down modulation during visual mental imagery

Flavio Ragni[1], Caterina Pedersini[3], Carlo Marzi[3], Nivedita Agarwal[1,2] and Angelika Lingnau[1,4*]

[1]Center for Mind/Brain Science (CIMeC), University of Trento, 38068 Rovereto (TN), Italy

[2]Department of Neurology, Santa Maria del Carmine Hospital, 38068 Rovereto (TN), Italy

[3]Department of Neuroscience, Biomedicine and Movement, University of Verona, 37134 Verona (VR), Italy

[4]Deparment of Psychology, Royal Holloway University of London, TW20 0EX, Egham (London) UK

3.1 Abstract

Following lesions affecting retrochiasmatic visual pathways, one of the most common deficits is homonymous hemianopia. This visual impairment is characterized by the loss of sight in one half of the visual field and has a profound impact on patient's emotional and social wellbeing. The low chances of spontaneous recovery in this clinical population makes research and development of rehabilitation techniques of crucial importance. Visual mental imagery refers to the ability to generate internal representations of external objects in the absence of perceptual stimulation. In normal sighted individuals, visual imagery recruits a network of prefrontal, parietal and inferotemporal areas, and early visual cortex (EVC). Several studies indicated preserved visual imagery abilities in hemianopic patients, both in the sighted and damaged hemifield. In the present study, we aimed to examine whether it is possible to recruit individual portions of early visual cortex by means of visual mental imagery both in normal sighted participants and in hemianopic patients. To this aim, we tested a group of N=11 normal sighted participants and N=5 hemianopic patients, and measured their selective recruitment of different portions of EVC during visual imagery in different quadrants of the visual field. We found a spatial selective recruitment of EVC in normal sighted participants and in the healthy hemisphere of hemianopic patients. Our results provide evidence for the possibility to recruit individual portions of early visual cortex in normal sighted participants, exploiting the top-down modulation occurring during visual mental imagery. In our sample of hemianopic patients, the same top-down recruitment of low-level visual areas was limited to the quadrants pertaining to the sighted hemisphere. However, we found a substantial within-hemisphere variability in the recruitment of early visual cortex in hemianopic patients, which does not allow us to provide conclusive results with respect to the damaged hemisphere. Overall, our results confirm the possibility to modulate the activity of low-level visual areas by means of the top-down modulation originating in higher-level areas during visual imagery.

3.2 Introduction

Among the wide range of visual field defects, the most common is homonymous lateral hemianopia (Rowe et al., 2009). This deficit is characterized by the abolition of one half of the visual field, due to lesions affecting the optic chiasm or more posterior visual pathways, such as the optic trait, optic radiations or primary visual cortex (V1). The most common cause of homonymous hemianopia is arterial infarctions (70%), followed by tumors (15%), and hemorrhages (5%; Pambakian & Kennard, 1997). The inability to perceive stimuli in the blind portion of the visual field has a profound negative impact on patients' daily life activities, causing severe impairments in driving, reading, and navigating in the external environment. This, in turn, greatly increases the risk of incurring in domestic injuries, with significant repercussions on emotional and social wellbeing (Vu et al., 2004).

Visual mental imagery refers to the ability to visualize, inspect and manipulate a mental representation of a percept, in the absence of any visual stimulation from the external world (Kosslyn, 1994). In healthy individuals, visual mental imagery recruits a network of prefrontal, parietal and inferotemporal areas (Mechelli et al., 2004; Dijkstra et al., 2017; Winlove et al., 2018), as well as the primary visual cortex (Kosslyn, 1981; 2005). In light of its retinotopical organization, this area could serve as a substrate where mental images are reenacted, acquiring their resemblance with real objects (Kosslyn, 1994). Despite their visual impairment, hemianopic patients retain the ability to perform visual mental imagery, both in the sighted and in the damaged hemifield. As an example, Marzi et al. (2006) described the case of patient CA suffering from right homonymous hemianopia due to a lesion of the optic radiation, who reported to be able to perform visual mental imagery in the affected hemifield. Recent studies revealed that visual mental imagery recruits a similar network of extrastriate and parietal areas in hemianopic participants (Bridge et al., 2012), and maintains a similar pattern of spontaneous eye-movements as healthy individuals (Gbadamosi and Zangemeister, 2001). These results might suggest that, in spite of their visual field defect, patients suffering from homonymous hemianopia employ the same top-down strategies during the generation of a mental image of an external stimulus as normal sighted participants.

Here we aimed to assess whether the top-down modulation occurring during visual mental imagery could lead to a quadrant selective recruitment of early visual cortices, both in healthy individuals and hemianopic patients. If this were revealed to be true and visual mental imagery would prove to be effective in inducing a quadrant specific activation in low-level visual areas, we could hypothesize the development of rehabilitation techniques based on visual imagery training. In fact, following lesions affecting retrochiasmatic visual pathways a consistent portion of hemianopic patients presents functionally preserved but deafferentated portions of early visual cortex. The top-down re-activation of these silenced visual areas as a consequence of the lesion could lead to the induction of plastic mechanisms of recovery in hemianopic patients, with the hope of reinstating perceptual awareness.

To assess the feasibility of the top-down modulation occurring during visual imagery in inducing a quadrant selective recruitment of individual portions of early visual cortex, we ran a pilot fMRI study in N=11 normal sighted participants. In a second phase of the study, we then applied the same paradigm to N=5 hemianopic patients. Both groups were tested in a block design and asked to perform visual mental imagery in the four quadrants of the visual field. For each dorsal and ventral portion of EVC, we computed a spatial selectivity index, aimed at measuring their selective recruitment during our imagery task. We found a quadrant selective recruitment of EVC in healthy participants and in the healthy hemisphere, but not the affected hemisphere of hemianopic patients. Our results indicate that, when asked to imagine a small stimulus in one of the four quadrants of the visual field, healthy participants exhibit a spatially selective recruitment of primary visual cortex in the corresponding visual field location. Hemianopic patients exhibited an analogous spatial selective recruitment of EVC, which was limited to the upper and lower quadrants of the sighted hemifield.

3.3 Materials & Methods

3.3.1 Normal sighted participants

To establish whether our paradigm is suitable to induce and measure a selective recruitment of a specific portion of EVC by means of visual mental imagery, we conducted a pilot fMRI study in N = 11 normal-sighted participants (6 females, mean age 29.4) prior to testing hemianopic patients. All participants had normal or corrected-to-normal vision and had no history of neurological or psychiatric disease. Before taking part in the study, all participants gave their written informed consent. The study was approved by the Ethics Committee for research involving human participants at the University of Trento, Italy. Healthy participants were tested at the University of Trento (Italy) on a 4T scanner.

3.3.2 Hemianopic patients

Five hemianopic patients (1 female, mean age 53) with different post-chiasmatic lesions participated in the study (for details, see *Figure 3.1* and *Table 3.1*). All patients were diagnosed with hemianopia at least 3 months prior to the scanning session. Site and extent of the lesion were assessed by MRI structural scanning in the Department of Neurology of Santa Maria del Carmine (Rovereto, Italy) and Borgo Roma Hospital (Verona, Italy), whereas visual field defect was assessed by means of Humphrey's clinical campimetry (see *Figure 3.1*). Exclusion criteria were: pre-existing neurological or psychiatric disorders, history of drugs or alcohol abuse, presence of a general cognitive impairment as revealed by a score equal to or less than 24 on the Mini Mental State Examination (MMSE; Folstein et al., 1975), and presence of a spatial attention deficit (i.e. hemineglect). Recruitment took place in the Department of Neurology of Santa Maria del Carmine Hospital (Rovereto, Italy), and in the Department of Neuroscience, Biomedicine and Movement of the University of Verona (Verona, Italy). Patients recruited in the Department of Neuroscience, Biomedicine and Movement of the University of Verona were assessed for the presence of attentional impairments by means of a pen and paper neuropsychological battery, including: Diller letter H cancellation (Diller et al., 1974), Line Bisection (Schenkenberg et al., 1980) and Bell cancellation test (Gauthier et al., 1989). In order to assess the

impact of visual impairments on everyday life, patients were evaluated with the Visual Function Questionnaire (VFQ25; Mangione et al., 1960). Before taking part in the study, all participants gave their written informed consent. The study was approved by the Ethics Committee for research involving human participants at the University of Trento, Italy and by the Azienda Ospedaliera Universitaria Integrata (AOUI) of Verona, Italy.

N=2 patients (CG and PG in *Table 3.1*) recruited in the Department of Neurology of Santa Maria del Carmine Hospital (Rovereto, Italy) were tested at the University of Trento (Italy) on a 4T scanner. The remaining three were tested at the Department of Neuroscience, Biomedicine and Movement of the University of Verona (Verona, Italy), on a 1.5T scanner.

Details concerning age, sex, lesion site, scanner setup and visual field defects of patients are summarized in *Table 3.1*.

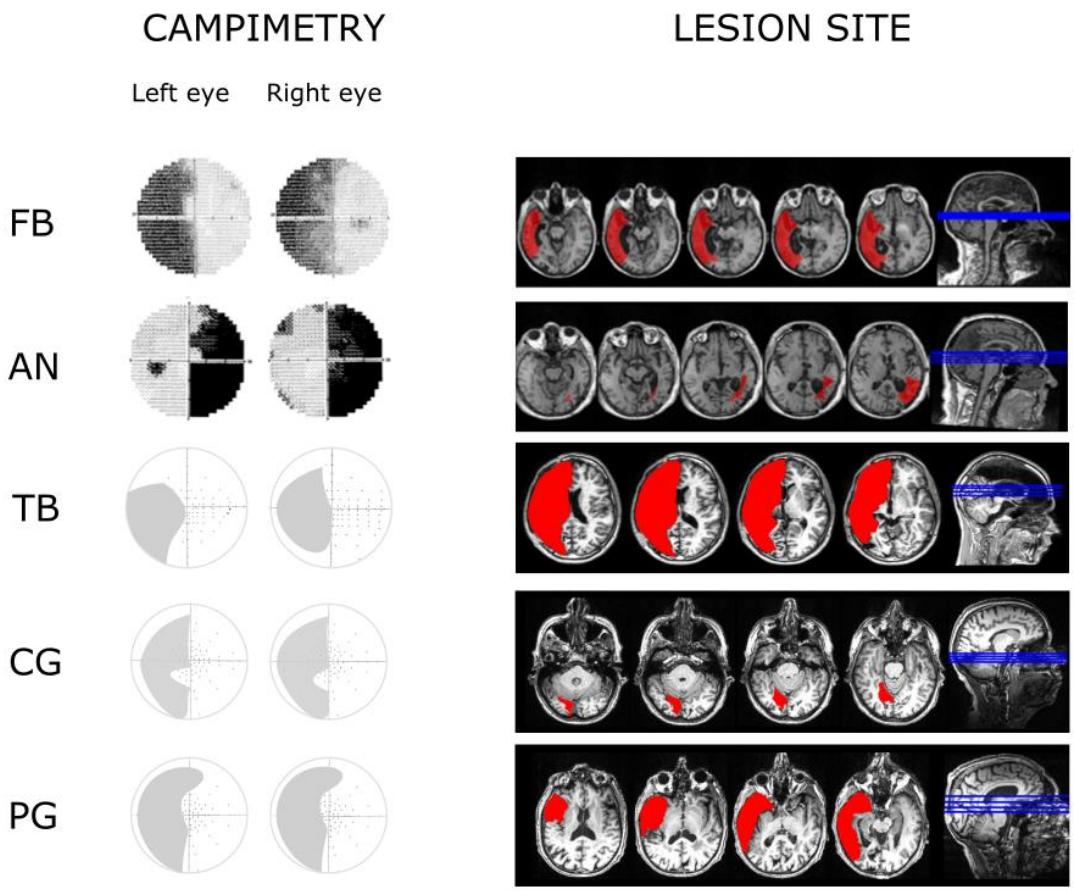

Figure 3.1. Patients' campimetry and lesion sites. For each patient, the output from Humphrey's clinical campimetry is reported (left), followed by MR T1 contrast images (right). Lesion site is highlighted in red.

Patient	Age	Gender	Lesion	Scanner	Visual field defect
FB	49	F	Extensive lesion mainly involving the right temporal and parietal lobes, with development of a poro-encephalic cavity in the temporal lobe and ex-vacuo dilatation of the right lateral ventricle. In the occipital lobe, the lesion involves the superior and part of the middle occipital gyri. Right optic radiation was interrupted. The other parts of occipital lobe are preserved.	1.5T	Left lateral homonymous hemianopia
AN	54	M	Lesion involving the left temporo-parietal lobe, with extension to the occipital lobe in the superior and middle occipital gyri. The alteration of the white matter in the occipital lobe suggests an involvement of the upper part of left optic radiation.	1.5T	Right lateral homonymous hemianopia
TB	22	M	Traumatic lesion involving the right cerebral hemisphere (dissection of the right carotid artery). In the occipital lobe, the lesion involves part of the right optic radiation and the ventral portion of primary visual cortex.	1.5T	Left lateral homonymous hemianopia
CG	69	F	Ischemic lesion involving the middle occipital gyrus in the right hemisphere.	4T	Left lateral homonymous hemianopia
PG	71	M	Ischemic lesion involving the right temporo-parietal lobe.	4T	Left lateral homonymous hemianopia

Table 3.1. Patients' clinical details. For each patient, age, gender and a brief description of the location and extent of the lesion are reported, followed by details about the type of scanner and visual field defect.

3.3.3 Setup

4T scanner. Visual stimuli were back-projected to a screen via a liquid crystal projector (OC EMP 7900, Epson Nagano, Japan; frame rate: 60 Hz; screen resolution: 1280x1024 pixels). Participants laid horizontally in the scanner in a conventional configuration and viewed the screen binocularly through a rectangular mirror (17.8°x13.4° of visual angle), positioned on the head coil. The auditory cue was delivered by means of MR-compatible headphones. Button presses were collected via an MR-compatible response button (Lumina LP 400, Cambridge Research Systems). Stimulus presentation, response collection, and synchronization with the scanner were controlled using "ASF" (Schwarzbach, 2011), based on MATLAB (MathWorks, Natick, MA, U.S.A.) and the Psychtoolbox-3 for Windows (Brainard, 1997).

1.5T scanner. Visual stimuli were displayed on a MR compatible monitor (Nordic Neuro Lab 32", NordicNeuroLab, Norway; frame rate: 60 Hz; screen resolution: 1920x1080 pixels). Participants laid horizontally in the scanner in a conventional configuration and viewed the screen binocularly through a mirror, positioned on the head coil. The auditory cue was delivered by means of MR-compatible headphones. Button presses were collected via an MR-compatible response button (NordicNeuroLab, Norway). Stimulus presentation, response collection, and synchronization with the scanner were controlled using "ASF" (Schwarzbach, 2011), based on MATLAB (MathWorks, Natick, MA, U.S.A.) and the Psychtoolbox-3 for Windows (Brainard, 1997).

3.3.4 Experimental design

To test whether it is possible to selectively recruit a specific portion of EVC by means of visual mental imagery, we employed a block design. To assess the feasibility of this approach, we first conducted a pilot test on normal sighted participants and then applied the same procedure to hemianopic patients. Both groups then took part in one single experimental session, consisting of a short familiarization with the task outside the scanner (~10 minutes), a structural scan (~5 minutes), and 5 functional runs (~9 minutes each). Each functional run started and ended with 12 seconds of rest and consisted of 20 trials.

Imagery condition. The imagery condition started with the presentation of a reference frame, composed of a central fixation cross and four gray squares, placed in the upper and lower portions of the screen - on the left and on the right side with respect to the central vertical meridian (*Figure 3.2*). This phase served as a reference for the participants to understand in which portion of the screen they will have to perform the task next. After two seconds, the four reference squares disappeared, leaving only the gray central fixation cross, which remained onscreen for 12 seconds (ITI). An auditory cue (i.e. “upper left”, “upper right”, “lower left” or “lower right”; 3 seconds) instructed participants in which quadrant they will have to perform the task next. After the cue, the central cross turned green and participants had to imagine a gray square in the quadrant indicated by the recorded voice, trying to keep the same spatial position and size of the reference frame they saw at the beginning of the experimental run. Imagery had to be performed for 12 seconds. After this delay, the central fixation cross turned gray again, signaling the start of the following trial. Throughout the whole experimental run, participants were instructed to keep their gaze on the central fixation cross.

Attention condition. The attention condition (*Figure 3.2*) was very similar to the imagery condition, except in the following aspects. After the presentation of the auditory cue, participants only had to pay attention to the quadrant indicated by the voice (12 seconds) without performing any mental operation. As in the imagery condition, fixation had to be maintained on the central cross throughout the whole experimental run. Note that the attention condition was not used for the purpose of this study and thus will not be described in the following sections (for additional information, see *Appendix*).

Perception condition. To localize the portion of early visual cortex responsible for processing the different quadrants of the visual field, participants performed a perception condition (*Figure 3.2*). The perception condition followed the same configuration as the imagery and attention conditions. At the beginning of the experimental run, participants were presented with the reference frame (2 seconds) followed by a gray central fixation cross (12 seconds). After the auditory cue (i.e. “upper left”, “upper right”, “lower left” or “lower right”; 3 seconds), participants were presented with a gray and white checkerboard in the quadrant indicated by the voice.

The checkerboard, comprising of an area the same size as the individual squares in the reference frame, started flickering with a frequency of 1.5 Hz for 12 seconds. Similar to the other conditions, participants were instructed to keep their gaze at the central fixation cross throughout the entire experimental run.

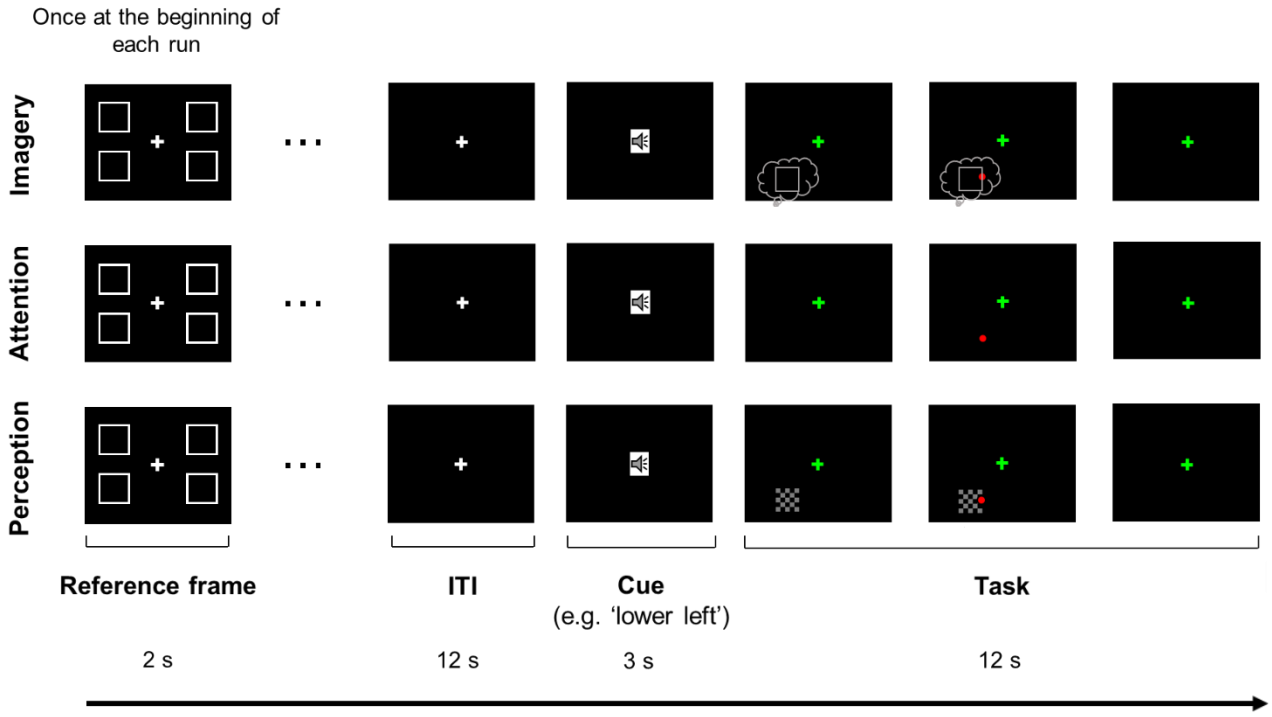

Figure 3.2. Task overview, normal sighted participants. Schematic representation of the imagery (top panel), attention (mid panel) and perception (bottom panel) condition. Each run started with the presentation of a reference frame (2 seconds), indicating the four quadrants of the visual field. Participants saw a white fixation cross in the center of the screen for 12 seconds (ITI). Next, an auditory cue indicated one of the four quadrants of the visual field (i.e. "upper left", "upper right", "lower left", "lower right"). Following a color change of the central fixation cross (i.e. from white to green), participants had to imagine a small gray square in the corresponding portion of the visual field, for a delayed period of 12 seconds. After this interval, the central cross returned white, signaling the start of the next trial. The attention condition followed the same logic except that, after the auditory cue, participants had to attend the quadrant indicated by the voice, instead of performing visual mental imagery. In the perception condition, after the auditory cue, subjects saw a contrast-reversing black and white checkerboard, flickering at the location indicated by the voice. In all three tasks, fixation had to be maintained on the central cross throughout the whole run.

To ensure that participants followed the instructions, an attention-control task was embedded in all three conditions. During the task period of each of the conditions (*Figure 3.2*), a red dot appeared in one of the 4 quadrants; participants were instructed to press a response button as soon as they detected the dot. In 60%

of trials, the red dot appeared in the quadrant indicated by the auditory cue (valid cue), whereas in the remaining 40%, the dot appeared in one of the remaining three quadrants (invalid cue). Reaction times (RTs) were recorded.

Healthy participants performed 2 runs of visual imagery, 2 runs of attention, and 1 run of perception condition, for a total of 5 experimental runs (100 trials, 5 for each factorial combination of task (3) and visual quadrant (4)). The order of the trials within each run was randomized. Four participants started the experimental session performing two runs of imagery task, followed by two runs of attention task (AABB design); the remaining seven followed the opposite order (BBAA design). The perception task was always performed as the last functional run.

To test whether also hemianopic patients exhibit a spatially selective recruitment of EVC during visual mental imagery, we used an experimental design very similar to the one adopted for normal sighted participants except for the following changes. In order to reduce the duration of the scanning session and to keep patients as comfortable as possible, the attention condition was not included. Each patient then took part in one single experimental session, consisting of a structural scan (~5 minutes) and 3 functional runs (~9 minutes each, 2 runs for the visual imagery task, and 1 run for the perception task). Moreover, before the start of the experimental session, each patient took part in an intensive training outside the scanner were they performed a short version of the imagery task. The aim of the training was to assess the correct understanding of task requirements and, most importantly, the ability of each patient to perform visual mental imagery at the correct spatial position.

3.3.5 Data acquisition

4T scanner. Data were collected using a 4T Bruker MedSpec Biospin MR scanner equipped with an eight-channel birdcage head coil. Functional data were acquired using an EPI sequence (TE/TR = 28.0/2000.0, flip angle = 73°, matrix size = 64x64, 30 interleaved slices, in-slice resolution 3 mm). Slices were axial, slightly tilted to be approximately parallel to the calcarine sulcus in order to optimize brain coverage. Two-hundred seventy-eight volumes were acquired for each functional run.

To be able to coregister the low-resolution functional images to a high-resolution anatomical scan, we acquired a T1-weighted anatomical scan (magnetization-prepared rapid-acquisition gradient echo; TR: 2700 ms; voxel resolution: 1 x 1 x 1 mm; TE: 4.18 ms; FA: 7°; FOV: 256 x 224 mm; 176 slices; generalized autocalibrating partially parallel acquisition with an acceleration factor of 2; inversion time: 1020 ms).

1.5T scanner. Data were acquired using a 1.5 T Philips MR scanner at the Borgo Roma Hospital (Verona, Italy), using a 15-channel head coil. Functional data were acquired using an EPI sequence (TE/TR = 35.0/2000.0, flip angle = 90°, matrix size = 64x64, 30 ascending slices, voxel resolution 2x2x4 mm). The slices were axial, slightly tilted to be approximately parallel to the calcarine sulcus in order to optimize brain coverage. Two-hundred seventy-eight volumes were acquired for each functional run.

For the high resolution anatomical scan, we used a T1 – weighted sequence (magnetization-prepared rapid-acquisition gradient echo; TR: 7763 ms; voxel resolution: 1 x 1 x 1 mm; TE: 4.18 ms; 176 slices).

3.3.6 Data analysis

Behavioral analyses. Due to a communication problem with the 1.5T scanner that went undetected, behavioral responses and reaction times were not collected in N = 3 hemianopic patients (FB, AN and TB in *Table 3.1*). We report behavioral data from N = 11 normal sighted participants and N=2 hemianopic patients (CG and PG in *Table 3.1*).

fMRI data analysis

Preprocessing. Data were preprocessed and analyzed using FSL 5.1 (FMRIB's Software Library, https://fsl.fmrib.ox.ac.uk/fsl) in combination with custom software written in Matlab. To avoid T1 saturation, we discarded the first four volumes of each run. Preprocessing included motion correction to the mean image, followed by slice timing correction (ascending order), spatial smoothing (Gaussian kernel FWHM = 5 mm), and high-pass temporal filtering (t > 0.01 Hz) to remove frequency artefacts. Each functional scan was

registered to its corresponding coplanar high-resolution image with rigid body transformations and to the MNI152 standard brain using nonlinear transformation (twelve degrees of freedom).

Univariate RFX-GLM analysis. To examine the hemodynamic response during the imagery and perception condition, we performed a fixed effects (FFX) general linear model (GLM) analysis separately for the perception and imagery condition. For each individual participant, we created predictors for the four quadrants of the visual field (upper left (UL), lower left (LL), upper right (UR), lower right (LR)), resulting in a total of four predictors for each experimental run. In both conditions, predictors were time-locked to the onset of the imagery or perception delay (12 seconds). Each predictor was convolved with the canonical HRF. Parameters from 3D motion correction were included in the model as nuisance regressors.

ROI definition. To define the two dorsal (RHd, LHd) and ventral (RHv, LHv) portions of EVC responsible for the processing of the lower and upper quadrants of the visual field respectively, we analyzed data from the perception run in both normal sighted participants and hemianopic patients. We estimated the main contrast for each quadrant against the other three (e.g. UL>UR+LR+LL). For each functional contrast, we defined one ROI comprising those voxels responding to visual stimulation individually for each participant.

Hemianopic patients tested at lower field intensity (i.e. FB, TB, AN in *Table 3.1*) exhibited a weaker activation in the perception localizer scan, which resulted in the impossibility to create individual ROIs following the procedure described above. For this reason, we adopted a set of ROIs common for all hemianopic patients based on the activation in normal sighted participants. Results from the FFX GLM for the perception condition of all normal sighted participants were entered in a univariate random effects (RFX) GLM analysis (N=11), to identify portions of EVC responding to visual stimulation at group level. Based on this group analysis, we identified dorsal and ventral portions of EVC activated during visual stimulation of the four quadrants of the visual field *(Figure 3.3*; for a summary of peaks coordinates see *Appendix, Supplementary material: Chapter 3*). For patients scanned at high field intensity (i.e. CG and PG in *Table 3.1*), we adopted the same procedure as normal sighted participants. To create the dorsal and ventral ROIs for the damaged hemisphere, we mirrored the ROIs selected for the healthy hemisphere, flipping them on the x-axis with respect to the central sulcus.

Normal sighted participants and patients' group ROIs were binarized using FSLmaths. All ROIs were transformed from native space to MNI space by means of FMRIB's Linear Image Registration Tool (FLIRT; Jenkinson et al., 2001; 2002), as implemented in FSL 5.1.

a)

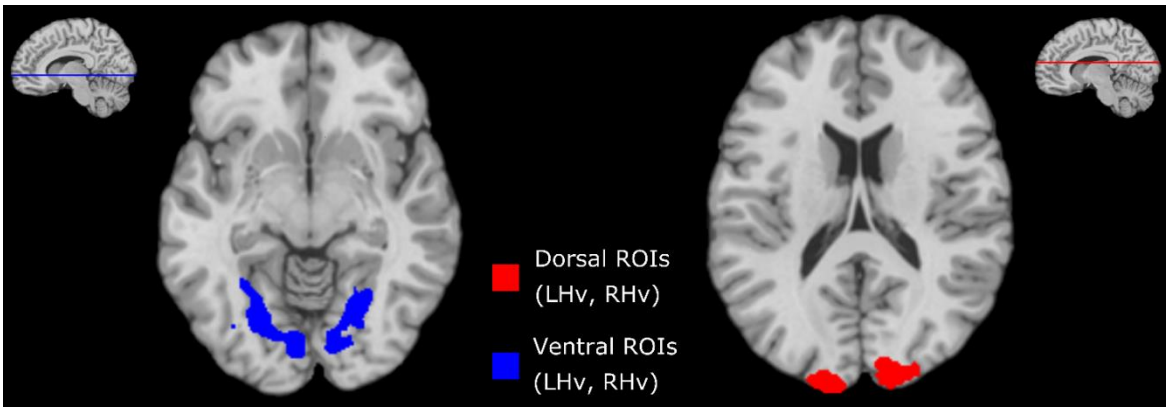

b)

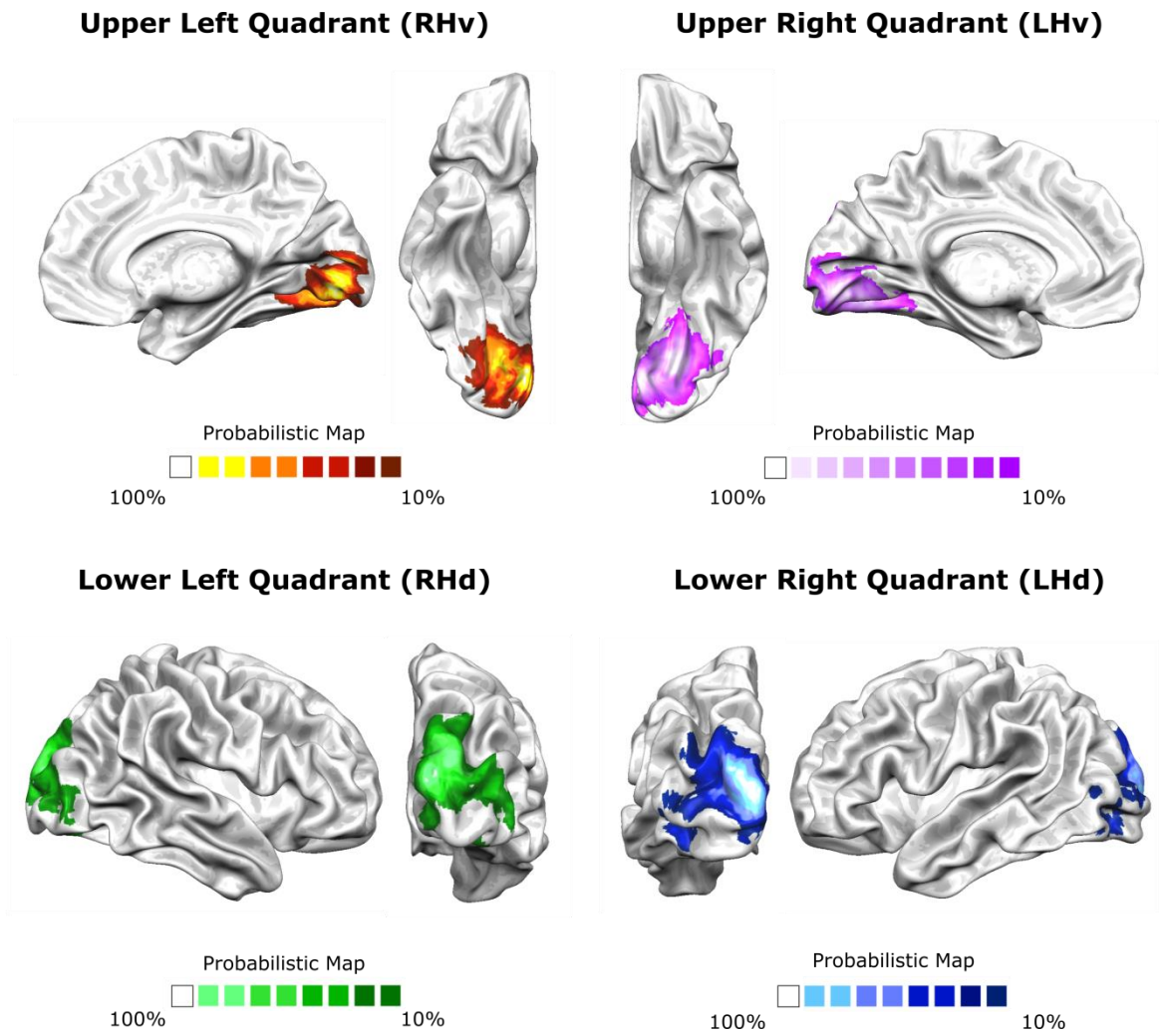

Figure 3.3. a) Position of the dorsal (red) and ventral (blue) ROIs, averaged across normal sighted participants. b) Probabilistic maps for the upper left (red), upper right (purple), lower left (green) and lower right (blue) quadrants. For each ROI, these maps represent the percentage of subjects leading to significant task activity at each spatial location.

Spatial selectivity index. To examine whether each portion of early visual cortex was selectively recruited when visual mental imagery was performed in the respective quadrant, we computed a spatial selectivity index. To compute the index, we used the following formula:

$$d' = \frac{BETA_{(pref)} - mean(BETA_{(npref)})}{BETA_{(pref)} + mean(BETA_{(npref)})}$$

where $BETA_{(pref)}$ is a vector of beta values from all voxels during preferred stimulation (e.g. UL for RHd) and $BETA_{(npref)}$ is a vector of beta values from the same set of voxels, averaged across stimulation within the remaining three quadrants (e.g. UR, LR and LL for RHd). Within each ROI, only the 100 voxels showing the highest beta estimates were selected.

Correlation between spatial selectivity index and behavioral measures. To understand whether individual differences in visual imagery abilities could result in differences in the recruitment of early visual cortex, we explored the relation between the spatial selectivity index and VVIQ scores (Marks, 1975). For each participant, we computed the linear correlation (Pearson correlation coefficient) between the spatial selectivity index averaged across the four quadrants of the visual field and VVIQ scores. VVIQ scores are expressed as an average between the score of visual mental imagery with eyes open and eyes closed (Amedi et al., 2005). Moreover, we also wanted to explore the relation between reaction times in the attentional control task and individual recruitment of early visual cortices. To this aim, we computed a second Pearson linear correlation between the spatial selectivity index, averaged across the four quadrants of the visual field, and RTs averaged across valid and invalid trials.

3.4 Results

3.4.1 Behavioral results

We analyzed RTs separately for valid trials (i.e. trials where the red dot was presented in the quadrant indicated by the auditory instruction) and invalid trials (i.e. trials where the red dot appeared in one of the remaining quadrants), in both normal sighted participants and hemianopic patients (*Figure 3.4*).

During the imagery task, RTs were not statistically different for both normal sighted participants [mean: 660ms ± 232.15] and hemianopic patients [mean: 687.75ms ± 83.75. Repeated measures ANOVA. Factors: group (normal sighted, hemianopic), trial type (valid, invalid). Main effect of group: F(1,1)=14.883, p=0.161], and did not differ between valid and invalid trials [Main effect of trial type: F(1,1)=0.723, p=0.551. Interaction group*trial type: F(1,1)=19.67, p=0.141].

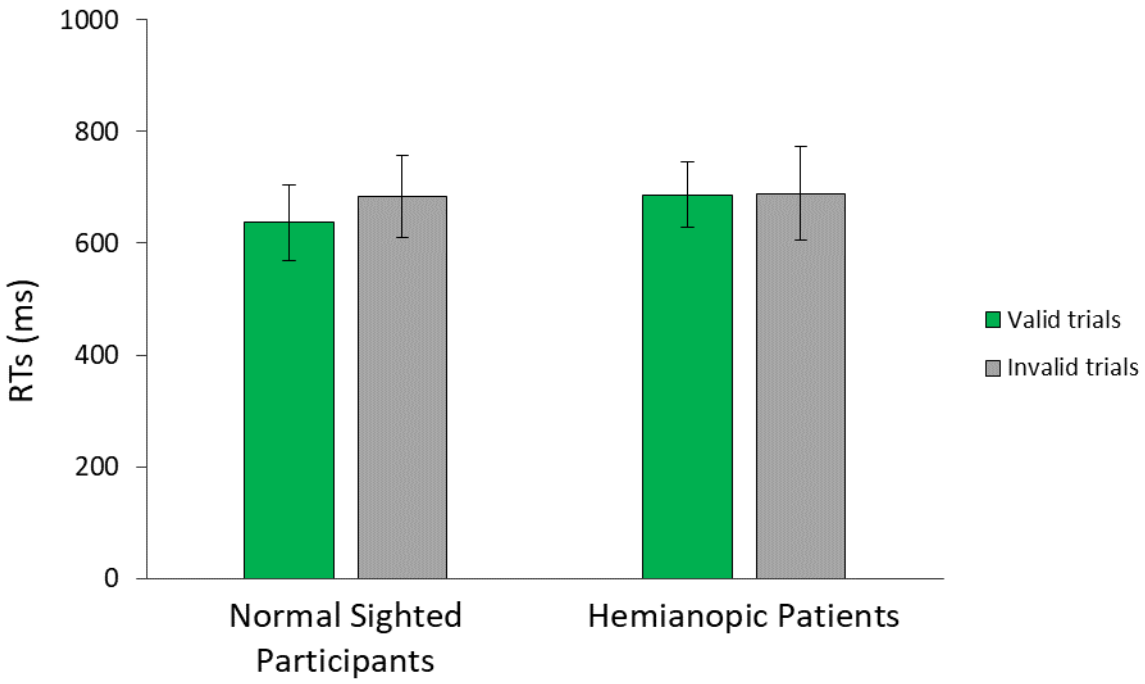

Figure 3.4. Behavioral results. RTs, separately for normal sighted participants and hemianopic patients (PG and CG). RTs were computed separately for valid trials (i.e. trials where the red dot was presented in the quadrant indicated by the auditory instruction) and invalid trials (i.e. trials where the red dot appeared in one of the remaining quadrants). RTs did not differ between the two groups, and were comparable across valid and invalid trials. Error bars represent the standard error of the mean (S.E.M.).

3.4.2 Selectivity index

To understand whether is possible to selectively recruit individual portions of early visual cortex (EVC) by means of visual mental imagery, we computed the selectivity index previously described (see *Material and Methods*). The same analysis was also performed for the attention condition in normal sighted participants (see *Appendix, Supplementary materials: chapter 3*).

In normal sighted participants, beta values were extracted from dorsal and ventral ROIs in early visual cortex created individually for each subject. Results are summarized in *Figure 3.5*. As can be seen, we obtained a spatially selective response during the visual mental imagery task in the dorsal and ventral ROIs of the left primary visual cortex [LHv: M=0.62, SD=0.54; t(10), p=0.003. LHd: M=0.73, SD=0.54; t(10), p=0.001], and in the corresponding dorsal ROI of the right hemisphere [RHv: M=0.50, SD=0.6; t(10), p=0.019]. The upper left quadrant did not reach statistical significance [RHd: M=0.24, SD=0.40; t(10), p=0.076]. No significant difference was reported between the different quadrants in the two hemifields [repeated measures ANOVA. Factors: quadrant (4 levels). Main effect of quadrant: F(3,30)=2.817, p=0.056].

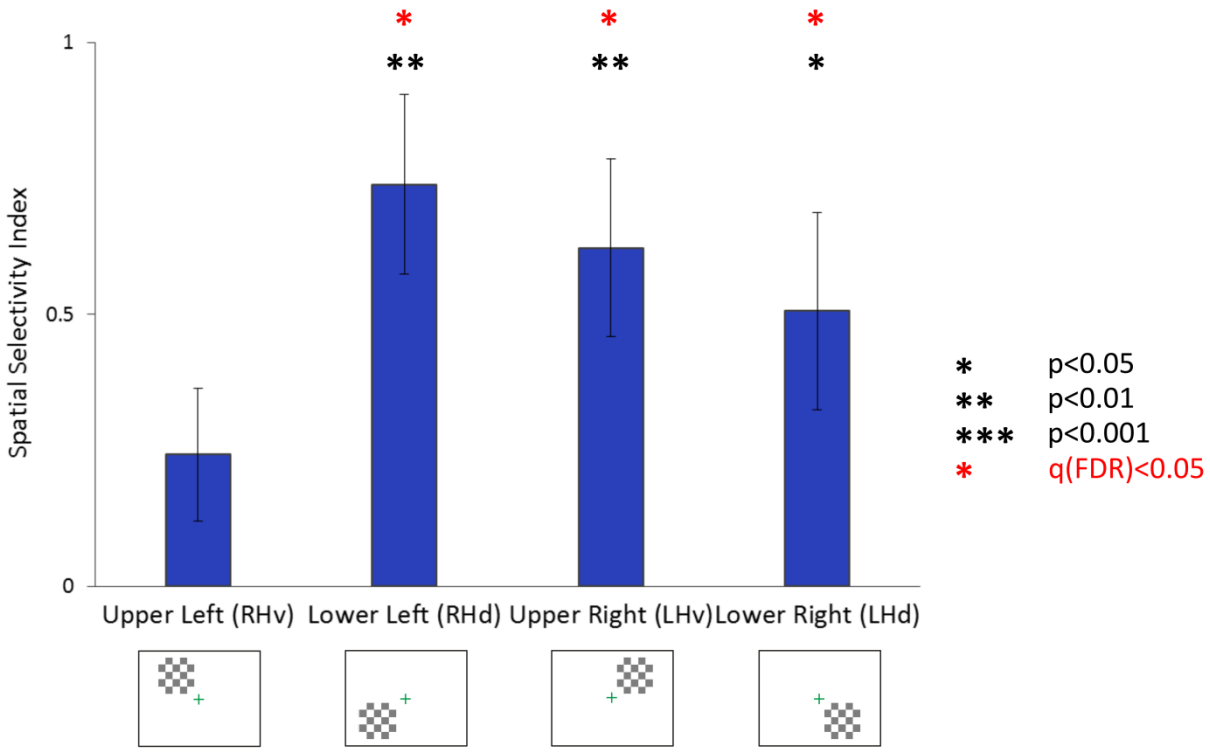

Figure 3.5. Normal sighted participants. Spatial selectivity index during the imagery condition, separately for the four ROIs in EVC corresponding to stimulation of the upper left, upper right, lower left and lower right quadrants. Results were corrected for multiple comparisons using a false discovery rate (FDR) < 0.05. RHv, right hemisphere ventral; LHv, left hemisphere ventral; RHd, right hemisphere dorsal; LHd, left hemisphere dorsal. Significance levels: one black asterisk, p<0.05; two black asterisks, p<0.01; three black asterisks, p<0.001, one red asterisk, q(FDR)<0.05. Error bars represents the standard error of the mean (S.E.M.).

Figure 3.6 shows the magnitude of the selectivity index averaged across the 4 quadrants, plotted separately for each individual normal sighted participant. We found an extensive variability between individuals in the ability to selectively recruit different portions of early visual cortex by means of visual mental imagery.

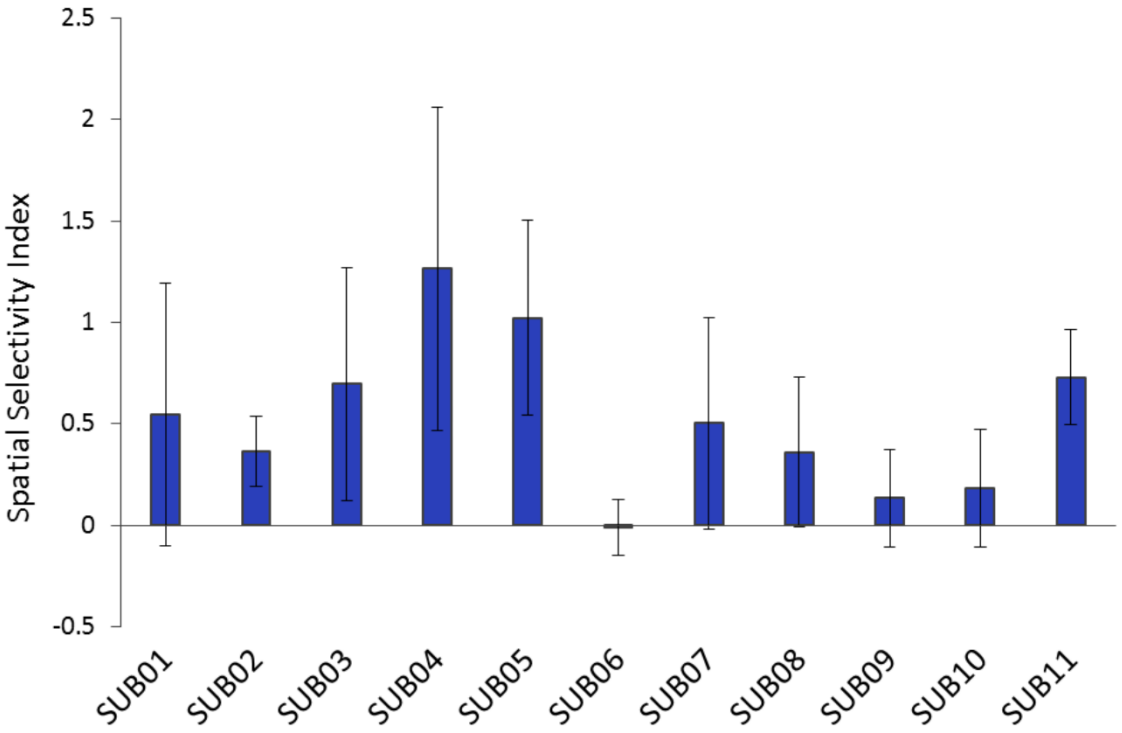

Figure 3.6. Normal sighted participants. Spatial selectivity index during the imagery condition, computed separately for each individual normal sighted participant. Error bars represent the standard deviation in the magnitude of the eccentricity effect across the four quadrants.

To examine whether individual abilities in performing visual mental imagery could result in individual differences in the recruitment of early visual cortex, we computed the linear correlation between vividness of mental imagery as assessed by the VVIQ, and the spatial selectivity index in the normal sighted participants group. As shown in *Figure 3.7*, we obtained no correlation between these two measures.

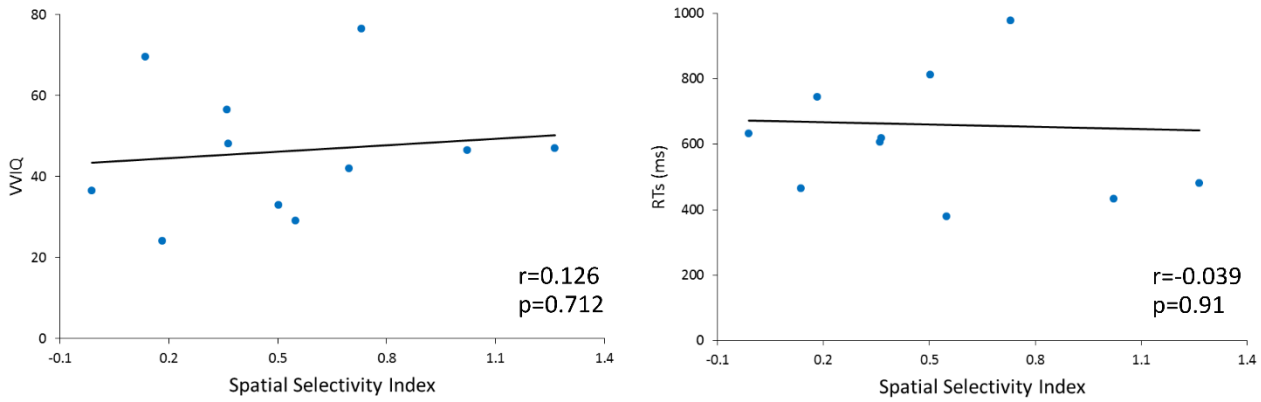

Figure 3.7. Normal sighted participants. Left panel: correlation between the average selectivity index across the four quadrants and the vividness of mental imagery as assessed by the VVIQ. Right panel: correlation between the average selectivity index across the four quadrants and reaction times in the attentional control task, averaged across valid and invalid trials.

To investigate the recruitment of the damaged and healthy hemispheres of hemianopic patients during visual mental imagery, we computed the same analysis as in normal sighted participants. The weak response in the perception localizer for hemianopic patients tested at low field intensity did not allowed us to create individual ROIs for patients FB, TB and AN. For this reason, beta values for all five hemianopic patients were extracted from dorsal and ventral ROIs in the two hemispheres defined based on the group analysis of normal sighted participants (see *Material and Methods*, *ROI definition* paragraph). For theoretical reasons, we considered the healthy and damaged hemispheres separately, collapsing the indexes of the dorsal and ventral ROIs constituting each hemisphere (*Figure 3.7*). We found a significant recruitment of early visual cortex during the imagery [M=0.38, SD=0.26; t(4)=3.34, p=0.029] and perception conditions [M=0.68, SD=0.38; t(4)=4.04, p=0.016] in the healthy hemisphere. In the damaged hemisphere, we found significant quadrant selective recruitment during perception [M=0.39, SD=0.15; t(4)=5.69, p=0.005], but not during imagery [M=0.1, SD=0.42; t(4)=0.55, p=0.609]. The spatial selectivity index did not differ significantly between the healthy [M=0.38, SD=0.26] and damaged [M=0.1, SD=0.42] hemispheres during the imagery condition [paired samples *t*-test: t(4) = 1.06, p = 0.349].

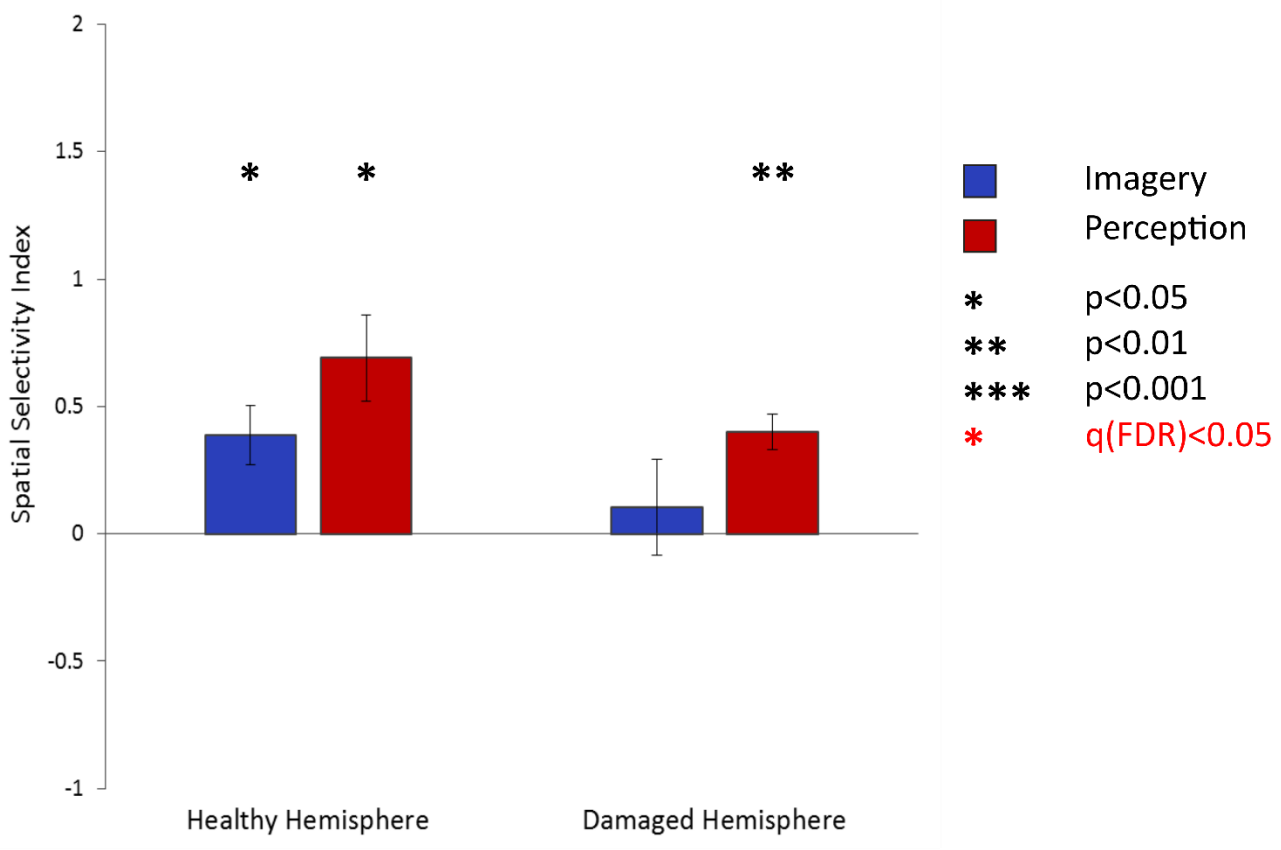

Figure 3.7. Hemianopic patients. Selectivity index computed for the healthy and damaged hemispheres during visual mental imagery. Beta values were extracted from dorsal and ventral ROIs in the two hemispheres defined based on the group analysis of normal sighted participants. For each hemisphere, we collapsed data from the corresponding dorsal and ventral ROIs during the imagery condition. Results were corrected for multiple comparisons using a false discovery rate (FDR) < 0.05. Significance levels: one black asterisk, p<0.05; two black asterisks, p<0.01; three black asterisks, p<0.001, one red asterisk, q(FDR)<0.05. Error bars represents the standard error of the mean (S.E.M.).

Figure 3.8 shows the selectivity index for the imagery and perception conditions, plotted separately for dorsal and ventral ROIs. During the perception condition, we found a significant quadrant selective recruitment in the healthy hemisphere [ventral ROI: M=0.49, SD=0.33; t(4)=3.3, p=0.03; dorsal ROI: M=0.89, SD=0.48; t(4)=4.1, p=0.015] and in the dorsal ROI of the damaged hemisphere [M=0.62, SD=0.41; t(4)=3.381, p=0.028]. Due to the high variability between patients, during the imagery condition, the eccentricity index did not reach significance in any of the four quadrants of the visual field [healthy hemisphere: ventral ROI: M=0.76, SD=0.78; t(4)=2.19, p=0.094; dorsal ROI: M=0.013, SD=0.46; t(4)=0.064, p=0.952. Damaged hemisphere: ventral ROI: M=-0.21, SD=0.54; t(4)=-0.876, p=0.43; dorsal ROI: M=0.62, SD=0.41; t(4)=2.17, p=0.096].

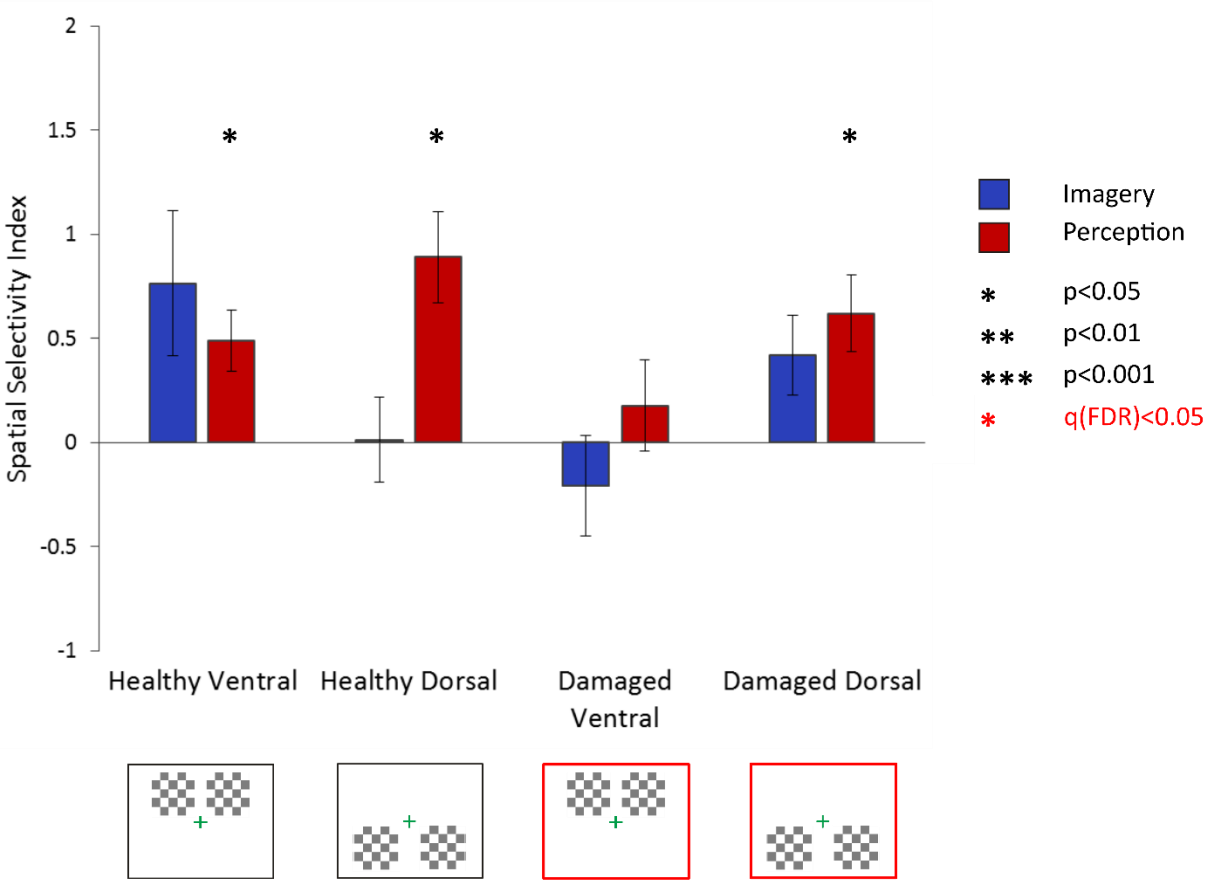

Figure 3.8. Hemianopic patients. Spatial selectivity index computed for the healthy and damaged hemispheres during the imagery condition. Beta values were extracted from dorsal and ventral ROIs in the two hemispheres defined based on the group analysis of normal sighted participants. Data from dorsal and ventral ROIs are shown separately for both the healthy and damaged hemispheres. Damaged ROIs are highlighted in red. Results were corrected for multiple comparisons using a FDR < 0.05. RHv, right hemisphere ventral; LHv, left hemisphere ventral; RHd, right hemisphere dorsal; LHd, left hemisphere dorsal. Significance levels: one black asterisk, p<0.05; two black asterisks, p<0.01; three black asterisks, p<0.001, one red asterisk, q(FDR)<0.05. Error bars represents the standard error of the mean (S.E.M.).

Considering the stronger activation during the perception localizer in hemianopic patients tested at high field intensity (see *Material and Methods*), we carried out additional analyses for patients PG and CG (*Figure 3.9*). Dorsal and ventral ROIs for healthy and damaged hemispheres were created based on the activation during the perception localizer, individually for each patient. The results show a within quadrant variability in the recruitment of early visual cortex, both in the healthy and in the damaged hemisphere [Patient CG. Healthy hemisphere: ventral ROI: selectivity index = 0.106; dorsal ROI: selectivity index = 0.494. Damaged hemisphere: ventral ROI: selectivity index = -0.061; dorsal ROI: selectivity index = 0.432. Patient PG. Healthy

hemisphere: ventral ROI: selectivity index = 1.05; dorsal ROI: selectivity index = -0.26. Damaged hemisphere: ventral ROI: selectivity index = 0.45; dorsal ROI: selectivity index = 1.513].

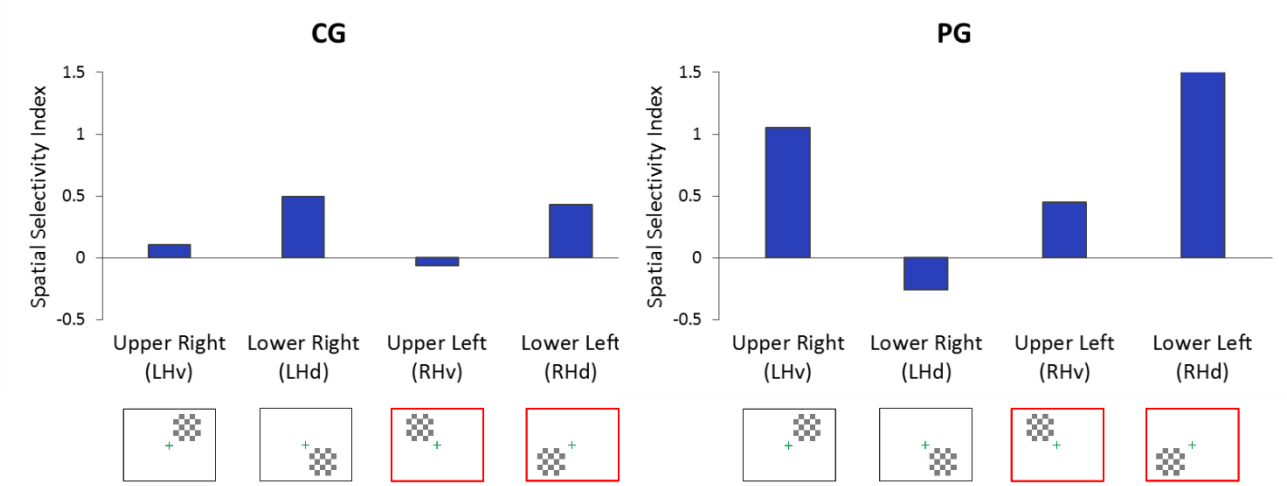

Figure 3.9. Hemianopic patients. Spatial selectivity index computed for the imagery condition in patients CG and PG. Beta values were extracted from dorsal and ventral ROIs in the two hemispheres defined based on the perception localizer, individually for each patient. Data from dorsal and ventral ROIs are shown separately for both the healthy and damaged hemispheres. Damaged ROIs are highlighted in red.

3.5 Discussion

We tested normal sighted individuals and hemianopic patients in a visual imagery paradigm. The aim of the study was two-folded: i) understanding whether it is possible to selectively recruit individual quadrants within the visual field by means of visual mental imagery, and ii) testing whether this ability is preserved in individuals affected by lesions to visual routes. Our results indicate that normal sighted participants are able to recruit retinotopically organized visual areas by means of visual mental imagery. Hemianopic patients exhibited a similar pattern of recruitment in the healthy hemifield, albeit with less strength. In the following sections, we will discuss the main results in more detail.

3.5.1 Visual imagery in healthy individuals

Our group of healthy participants showed a spatially selective recruitment of early visual cortex during visual mental imagery. In other words, when participants imagined a stimulus in one of the four quadrants, we found a significant recruitment of the portion of EVC processing the corresponding visual field location (e.g. ventral EVC in the right hemisphere) compared to when the same mental process was performed in the other three quadrants.

The recruitment of retinotopically organized visual areas during visual imagery is still a matter of extensive debate in the scientific community. Depictive theories of visual mental imagery (Kosslyn 1981; 2005) posits the internal generation of mental images to be dependent on a top-down modulation originating in prefrontal and parietal areas, reactivating representations of external entities stored in inferotemporal cortices. Ultimately, this chain of processes would lead to a recruitment of early visual areas, where in light of their retinotopical organization, mental images would be "depicted" acquiring their resemblance to real stimuli (Kosslyn, 1994). In the last few decades, a growing number of PET (Kosslyn et al., 1993; 1995; Thompson et al., 2001) and fMRI studies employing different paradigms (Klein et al., 2000; Ishai et al., 2002; O'Craven & Kanwisher, 2000; for a recent review see Winlove et al., 2018) supported this theory, reporting activation of primary visual cortex during visual mental imagery. On the other hand, several fMRI studies failed to report such activation (D'Esposito et al., 1997; Formisano et al., 2002; Ishai et al., 2000; Sack et al.,

2002). The functional role of early visual cortex during visual mental imagery is still an open question. In this debated scenario, our study provides further evidence of an involvement of early visual cortex during visual mental imagery.

Previous fMRI studies reporting a retinotopically-organized activation of early visual cortex during visual imagery used relatively large stimuli such as bow-tie shapes covering the horizontal and vertical meridians (7 deg. visual angle radius; Klein et al., 2004) and rotating wedges covering the whole visual field (12.3 deg. visual angle; Slotnick et al., 2005). By adopting a simple geometric-shape stimulus covering a smaller portion of the visual field (1.8 deg. visual angle), we were able to replicate these results, showing that participants are able to recruit specific portions of early visual areas by means of visual mental imagery. Nevertheless, we found a high interindividual variability in the quadrant specific recruitment during imagery. The magnitude of the selectivity index and the pattern of recruitment across the four quadrants of the visual field varied across healthy participants, with only a subset exhibiting a homogeneous recruitment of dorsal and ventral early visual cortex. Individual differences in visual imagery abilities are often reported in the literature and are quite common in neuroimaging studies using different paradigms (see e.g. Kosslyn & Thompson, 2003). Kosslyn et al. (1996) hypothesized this variability could be due to individual differences in the ability to perform visual mental imagery, with weaker EVC activation corresponding to slower reaction times in imagery tasks. Nevertheless, our analysis did not reveal any correlation between the average selectivity index across the four quadrants of the visual field and reaction times during the imagery task, or individual imagery ability as assessed by the VVIQ. Interindividual variability in performing visual imagery seems to be an external variable difficult to control in cognitive studies.

3.5.2 Visual imagery in hemianopic patients

Patients affected by homonymous hemianopia showed a different pattern of results in comparison to normal sighted participants. As expected, at group level, we detected a positive spatial selectivity index in the healthy hemisphere during the imagery task. We further observed a slightly positive spatial selectivity index in the affected hemisphere (i.e. lower visual quadrants); however, this did not reach statistical significance. Overall,

these results suggest that, similarly to normal sighted participants, hemianopic patients are able to selectively recruit portions of early visual cortex in the healthy hemisphere by means of visual mental imagery. However, the top-down modulation occurring during visual imagery, however, seems to not be effective in recruiting the lesioned hemifield. One potential explanation for this difference between the two hemispheres could be related to the extent and location of the lesion in the patients' group. To our knowledge, the only fMRI study investigating residual brain activity in hemianopic patients during imagery (Bridge et al., 2012), consisted in a single case study with a lesion limited to bilateral V1. Conversely, out of our five patients, four of them had extensive lesions covering not only retrochiasmatic visual pathways, but also portions of temporal and parietal cortices (see *Table 3.1* and *Figure 3.1*). One might argue that the failure in recruiting the damaged hemisphere during imagery can be due to altered or impaired communication between nodes of the visual imagery network and early visual cortex. Different studies showed that, as a results of a cerebral insult, alterations in functional connectivity between brain regions even distant from the lesion site, might occur (He et al., 2007; Grefkes & Fink, 2011). Diffusion tensor imaging (DTI) data from our patients would be necessary to confirm alterations in anatomical connectivity between regions of the visual imagery network. Considering the extent of the lesions in the patients' group, it is possible that the transfer of information between spared portions of early visual cortex in the damaged hemisphere and parietal (e.g. SPL) and prefrontal (e.g. IFG) areas might be reduced. These regions are considered to play a pivotal role in the top-down modulation of information necessary to perform visual imagery (Mechelli et al., 2004; Dentico et al., 2014; Dijkstra et al., 2017). If this was the case, we would have expected, in light of its structurally intact anatomical connectivity, a homogeneous increase of the selectivity index in dorsal and ventral ROIs of the healthy hemisphere but not in the corresponding portions of the damaged hemisphere. However, our data do not support this hypothesis. Indeed, the analysis of individual quadrants (see *Figure 3.8*) revealed a dramatic within-hemispheres variability, with dorsal and ventral portions of early visual cortex exhibiting differences in their recruitment, both in the healthy and in the damaged hemispheres.

Another plausible explanation is that the lack of recruitment of the damaged hemisphere is not due to an impaired top-down modulation over low-level visual areas, but to a generalized variable recruitment of individual quadrants that affect both hemispheres, which might not be related to the lesion. This inter-

individual variability in imagery abilities is reported in different studies conducted on healthy participants (see Winlove et al., 2018), and might be even more prominent after brain damage. Considering the difficulties of some participants in performing visual imagery, it could be desirable to implement a more intense training session to ease the performance to the actual task, and possibly obtain a more reliable recruitment of early visual cortex. In fact, previous results from our lab (Andersson et al., 2018, *under review*) indicated that normal sighted participants can learn to self-regulate BOLD signal in early visual cortex during imagery tasks. When provided with a real-time auditory feedback based on the BOLD signal of V1 (real-time fMRI; Sulzer et al., 2013), participants learned to up- and down-regulate brain activity by means of visual mental imagery. A similar approach could be exploited in clinical populations.

We acknowledge that we were able to only include a limited number of patients. Additional data would be required to better assess the possibility to recruit the damaged hemisphere of hemianopic patients by means of visual mental imagery. Moreover, the presence of a significant positive of the spatial selectivity index in the dorsal damaged ROIs during the perception condition raises the possibility that patients did not follow experimental instructions (i.e. keeping fixation in the center of the screen), at least in the perception condition. If this was the case, there is also the possibility that patients might have had difficulties in fulfilling task requirements in the imagery condition, and this in turn might explain the high variability of our results. However, another possible explanation is that ROIs created from group level analysis of normal sighted participants data might encompass voxels in early visual cortex of the damaged hemisphere which are still receiving visual inputs, and thus showing an increase of the spatial selectivity index during the perception condition. Further studies adopting strategies for controlling eye-movements, such as gaze control using eye-tracking, might be necessary to assess hemianopic patients ability to recruit early visual cortex.

3.5.3 Conclusions

In conclusion, our results are in line with the view that healthy participants are able to recruit early visual cortex by means of visual mental imagery. Moreover, this recruitment appears to be selective for individual quadrants within the visual field. This retinotopic organization is analogous to what is observed during

perception of external stimuli (Engels et al., 1997). Hemianopic patients showed the same spatially-selective top-down modulation over early visual cortex in the healthy hemisphere but not in the damaged. Analysis of individual quadrants highlighted a huge within-hemisphere variability in hemianopic patients and we acknowledge several limitations due to the sample size of both experimental groups. Even though this study did not provide conclusive results, it confirmed the possibility to modulate lower level visual areas by means of visual mental imagery in healthy individuals. Further studies considering a bigger sample of patients will be required to better delineate visual imagery abilities in hemianopic population.

Chapter 4.

Discussion and future perspectives

4.1 Thesis recap

In his lecture at MIT in 2009, Stephen Kosslyn began his talk by asking the audience three different questions: "What shape are Mickey Mouse's ears?", "Which is darker green, spinach or lettuce?" and finally "In which hand does the Statue of Liberty hold the torch?" Answers to all these questions are trivial but they constitute a perfect example of the impact visual imagery has on our daily life. To answer these questions the vast majority of people would proceed by visualizing a representation of an external object in their mind (i.e. Mickey Mouse, vegetables or the Statue of Liberty) recreated from memory, and inspect such internally-generated mental images to identify a specific feature (i.e. ear shape, color, position of the torch) critical to answer the question. Without even noticing, we perform this cognitive process during the day to accomplish both simple tasks, as in the aforementioned example, and most complex forms of planning and problem solving.

Early studies on visual mental imagery mainly focused on its similarities with perception (Shepard & Metzler, 1971; Hayes, 1973; Kosslyn et al., 1973) and on the involvement of early visual areas in the internal generation of mental images of external objects (e.g. Amedi et al., 2005; Klein et al., 2000; 2004; Kosslyn et al., 1993; 1995; Ishai et al., 2000; Slotnick et al., 2005). In recent years, the advent of more complex data analysis techniques, such as MVPA (Haxby et al., 2014), shifted the focus of mental imagery research from the traditional functional mapping approach to the investigation of the representational content of the brain areas involved. In particular, several studies (Cichy et al., 2011; Lee et al., 2012; Reddy et al., 2010; Stokes et al., 2009) showed that visual mental imagery of complex stimuli (e.g. faces, scenes, objects) could be decoded

from patterns of neural activity in specific category selective extrastriate areas (e.g. FFA, PPA, LOC). However, few studies focused specifically on early visual areas (Albers et al., 2013), leaving their representational content during visual mental imagery an open question. It is important to also point out that the top-down modulation occurring during visual mental imagery (Mechelli et al., 2004; Dijkstra et al., 2017) could have important implications for clinical practice, in particular for the rehabilitation of visual field defects.

With the present work, we tried to pursue a more holistic view, investigating two different but at the same time interconnected questions. On one hand, we tried to clarify the role of early visual cortex in visual mental imagery, combining both univariate and multivariate analyses. Specifically, in Study 1 (Chapter 2), we explored the level of complexity in the information represented in early visual areas during visual mental imagery, employing stimuli pertaining to different semantic categories. In Study 2 (Chapter 3), we adopted a univariate approach to establish whether mental imagery is capable to induce a selective recruitment of portions of V1 in healthy individuals and in a group of hemianopic patients. On the other hand, in Study 1 using a multivariate searchlight analysis approach, we aimed to understand how the information on what is being imagined by the individual is represented in the other nodes constituting the visual imagery network, and what this can tell us about their different functional specialization.

4.1.1 Summary of main experimental findings

With the first study (Chapter 2), we tested the representational content of early visual cortex during visual mental imagery. In particular, we investigated whether both V1 and V2 could encode the identity of different imagined stimulus categories (i.e. Lowercase Letters, Objects and Simple Shapes) that has not been used in previous MVPA studies. Moreover, we were also interested in understanding whether the same information could be represented in brain areas outside early visual cortex and to which degree it was shared with perception of the same stimuli. We designed a delayed spatial judgment task in which participants were required to establish the position of a dot with respect to the stimulus they were instructed to imagine or observe right before.

To answer our first question (i.e. the representational content of early visual cortex during imagery), we performed a ROI-based MVPA analysis. Results showed that both V1 and V2 encode the identity of imagined stimulus categories during our task.

To address our second question, we performed a searchlight-based MVPA analysis, which allowed us to investigate whether other brain areas outside early visual cortex could contain information about imagined stimulus categories. Our results revealed a network of inferotemporal (LOC), parietal (SPL, aIPS) and prefrontal (PMd) areas involved in encoding complex stimulus categories.

Moreover, using a cross-decoding approach, we investigated whether perceived and imagined stimuli would rely on similar neural representations. We found significant cross-decoding in a subset of the considered regions (V1, LOC, SPL, left aIPS, left IPL), indicating shared representations between imagery and perception. The presence of a significant within-condition encoding in both temporal and parietal areas can be interpreted in light of previous studies, suggesting the existence of two distinct pathways engaged during visual mental imagery. Occipito-temporal cortices constitute the “ventral” network, which is considered to represent the content of mental images. Regions within parietal and premotor cortices form the “dorsal” network, involved in encoding spatial features of imagined stimuli (Sack et al., 2012).

In the second study (Chapter 3), we aimed to understand whether it is possible to induce a retinotopically-organized recruitment of early visual cortex by means of visual mental imagery in healthy individuals. If this was revealed to be true, it would be possible to hypothesize the application of the same experimental protocol to patients suffering from visual field defects, with the aim to recruit preserved but silenced portions of early visual cortex within the damaged hemisphere. This top-down modulation on spared low-level visual areas could potentially lead to the development of rehabilitative interventions, with the hope of inducing plastic mechanisms of change in the damaged brain, reinstating perceptual awareness. We tested whether imagining a relatively simple stimulus (i.e. small gray square) in one of the four quadrants of the visual field could lead to an activation of the portion of EVC processing the corresponding visual field location. Moreover, by performing the same task in a group of patients suffering from homonymous hemianopia, we investigated whether the same top-down modulation of EVC was still possible after lesions involving retrochiasmatic visual pathways. We computed a spatial selectivity index to measure the selective recruitment of the two

dorsal and two ventral portions of V1 during our visual imagery task. Our results highlighted that healthy participants were able to selectively recruit specific quadrants within the visual field by means of visual mental imagery. However, this retinotopically organized activation of V1 was subjected to inter-individual variability, with only a subset of subjects exhibiting an homogeneous recruitment of both dorsal and ventral ROIs. On the other hand in hemianopic patients we detected a positive increase of the spatial selectivity index in the healthy hemisphere, but not in the damaged. Results in the hemianopic group were not conclusive, possibly due to the small sample size and the dramatic interindividual variability.

In the following paragraphs, I will discuss the main results of this thesis in light of the current literature, providing an overview about visual mental imagery and suggesting possible follow-up investigations.

4.2 What kind of information is represented in the visual imagery network during visual mental imagery

Visual mental imagery is a very recent topic in neuroscientific research. In particular, very little is known about the representational content of regions involved in imagery tasks. The current literature investigating this issue is lacking a comprehensive description of what type of information is processed and stored within different nodes of the network. Previous MVPA studies focused on specific regions within the inferior temporal cortex (i.e. FFA, PPA, LOC), well known for processing specific types of stimuli during perception (respectively faces, places, and objects) (Kanwisher et al., 1997; Epstein et al., 1999; Grill-Spector et al., 1999). Collectively, they showed that mental images of faces and scenes (Reddy et al., 2010; Cichy et al., 2011), letters (Stokes et al., 2009), and common objects (Lee et al., 2012) could be decoded from the same category-selective regions; these representations were similar to those elicited by perception. Overall, these studies remarked that visual mental imagery relies on similar neural substrates as perception. However, as previously stated, researchers focused on high-level perceptual regions, neglecting the representational content of striate visual cortices (i.e. V1 and V2). Considering the pivotal role attributed to V1 in the reenactment of internally generated mental representations during imagery (Bullier, 2001; Kosslyn, 2005), investigating its

representational content is of fundamental importance. Primary visual cortex has traditionally been considered to process low-level visual features of perceived stimuli, such as line orientation and contrast (Ward, 2010). The only imagery study focusing specifically on the representational contents of primary visual cortex (Albers et al., 2013) reported above-chance decoding for visual imagery of low-level stimuli (i.e. gratings) with different orientations. Given this fragmented scenario, we tried to consider all the regions involved in visual mental imagery as a network, providing a holistic view of this cognitive process. With the first study (Chapter 2), we highlighted that the identity of different stimulus categories is represented both in early visual cortices and in temporal and parietal regions. Importantly, we showed that V1 and V2 can represent high-level categorical information about imagined stimuli. In line with this view, recent fMRI studies showed the existence of nonretinal influences on early visual cortex via feedback connections that might transfer high level information to V1. Muckli et al. (2005) showed that movement paths in an apparent motion illusion can recruit primary visual cortex. Adopting an MVPA approach, Bannert and Bartels (2013) showed that information about the prototypical color of an object (e.g. yellow = banana) can be decoded in V1, even when the object is presented in grayscale. Similarly, Vetter et al. (2014) showed that it is possible to decode the identity of both real and imagined sounds from patterns of activation extracted from primary visual cortex. The same was possible also for different hand actions (i.e. reaching and grasping), performed both with eyes open and eyes closed (Monaco et al., 2018). Overall, these findings corroborated the hypothesis of a top-down modulation from higher-level areas to early visual cortex during visual imagery, carrying not only low-level features of imagined stimuli (i.e. orientation or spatial location), but possibly more abstract and semantic information.

It is plausible to hypothesize that top-down modulation would rely on regions outside early visual cortex that are involved in the generation and maintenance of mental images. Indeed, previous studies highlighted an increase of functional connectivity between prefrontal (Mechelli et al., 2004; Dijkstra et al., 2017) and parietal (Dentico et al., 2014) to occipital regions during imagery. Similar findings were also reported in studies involving other types of mental imagery that rely on different sensory modalities, such as motor and auditory. Motor imagery is defined as “internal rehearsal of a movement without any overt physical movement” (Szameitat, 2007), and is thought to rely on similar representations as those involved in motor planning

(Glover et al., 2004). Several studies showed that, similarly to what has been described in visual mental imagery, there is a strong overlap in functional activation between motor imagery and motor execution. In particular, two key regions have been consistently reported to be activated during the internal generation of movements: the supplementary motor area (SMA), a region involved in motor preparation, and the premotor cortex (PMC), an area responsible for internal representation of movements (Stephan et al., 1995; Gerardin et al., 2000; Lotze et al., 2006). Moreover, this activation has been shown to be accompanied by recruitment of parietal regions (SPL, IPL, aIPS; Dechent et al., 2004; Hanakawa et al., 2008). Analogous observations were made for auditory imagery. During the internal generation of sounds, activation of the secondary auditory cortex in the superior temporal gyrus (Halpern & Zatorre, 1999; Zatorre & Halpern, 2005) and of the supplementary motor area (Halpern et al., 2004) has been reported, along with the recruitment of parietal and prefrontal regions (Langheim et al., 2002).

The fact that imagery performed with different modalities induces similar functional activation within the brain led researchers to hypothesize the existence of a network of areas supporting all types of mental imagery. This modality-independent "core" network comprises higher-level regions of parietal and prefrontal cortices (Hassabis et al., 2007a; Daselaar et al., 2010; McNorgan, 2012) and could be responsible for the generation and maintenance of complex and coherent mental representations across all sensorimotor modalities. This supramodal activation of the "core" network has been suggested to be accompanied by a top-down recruitment of low-level sensory regions depending on the type of imagery being performed (e.g. early visual areas during visual mental imagery, auditory cortices during auditory imagery, etc.). We hypothesize a top-down modulation occurred also in our task, with a transfer of information between higher order areas and early sensory regions of the visual imagery network. We found that parietal (SPL, aIPS) and inferotemporal (LOC) regions host a representation of more complex stimulus categories as those found in V1. However, further investigations considering functional connectivity patterns between the considered regions would be required to confirm this hypothesis.

In the last few years, a growing number of studies allowed a more precise understanding of the complex interplay of brain regions involved in the top-down generation of mental images. In analogy with perception, also in visual mental imagery, a specialization in the processing of different aspects of the same information

has been found - a semantic ("what") component, representing the content of mental images, and a spatial ("where") component, representing the relations between parts of said mental images. These two types of information are considered to be processed by two separate routes: the former involving category-selective inferotemporal areas and the latter including premotor and parietal regions (Sack et al., 2012). This functional specialization is also supported by lesion studies, showing double dissociations after lesions in posterior cerebral regions. Some patients were not able to describe objects from memory highlighting an impairment to the "what" component, while others had difficulties in describing spatial relations from memory, indicating impairments to the "where" component (Levine et al., 1985). Nevertheless, little is known about the information encoded in the regions involved in imagery and how this information is distributed within the network. Future studies should investigate these issues, focusing on the mechanisms underlying functional connectivity between the different nodes of the visual imagery network.

4.3 The recruitment of early visual areas during visual mental imagery

A matter of debate in visual mental imagery research exists in defining the involvement of low-level visual areas (i.e. V1 and V2). Since the first studies on visual mental imagery, it was clear that imagined stimuli are affected by the same constraints as perceived objects (Shepard & Metzler, 1971; Hayes, 1973; Kosslyn et al., 1973). These observations led to the formulation of the so called "depictive" theory of visual mental imagery (Kosslyn, 1981; 2005). According to this theory, similar neural mechanisms underlie both imagery and perception. However, the flow of information during the two cognitive processes is assumed to be reversed. During perception, information is passed from the retina to the optic nerve, the optic trait and optic radiations to early visual cortex, and from there is conveyed to high-level regions in parietal and inferotemporal cortices (Ungerleider & Haxby, 1994). On the other hand, during imagery the internal generation of mental images has been suggested to start with top-down signals originating from frontal regions (i.e. IFG) and directed towards parietal (i.e. SPL, IPS) and inferotemporal cortices (i.e. LOC, PPA, FFA; Mechelli et al., 2004; Dentico et al., 2014; Dijkstra et al., 2017). This "top-down" modulation has been

suggested to ultimately lead to a recruitment of early visual cortex (Kosslyn, 1981; 2005). Many studies tried to address the involvement of early visual areas during imagery, reporting conflicting results.

A consistent number of PET (Kosslyn et al., 1993; 1995; Shin et al., 1999) and fMRI (Amedi et al., 2005; Klein et al., 2000; Ishai et al., 2002; O'Craven & Kanwisher, 2000; Slotnick et al., 2005) studies showed activation of primary visual cortex during imagery. In Study 2 (Chapter 3) we confirmed the possibility of up- and downregulating the activity of early visual cortex by means of visual mental imagery. Moreover, we highlighted that small stimuli (i.e. square) covering selective quadrants within the visual field are capable inducing a retinotopically-organized activation of V1 during visual mental imagery, in line with previous studies (Klein et al., 2004; Slotnick et al., 2005).

On the other hand, other fMRI studies failed to report V1 activation during visual mental imagery (Ishai et al., 2000; Formisano et al., 2002; Sack et al., 2002). There are two possible factors influencing the involvement of early visual cortex: the characteristics of the adopted task and the variability in the recruitment of V1 between participants. Concerning the first factor, several studies indicate that V1 recruitment is stronger when participants are required to inspect high-resolution details of internally-generated mental images (Kosslyn & Thompson, 2003). Instead other types of tasks requiring spatial imagery, instead, have been shown to induce a less reliable activation of V1. Indeed, these types of tasks rely on parietal cortices storing topographically organized representations of imagined stimuli (Sereno et al., 2001; Sack et al., 2008; 2012). The central role of task requirements in visual mental imagery studies has been also remarked upon in this thesis.

The task we designed for Study 1 (Chapter 2) had a strong spatial component, which required participants to imagine each stimulus in a specific spatial position and to perform a delayed spatial judgment. In line with previous findings (Sereno et al., 2001; Sack et al., 2008; 2012), we found a stronger recruitment of parietal areas compared to V1. Conversely, in Study 2 (Chapter 3) participants were required to vividly imagine a stimulus in a portion of the visual field, but not to judge its spatial properties. We hypothesize that the characteristics of the task could explain the stronger and more reliable recruitment of early visual cortex we found in Study 2.

The second factor that might explain the variability in V1 recruitment can be attributed to the fact that some participants rely on early visual cortex to perform imagery more than others do. In Study 1, we did not find a reliable recruitment of primary visual cortex at the group level. However, a single-subject analysis revealed that the majority of participants exhibited little to no deactivation of V1, while a subset of them were able to up-regulate its activity during mental imagery. Interestingly, we found a positive correlation between activity in SPL and aIPS and accuracy in our imagery task, which indicates a pivotal role of parietal regions in supporting participants' ability to generate mental images. The same variability was found in Study 2, where only some participants of the healthy group showed a reliable quadrant selective recruitment of the dorsal and ventral portions of early visual cortex. This inter-individual variability has been extensively reported in visual imagery literature using different paradigms (Kosslyn et al., 1996; Klein et al., 2004; Slotnick et al., 2005; Pearson et al., 2015). To date, there is no general consensus regarding possible reasons underlying this discrepancy in V1 activation across participants and studies. One possible explanation is that some of the individual differences reported in striate cortex activity might be related to the efficacy of the underlying information processing. Kosslyn et al. (1996), for example, showed that participants exhibiting the least increase in V1 activity also performed slowest on the imagery task. Moreover, in a subsequent study (Kosslyn & Thompson, 2003), authors suggested that such differences might be due to the type of imagery being used, with the requirement to inspect high-resolution details of mental images playing a key role in early visual cortex recruitment. More recently, different investigations highlighted a link between recruitment of primary visual cortex and vividness of visual mental imagery (Amedi et al., 2005; Cui et al., 2007; Dijkstra et al., 2017b), with participants reporting more robust and vivid mental imagery as assessed by different measures (i.e. VVIQ; Marks, 1973) exhibiting stronger V1 recruitment. However, the opposite pattern of correlation was reported by other studies (Daselaar et al., 2010; Fulford et al., 2018), leaving the interplay of factors inducing a modulation of primary visual cortex during visual mental imagery still an open question.

4.4 Visual mental imagery in clinical rehabilitation

Traditionally, clinical interventions for patients suffering from visual field defects were aimed at providing strategies and devices that could compensate the deficit in everyday life (Pouget et al., 2012). Recently, a new line of research started considering the possibility of adopting imagery tasks as a form of rehabilitative intervention in clinical practice. In this thesis, we focused on a particular clinical population, suffering from homonymous hemianopia. In normal sighted individuals, the visual information follows a specific pathway during perception of external stimuli, going from the retina to the optic nerve, the optic radiation and the LGN, and from there conveyed to the primary visual cortex via the optic radiations. In V1, information about low-level visual features of external stimuli (e.g. line orientations, colors, spatial frequencies) are extracted. Visual input is then sent from primary visual cortex to inferotemporal (i.e. "what" pathway) and parietal (i.e. "where" pathway) cortices, responsible for stimuli identification and spatial features processing (Ward, 2010). After lesions affecting retrochiasmatic visual pathways (i.e. from the optic traits to the occipital lobe), patients experience homonymous hemianopia, a specific class of visual field defects characterized by the abolition of one half of the visual field. The vascular nature of this deficit makes spontaneous recovery possible but chances of full-field recovery are scarce (Pambakian & Kennard, 1997), leading to repercussions on daily life activities (Vu et al., 2004).

Early visual areas in hemianopic patients are often preserved. Nevertheless, visual information might not reach these regions due to the damage affecting visual pathways. We hypothesized that, by bypassing bottom-up damaged visual routes, we could exploit the top-down modulation of visual mental imagery to induce plastic mechanisms of change in the brain. Evidences of preserved imagery abilities after lesion affecting visual pathways are described in the literature (Bridge et al., 2006; Marzi et al., 2006).

In Study 2, we showed a retinotopic recruitment of early visual cortex during visual imagery in healthy participants. Based on these results, we hypothesized that visual imagery performed in the blind quadrant or hemifield of hemianopic patients could up-regulate the activity in the corresponding silenced portion of early visual cortex, reinstating perceptual awareness. We explored imagery abilities in a group of patients with homonymous visual field defect due to retrochiasmatic lesions not involving primary visual cortex. We

found a significant spatial-selective recruitment during the imagery task, which was limited to the healthy hemisphere of hemianopic patients. However, we found a substantial interindividual variability in the recruitment of both silenced and preserved portions of early visual cortex during imagery, which did not allow us to make strong statements about a possible rehabilitative use of imagery tasks. In the following paragraphs, we are going to consider possible caveats due to task and sample characteristics, and we will provide a possible follow-up line of research that might help to better address this new and poorly explored field.

4.5 Limitations

In the following section, I am going to consider three potential classes of limitations that could affect the conclusions of this thesis: i) analysis method, ii) the task, and iii) patients sample.

Among fMRI data analysis methods, multivariate pattern analysis (MVPA, Haxby et al., 2001) is a fairly new approach, whose use has grown substantially during the last decade. The possibility to examine distributed patterns of response in the brain represented a major paradigm change with respect to traditional univariate analysis, allowing researchers to examine more subtle aspects of neural activity. However, as other neuroimaging data analysis approaches, MVPA comes with technical limitations, which have to be taken into account (Etzel et al., 2013; Todd et al., 2013). As an example, results of searchlight analyses can be affected by searchlight size and classifiers parameters, which can create distortions (i.e. misidentification of a cluster as informative or failing to detect truly informative voxels) at both single subject and group levels. This aspect has to be considered when looking at results from different neuroimaging studies as they might be the cause of inconsistencies and thus difficulties in interpretation. Another problem related to searchlight-based MVPA approaches is the low statistical power when correcting results for multiple comparisons, which is due to the substantial amount of voxel comprised within a brain volume (> 50.000). A potential way to address this issue is represented restricting the searchlight-based MVPA analysis to the cortical surface (i.e. gray-white matter boundaries). This surface-based approach, in fact, allows a lower correction for multiple comparisons because inferences are only drawn on grey matter voxels and not on the whole-brain volume.

Regarding the second class of limitations, visual mental imagery is a covert process, taking place in the privacy of one's own mind. This "inherently private nature" of visual mental imagery (Pearson et al., 2015) entails several practical problems when it comes to assessing it in an experimental environment. In particular, establishing whether a participant is actively engaging in visual mental imagery during the experimental session represents a major challenge. To overcome this constraint, researchers developed different paradigms which allowed them to obtain indirect measures of visual imagery performances. Examples of these strategies are mental rotation paradigms (Shepard & Metzler, 1971) or mental image exploration (e.g. Kosslyn et al., 1995; Klein et al., 2000). In Study 1, we addressed this issue by designing a task that allowed us to evaluate the quality and strength of visual imagery. The behavioral measurement of accuracy in our delayed spatial judgment task allowed monitoring the real engagement of participants in visual mental imagery. In Study 2, we chose not to continue with the same strategy but to adopt a simpler attention control task. While imaging in one of the four quadrants of the visual field, both normal sighted participants and hemianopic patients could see a red dot, either in the quadrant where they were imaging (i.e. valid trials) or in one of the other three (i.e. invalid trials). We expected that the shift of attentional resources directed towards a quadrant during imagery allowed a faster detection of a visually presented stimulus. Contrary to our predictions, we did not find a significant difference in RTs between valid and invalid trials. The absence of a difference in RTs between valid and invalid trials for hemianopic patients, which is present for normal sighted participants, might indicate that the former experimental group did not correctly perform the task, moving their gaze around the screen instead of maintaining fixation on the central cross. It has to be noted that our task, particularly the detection of the red dot during catch trials, was probably more challenging for hemianopic patients than for normal sighted participants. It is possible that the lack of experience in performing cognitive tasks in the noisy scanner environment might have affected the patients' abilities to detect the quick appearance of the red dot. This observation is also confirmed by the higher number of missed responses of two hemianopic patients with respect to normal sighted participants. However, another plausible explanation is that our control task was not salient enough to deviate participants' attention from the concurrent visual imagery task. In fact, to be performed correctly visual mental imagery entails a high-load on cognitive resources and it is thus possible that the size or the position of the red dot within the

quadrant were not optimal to induce a rapid attention shift. The small number of data available represents a limitation in the interpretation of the results and additional data would be necessary to disambiguate between these possible causes.

One last important aspect to address concerns our investigation of visual imagery-related activation in hemianopic patients. As it is often the case in clinical research, contact and recruitment of particular clinical populations represents a major challenge. These difficulties are further enhanced by the presence of additional exclusion criteria, necessary to ensure safety in an fMRI environment. As an example, it is fundamental that participants undergoing fMRI scanning do not have any metal or electronic implants in their body. The relative advanced age of individuals most frequently affected by homonymous hemianopia (i.e. 50-70 years old; Pambakian & Kennard, 1997) makes the presence of these devices more likely, increasing the exclusion rate. Prior to the execution of Study 2, in collaboration with the Neurology Department of Santa Maria del Carmine Hospital (Rovereto, Italy), I reviewed clinical records of neurology patients hospitalized between 2013 and 2015. Based on these records, we selected a total of 14 patients suffering from visual field defects (i.e. hemianopia or quadrantanopia). Out of this sample, only 6 patients revealed to be high-field MR compatible (i.e. 4T). We acknowledge that a larger sample size could increase the power of Study 2 and give better understanding of the mechanisms underlying visual mental imagery in hemianopia.

4.6 Future directions

Overall, the studies presented in this thesis contributed to highlighting the organization of the visual imagery network, both in healthy individuals and in patients suffering from lesion to retrochiasmatic visual pathways. Adopting different analysis approaches (univariate analysis and MVPA), we aimed to investigate the involvement of different brain areas in visual mental imagery and their representational content. However, the results of the current thesis also revealed a number of questions which should be followed up on in further investigations.

Despite the growing amount of studies on visual mental imagery highlighting the role of different brain regions in this process, very little is known about the temporal dynamics occurring during the internal generation of mental images. Future studies could exploit the high temporal resolution of magnetoencephalography (MEG) and EEG to further investigate the temporal dynamics occurring during visual mental imagery. For example, such studies could focus on interhemispheric communication, investigating the temporal relationship of activation between homologous areas of the visual imagery network. In fact, little is known about the role of the right hemisphere in visual mental imagery. Several studies indicated a prominent role of the left hemisphere nodes of the visual imagery network in the top-down processes involved both in the generation and maintenance of mental images (see Winlove et al., 2018). The previously suggested studies could clarify the exact contribution of the right hemisphere in visual imagery, and its potential compensative role after lesions affecting left nodes of the visual imagery network. Another poorly investigated issue relates to the individuation of which stimulus parameters could maximize the strength of visual mental imagery. In the vast majority of visual imagery studies, stimuli are selected from standardized databases or created ex-novo by researchers. However, self-reports of both healthy individuals and hemianopic patients collected during the debriefing of Study 1 and Study 2 suggest there might be an additional element to consider. Visual imagery research might benefit from adopting a "tailored" approach, consisting of the selection of stimuli that have an affective and personal value for each single participant. It is possible this could have an impact on both the vividness and the strength of internally-generated mental images, improving participants' self-efficacy and performances during tasks. Future research could investigate whether visual imagery of stimuli pertaining to the same semantic category but with different personal valence (i.e. familiar vs. unfamiliar) could modulate the strength of the activation in the different nodes of the visual imagery network or induce activation in different brain areas.

Following another potential line of research, a matter of further investigation would be exploring the neural basis underlying individual differences in visual mental imagery abilities across individuals. Since the first investigations on this cognitive ability, it has been clear that individuals differ widely in the strength and vividness of mental images they are able to generate (Marks, 1973). Several studies have tried to explain this phenomenon, linking visual imagery abilities to the surface size of primary visual cortex (i.e. smaller V1 is

associated with stronger visual imagery; Bergmann et al., 2016), or with its increased (Amedi et al., 2005; Cui et al., 2007; Dijkstra et al., 2017) or decreased (Daselaar et al., 2010; Fulford et al., 2018) activation during imagery tasks. However, the exact neural basis underlying differences in vividness between participants is still unclear. Future studies directly addressing this issue might be of fundamental importance in expanding our knowledge about the brain mechanisms underlying visual mental imagery.

Finally, to understand whether visual imagery could be considered a real tool for rehabilitation in clinical practice, it would be important to investigate its ability to induce long or short-term plastic changes in the brain. In particular, it would be interesting to understand whether an imagery based training, repeated over the course of multiple sessions, could induce changes in functional connectivity within the areas comprised in the visual imagery network. Different studies (Albert et al., 2009; Lewis et al., 2009) showed that it is possible to detect changes in functional connectivity, which persists beyond the duration of a task using visual and motor paradigms. If this were revealed to be true, it would be possible to hypothesize clinical intervention based on visual imagery paradigms.

4.7 Conclusion

In conclusion, with the studies presented in this thesis, we aimed to expand the knowledge about visual mental imagery and the vast network of areas involved in this cognitive process. By employing multivariate approaches to fMRI data analysis, we provided evidence for distinct roles of parietal and premotor areas, involved in processing the spatial layout of imagined stimuli and temporal regions, representing the content of internally generated representations. Moreover, we also showed that early visual cortex is able to access both types of information via feedback connections during visual imagery. In addition, we demonstrated that the top-down modulation of low-level visual areas occurring during visual mental imagery is feasible to recruit retinotopically-organized early visual cortex, both in normal sighted participants and in the healthy hemisphere of hemianopic patients. Albeit preliminary, these results open up new perspectives on the potential use of visual mental imagery as a rehabilitation tool in the clinical treatment of visual field defects.

Appendix

Supplementary materials: chapter 2

ROI-based MVPA – Individual stimulus exemplars. To understand whether it is possible to decode not only stimulus categories but also single stimulus exemplars, we performed an additional ROI-based MVP analysis. For each individual block, we created predictors for each stimulus in the perception and imagery condition. This resulted in 12 predictors for each experimental run (2 for letter "e", 2 for letter "n", 2 for pen, 2 for watch, 2 for triangle and 2 for circle). Nuisance regressors were identical to those employed for the between-category ROI-based MVPA (see *Chapter 2*, paragraph *2.4.7 Data Analysis*). Using a leave-one-run-out cross-validation method, we tested the ability of the classifier to discriminate between the six stimulus exemplars, across categories during the perception and imagery condition. Moreover, to the similarity between the representation of imagined and perceived stimulus exemplars in early visual areas, we performed a cross-decoding analysis. To assess the significance of the decoding accuracy, individual accuracy scores were entered into a two-tailed one-sample t-test across participants against chance decoding (16,67%), separately for each ROI. Statistical results were corrected for multiple comparisons (number of ROIs x number of tests) using the FD method (Benjamini and Yekutieli, 2001).

Figure S1 shows the results for the ROI-based MVP analysis, separately for V1, V2 and a control region (ventral bilateral striatum). We found above chance decoding for the six stimulus exemplars in both V1 and V2 during the perception (V1: mean accuracy 23.25% ± 5.5%; two-tailed one-sample *t* test: $t_{(20)}$= 5.499, p<0.001. V2: mean accuracy 24.84% ± 6.8%; two-tailed one-sample *t* test: $t_{(20)}$= 5.502, p<0.001) and the imagery condition (V1: mean accuracy 20.40% ± 6.6%; two-tailed one-sample *t* test: $t_{(20)}$= 2.573, p=0.018. V2: mean accuracy 21.35% ± 4.7%; two-tailed one-sample *t* test: $t_{(20)}$= 4.563, p<0.001). In addition, we found above-chance cross-classification accuracy in both V1 (mean accuracy 20.32% ± 5.7%; two-tailed one-sample *t* test: $t_{(20)}$= 2.915, p=0.008) and V2 (mean accuracy 21.35% ± 5.6%; two-tailed one-sample *t* test: $t_{(20)}$= 3.925, p<0.001). Classification accuracy did not reach significance in the ventral bilateral striatum (Perception: mean accuracy 18.33% ± 4%; two-tailed one-sample *t* test: $t_{(20)}$= 1.1887, p=0.073. Imagery condition: mean accuracy 18.81%

± 5.8%; two-tailed one-sample *t* test: $t_{(20)}$= 1.693, p=0.106. Cross-decoding condition: mean accuracy 18.41% ± 3.9%; two-tailed one-sample *t* test: $t_{(20)}$= 0.087, p=0.931).

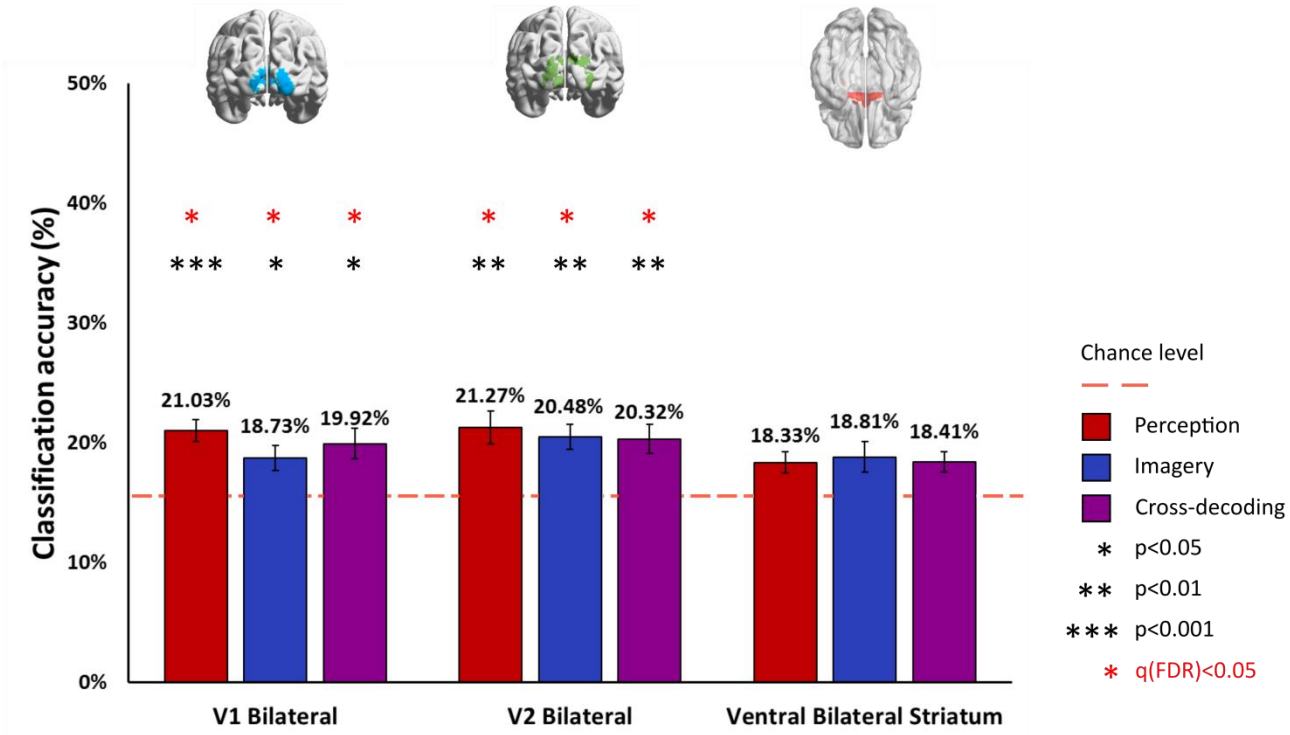

Figure S1. Results of the between-stimulus exemplars ROI-based MVP analysis. Mean decoding accuracy as a function of stimulus exemplar, separately for V1, V2, and a control ROI (ventral bilateral striatum). Blue bars, perception condition. Red bars, imagery condition. Purple bars, cross-decoding condition. Statistical significance was assessed by means of a one-sample t-test against chance (50%). Results were corrected for multiple comparisons using a FDR < 0.05. Significance levels: one black asterisk, p<0.05; two black asterisks, p<0.01; three black asterisks, p<0.001; one red asterisk, q(FDR)<0.05. Error bars: standard error of the mean (S.E.M.).

Tables

Univariate analysis – Perception condition

Area	Cluster Index	Voxels	MAX	MAX X (mm)	MAX Y (mm)	MAX Z (mm)
Right V2	2	21778	7.11	28	-94	-4
Left Dorsal Premotor Cortex (PMd)	1	1395	5.25	-42	8	62

Table S1. Univariate analysis, perception condition. *Table reporting the different clusters resulting from the univariate contrast perception > baseline. Size, location (in MNI coordinates) and anatomical assignments based on the Juelich Histological Atlas are reported.*

Area	Cluster Index	x	y	z
Right Ventral V3	2	28	-94	-4
Right Ventral V3	2	26	-90	-18
Right V2	2	20	-94	-12
Right V2	2	34	-94	-12
Right V1	2	18	-102	-2
Right Ventral V3	2	26	-92	10
Left Dorsal Premotor Cortex (PMd)	1	-42	8	62
Left Dorsal Premotor Cortex (PMd)	1	-26	2	52
Left Broca's Area (BA 44)	1	-48	14	34
Left Broca's Area (BA 44)	1	-44	12	34
Left Broca's Area (BA 44)	1	-44	6	42

Table S2. Univariate analysis, perception condition. *Local maxima for clusters listed in table S1. Location (in MNI coordinates) and anatomical assignments based on the Juelich Histological Atlas are reported.*

Univariate analysis – Imagery condition

Area	Cluster Index	Voxels	Z-MAX X (mm)	Z-MAX Y (mm)	Z-MAX Z (mm)
Left Primary Somatosensory Cortex (S1)	2	1310	-48	-40	62
Left Dorsal Premotor Cortex (PMd)	1	576	-26	0	52

Table S3. Univariate analysis, imagery condition. Table reporting the different clusters resulting from the univariate contrast imagery > baseline. Size, location (in MNI coordinates) and anatomical assignments based on the Juelich Histological Atlas are reported.

Area	Cluster Index	X	Y	Z
Left Primary Somatosensory Cortex (S1)	2	-48	-40	62
Left Anterior Intraparietal Sulcus (aIPS)	2	-36	-42	44
Left Inferior Parietal Lobule (IPL)	2	-54	-42	54
Left Anterior Intraparietal Sulcus (aIPS)	2	-34	-32	38
Left Primary Somatosensory Cortex (S1)	2	-46	-30	46
Left Superior Parietal Lobule (SPL)	2	-32	-58	66
Left Premotor Cortex (PMd)	1	-26	0	52

Table S4. Univariate analysis, Imagery condition. Local maxima for clusters listed in table S3. Location (in MNI coordinates) and anatomical assignments based on the Juelich Histological Atlas are reported.

Univariate differences in activation between categories

Area	Cluster Index	Voxels	Z-MAX X (mm)	Z-MAX Y (mm)	Z-MAX Z (mm)
Right V2	6	1421	24	-92	24
Right Primary Somatosensory Cortex (S1)	5	662	44	-28	48
Left V4	4	521	-18	-80	-14
Right Broca's Area (BA 44)	3	348	48	8	32
Left Primary Somatosensory Cortex (S1)	2	219	-52	-26	40
Left Dorsal Premotor Cortex (PMd)	1	214	-24	2	52

Table S5. Differences in univariate activation between stimulus categories. Table reporting the different clusters resulting from the univariate contrast lowercase letters > simple shapes. Size, location (in MNI coordinates) and anatomical assignments based on the Juelich Histological Atlas are reported.

Searchlight-based analysis – Perception Condition

Area	Cluster Index	Voxels	MAX X (mm)	MAX Y (mm)	MAX Z (mm)
Left V5	5	3300	-42	-75	-9
Left Inferior Parietal Lobule (IPL)	4	83	-54	-42	48
Left Superior Parietal Lobule (SPL)	3	42	-6	-36	39
Left Inferior Parietal Lobule (IPL)	2	19	-45	-54	54
Right Inferior Parietal Lobule (IPL)	1	12	63	-33	36

Table S6. Searchlight-based MVP analysis – Perception condition. Table reporting the different clusters resulting from the MVP classification analysis in the perception condition. Size, location (in MNI coordinates) and anatomical assignments based on the Juelich Histological Atlas are reported.

Area	Cluster Index	X	Y	Z
Left V5	5	-42	-75	-9
Left V2	5	-24	-99	-6
Left V5	5	-39	-69	-12
Right V1	5	12	-102	0
Left Ventral V3 (V3v)	5	-21	-96	-12
Left Ventral V3 (V3v)	5	-18	-96	-3
Left Inferior Parietal Lobule (IPL)	4	-54	-42	48
Left Primary Somatosensory Cortex (S1)	4	-48	-27	42
Left Anterior Intraparietal Sulcus (aIPS)	4	-42	-42	42
Left Primary Somatosensory Cortex (S1)	4	-42	-30	51
Left Anterior Intraparietal Sulcus (aIPS)	4	-48	-42	48
Left Primary Somatosensory Cortex (S1)	4	-48	-27	51
Left Superior Parietal Lobule (SPL)	3	-6	-36	39
Left Superior Parietal Lobule (SPL)	3	-12	-48	24
Left Superior Parietal Lobule (SPL)	3	-6	-51	45
Left Inferior Parietal Lobule (IPL)	2	-45	-54	54
Left Superior Parietal Lobule (SPL)	2	-36	-54	63
Left Inferior Parietal Lobule (IPL)	2	-51	-54	51
Right Inferior Parietal Lobule (IPL)	1	63	-33	36
Right Inferior Parietal Lobule (IPL)	1	54	-42	42
Right Inferior Parietal Lobule (IPL)	1	60	-42	36
Right Inferior Parietal Lobule (IPL)	1	57	-36	36

Table S7. Searchlight-based MVP analysis – Perception condition. Local maxima for clusters listed in table S7. Location (in MNI coordinates) and anatomical assignments based on the Juelich Histological Atlas are reported.

Searchlight-based MVPA – Imagery condition

Area	Cluster Index	Voxels	MAX X (mm)	MAX Y (mm)	MAX Z (mm)
Left Anterior Intraparietal Sulcus (aIPS)	9	475	-27	-63	33
Right Superior Parietal Lobule (SPL)	8	234	24	-63	60
Right V1	7	117	6	-93	9
Left LOC	6	89	-48	-60	-9
Left Dorsal Premotor Cortex (PMd)	5	25	-60	9	30
Right LOC	4	24	39	-72	-12
Right Primary Somatosensory Cortex (S1)	3	18	51	-21	54
Right V4	2	17	36	-84	-3
Right Inferior Parietal Lobule (IPL)	1	16	45	-78	24

Table S8. Searchlight-based MVP analysis – Imagery condition. Table reporting the different clusters resulting from the MVP classification analysis in the imagery condition. Size, location (in MNI coordinates) and anatomical assignments based on the Juelich Histological Atlas are reported.

Area	Cluster Index	Value	x	y	z
Left Anterior Intraparietal Sulcus (aIPS)	9	8.2	-27	-63	33
Left Inferior Parietal Lobule (IPL)	9	5.75	-33	-75	27
Left Superior Parietal Lobule (SPL)	9	5.64	-30	-54	60
Left Superior Parietal Lobule (SPL)	9	5.41	-30	-48	63
Left Primary Somatosensory Cortex (S1)	9	5.41	-39	-39	63
Left Inferior Parietal Lobule (IPL)	9	5.3	-48	-33	39
Right Superior Parietal Lobule (SPL)	8	6.35	24	-63	60
Right Superior Parietal Lobule (SPL)	8	5.55	27	-69	51
Right Superior Parietal Lobule (SPL)	8	4.89	21	-69	60
Right Anterior Intraparietal Sulcus (aIPS)	8	4.51	33	-48	45
Right Superior Parietal Lobule (SPL)	8	4.5	30	-69	39
Right Primary Somatosensory Cortex (S1)	8	4.38	24	-39	54
Right V1	7	5.56	6	-93	9
Right V2	7	5.27	15	-102	15
Right V1	7	5.16	12	-87	3
Left V2	7	4.92	-12	-87	18
Right V1	7	4.63	27	-93	30
Right V1	7	4.62	12	-99	9

Table S9. Searchlight-based MVP analysis – Imagery condition. Local maxima for clusters listed in table S8. Location (in MNI coordinates) and anatomical assignments based on the Juelich Histological Atlas are reported.

Searchlight-based MVPA – Cross-condition decoding

Area	Cluster Index	Voxels	MAX X (mm)	MAX Y (mm)	MAX Z (mm)
Left LOC	9	208	-57	-54	-6
Left Superior Parietal Lobule (SPL)	8	109	-21	-51	60
Left Inferior Parietal Lobule (IPL)	7	75	-42	-72	27
Left Primary Somatosensory Cortex (S1)	6	30	-48	-36	54
Right Superior Parietal Lobule (SPL)	5	24	15	-66	54
Left Primary Somatosensory Cortex (S1)	4	22	-45	-18	42
Left Anterior Intraparietal Sulcus (aIPS)	3	15	-36	-33	39
Right V2	2	15	9	-93	27
Left Inferior Parietal Lobule (IPL)	1	13	-33	-84	36

Table S10. Searchlight-based MVP analysis – Cross-decoding condition. Table reporting the different clusters resulting from the MVP classification analysis in the Cross-decoding condition. Size, location (in MNI coordinates) and anatomical assignments based on the Juelich Histological Atlas are reported.

Supplementary materials: chapter 3

Group ROIs – Normal Sighted Participants

ROI	Cluster Index	Voxels	Z-MAX X (mm)	Z-MAX Y (mm)	Z-MAX Z (mm)
RHd (Lower Left Quadrant)	4	684	46	-74	6
LHv (Upper Right Quadrant)	3	596	-24	-70	-10
LHd (Lower Right Quadrant)	2	385	-12	-98	10
RHv (Upper Left Quadrant)	1	352	24	-66	-8

Table S6. Position of the dorsal (red) and ventral (blue) ROIs, averaged across normal sighted participants.

Normal Sighted Participants – Attention Condition

To understand whether directing attention to individual quadrants within the visual field could induce a selective recruitment of individual portions of EVC, we computed the spatial selectivity index in analogy to the imagery and perception condition (see *Chapter 3.3, Material and Methods*). This analysis was performed for normal sighted participants only.

Results are summarized in *Figure S2*. As can be seen, we obtained a spatially-selective recruitment during the attention condition in the dorsal and ventral ROIs of the left primary visual cortex [LHv: M=0.448, SD=0.298; $t(10) = 4.987$, $p<0.001$. LHd: M=0.54, SD=0.662; $t(10) = 2.707$, $p=0.022$], and in the corresponding dorsal and ventral ROIs of the right hemisphere [RHv: M=0.276, SD=0.398; $t(10) = 2.307$, $p=0.044$. RHd: M=0.665, SD=0.516; $t(10) = 4.272$, $p=0.0016$].

Moreover, to understand whether there are differences in the recruitment of early visual cortex between visual mental imagery and attention, we compared the selectivity index computed in the two tasks by means of a repeated measures ANOVA (factors: experimental condition, quadrants). The analysis did not highlight significant differences in the magnitude of the spatial selectivity index between the imagery and attention condition [main effect of experimental condition: $F(1, 10) = 0.156$, $p = 0.701$]. We found an overall weaker recruitment of the upper left quadrant with respect to the lower left and upper right quadrants [main effect

of quadrant: F(3, 30) = 4.032, p = 0.016; paired-samples t-tests: Lower Left (M = 0.53, SD = 0.3) vs Upper Left (M = 0.26, SD = 0.30); t(10) = 2.591, p = 0.027. Upper Right (M = 0.70, SD = 0.36) vs Upper Left (M = 0.26, SD = 0.30); t(10) = 4.046, p = 0.002]. No interaction effect between quadrants and experimental condition was found [interaction experimental condition*quadrant: F(3, 30) = 0.24 7, p = 0.862. *Figure S4*]

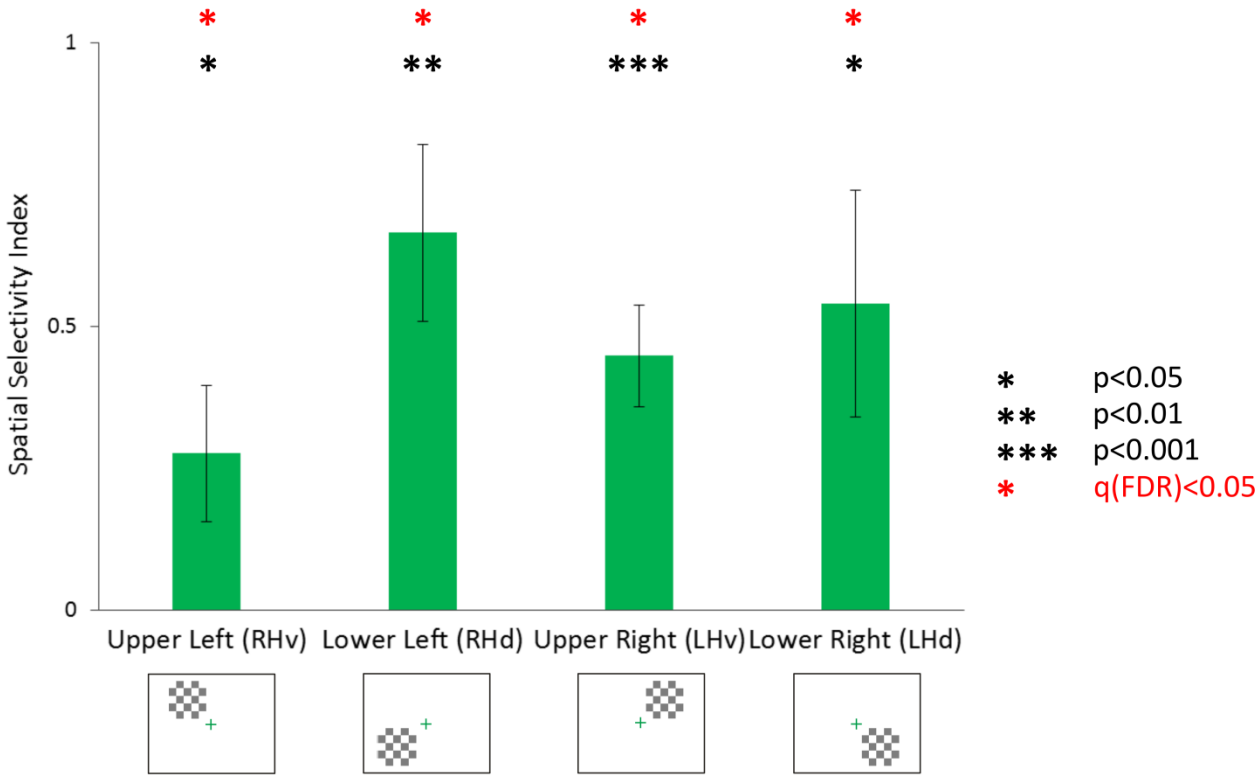

Figure S2. Normal sighted participants. Spatial selectivity index during the attention condition, separately for the four ROIs in early visual cortex (EVC) corresponding to stimulation of the upper left, upper right, lower left and lower right quadrant. Results were corrected for multiple comparisons using a FDR < 0.05. RHv, right hemisphere ventral; LHv, left hemisphere ventral; RHd, right hemisphere dorsal; LHd, left hemisphere dorsal. Significance levels: one black asterisk, p<0.05; two black asterisks, p<0.01; three black asterisks, p<0.001, one red asterisk, q(FDR)<0.05. Error bars represents the standard error of the mean (S.E.M.).

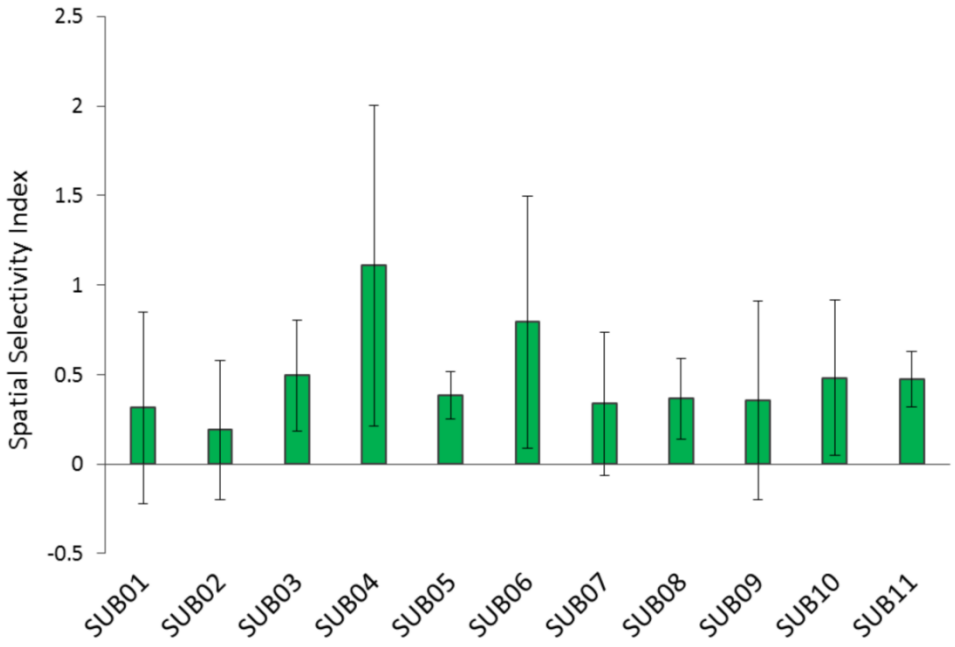

Figure S3. Normal sighted participants. Spatial selectivity index during the attention condition, computed separately for each individual normal sighted participants. Error bars represents the standard deviation in the magnitude of the eccentricity effect across the four quadrants.

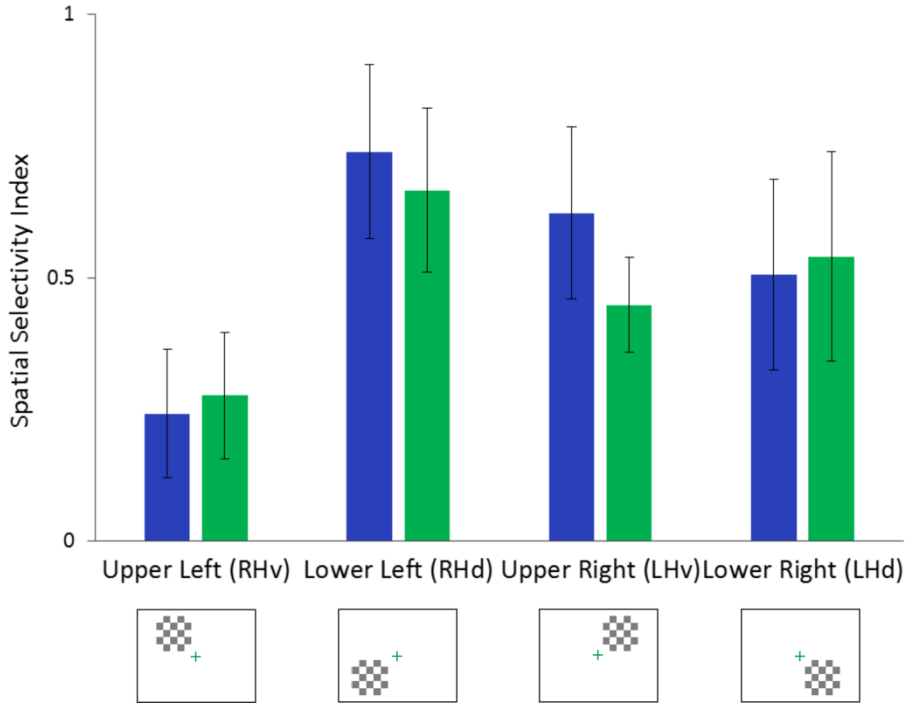

Figure S4. Normal sighted participants. Comparison between the spatial selectivity index during the imagery (Blue) and attention condition (green), computed separately for each individual normal sighted participants. Error bars represents the standard error of the mean (S.E.M.).

Hemianopic Patients – Spatial Selectivity Index

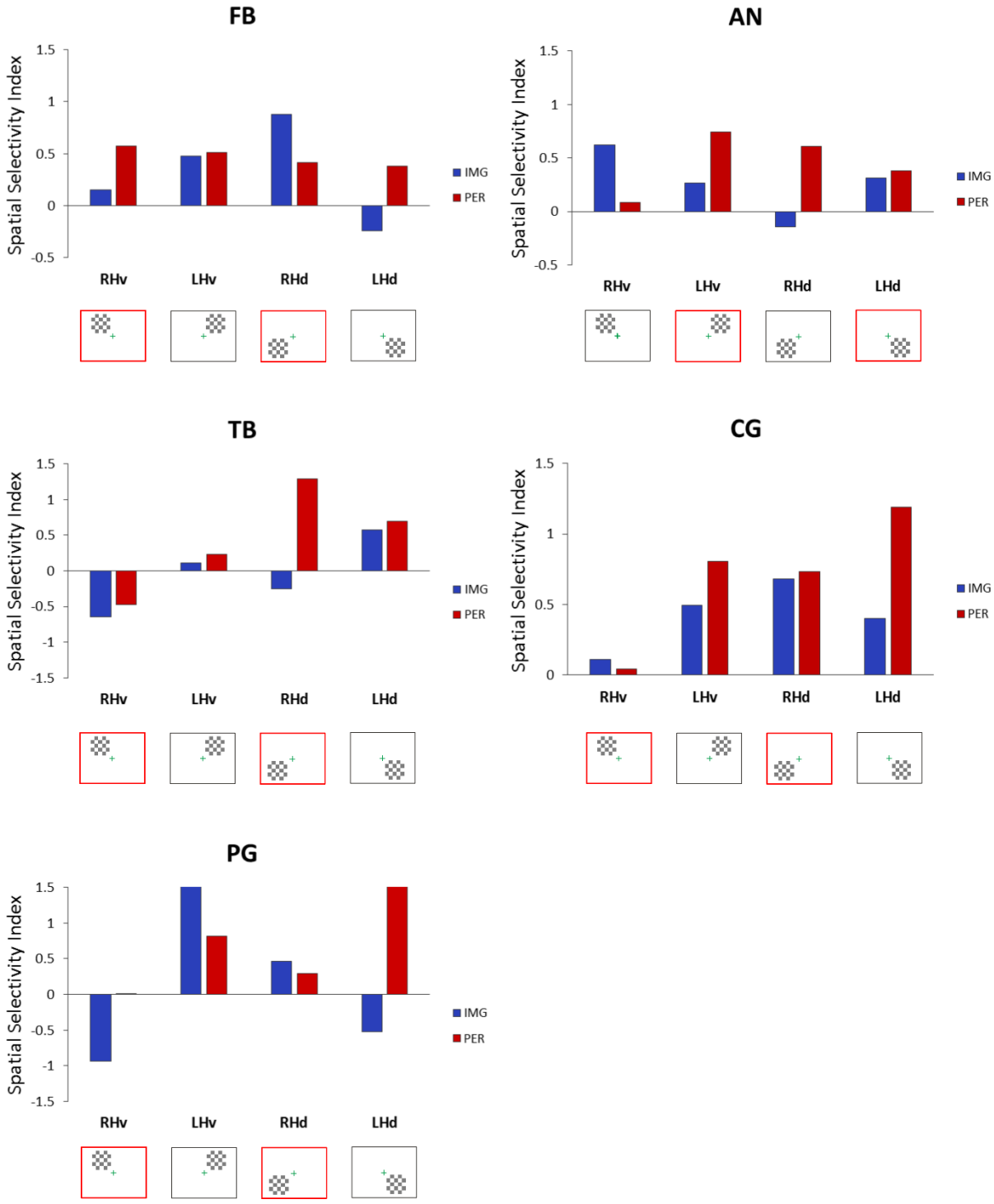

Figure S5. Spatial selectivity index computed for the imagery and perception condition, individually for each hemianopic patient. Beta values were extracted from dorsal and ventral ROIs in the two hemispheres defined based on the group results in normal sighted participants. Data from dorsal and ventral ROIs are shown separately for both the healthy and damaged hemisphere. Damaged ROIs are highlighted in red.

References

Albers, A. M., Kok, P., Toni, I., Dijkerman, H. C., & de Lange, F. P. (2013). Shared representations for working memory and mental imagery in early visual cortex. *Current Biology*, *23*(15), 1427–31. http://doi.org/10.1016/j.cub.2013.05.065

Albert, N. B., Robertson, E. M., Mehta, P., & Miall, R. C. (2009). Resting state networks and memory consolidation. *Communicative & Integrative Biology*, *2*(6), 530–2. http://doi.org/10.4161/CIB.2.6.9612

Amedi, A., Malach, R., & Pascual-Leone, A. (2005). Negative BOLD differentiates visual imagery and perception. *Neuron*, *48*(5), 859–872. http://doi.org/10.1016/j.neuron.2005.10.032

Anderson, R., & Bower, G. H. (1974). A propositional theory of recognition memory. *Memory & Cognition*, *2*(3), 406–412. http://doi.org/10.3758/BF03196896

Andersson, P., Ragni, F., & Lingnau, A. (in revision). Visual imagery during real-time fMRI neurofeedback from occipital and superior parietal cortex.

Bannert, M. M., & Bartels, A. (2013). Decoding the yellow of a gray banana. *Current Biology*, *23*, 2268–2272. http://doi.org/10.1016/j.cub.2013.09.016

Behrmann, M., Moscovitch, M., & Winocur, G. (1994). Intact visual imagery and impaired visual perception in a patient with visual agnosia. *Journal of Experimental Psychology: Human Perception and Performance*, *20*(5), 1068–1087. http://doi.org/10.1037/0096-1523.20.5.1068

Benjamini, Y., & Yekutieli, D. (2001). The control of the false discovery rate in multiple testing under dependency. *Annals of Statistics*, *29*(4), 1165–1188. http://doi.org/10.1214/aos/1013699998

Bergmann, J., Genç, E., Kohler, A., Singer, W., & Pearson, J. (2016). Smaller primary visual cortex is associated with stronger, but less precise mental imagery. *Cerebral Cortex*, *26*(9), 3838–3850. http://doi.org/10.1093/cercor/bhv186

Bisiach, E., & Luzzatti, C. (1978). Unilateral neglect of representational space. *Cortex*, *14*(1), 129–33. Retrieved from http://www.ncbi.nlm.nih.gov/pubmed/16295118

Bowers, A. R., Keeney, K., & Peli, E. (2008). Community-based trial of a peripheral prism visual field expansion device for hemianopia. *Archives of Ophthalmology*, *126*(5), 657–64. http://doi.org/10.1001/archopht.126.5.657

Brainard, D. H. (1997). The Psychophysics Toolbox. *Spatial Vision*, *10*, 433–436.

Bridge, H., Harrold, S., Holmes, E. a., Stokes, M., & Kennard, C. (2012). Vivid visual mental imagery in the absence of the primary visual cortex. *Journal of Neurology*, *259*(6), 1062–1070. http://doi.org/10.1007/s00415-011-6299-z

Bullier, J. (2001). *Integrated model of visual processing*. *Brain Research Reviews* (Vol. 36).

Cattaneo, Z., Vecchi, T., Pascual-Leone, A., & Silvanto, J. (2009). Contrasting early visual cortical activation states causally involved in visual imagery and short-term memory. *European Journal of Neuroscience*, *30*(7), 1393–1400. http://doi.org/10.1111/j.1460-9568.2009.06911.x

Chelazzi, L, Marzi CA, Panozzo G, Pasqualini N, Tassinari G, T. L. (1988). Hemiretinal differences in speed of light detection in esotropic amblyopes. *Vision Research*, *28*.

Christophel, T. B., Hebart, M. N., & Haynes, J.-D. (2012). Decoding the contents of visual short-term memory from human visual and parietal cortex. *Journal of Neuroscience*, *32*(38), 12983–12989. http://doi.org/10.1523/JNEUROSCI.0184-12.2012

Christophel, T. B., & Haynes, J. D. (2014). Decoding complex flow-field patterns in visual working memory. *NeuroImage*, *91*, 43–51. http://doi.org/10.1016/j.neuroimage.2014.01.025

Cichy, R. M., Heinzle, J., & Haynes, J. D. (2012). Imagery and perception share cortical representations of content and location. *Cerebral Cortex*, *22*(2), 372–380. http://doi.org/10.1093/cercor/bhr106

Cui, X., Jeter, C. B., Yang, D., Montague, P. R., & Eagleman, D. M. (2007). Vividness of mental imagery: individual variability can be measured objectively. *Vision Research*, *47*(4), 474–478. http://doi.org/10.1016/j.visres.2006.11.013

Daselaar, S. M., Porat, Y., Huijbers, W., & Pennartz, C. M. (2010). Modality-specific and modality-independent components of the human imagery system. *NeuroImage*, *52*, 677–685. http://doi.org/10.1016/j.neuroimage.2010.04.239

de Borst, A. W., Sack, A. T., Jansma, B. M., Esposito, F., De Martino, F., Valente, G., … Formisano, E. (2012). Integration of "what" and "where" in frontal cortex during visual imagery of scenes. *NeuroImage*, *60*(1), 47–58. http://doi.org/10.1016/j.neuroimage.2011.12.005

de Gelder, B., Tamietto, M., Pegna, A. J., & Van den Stock, J. (2014). Visual imagery influences brain responses to visual stimulation in bilateral cortical blindness. *Cortex*, *72*, 1–12. http://doi.org/10.1016/j.cortex.2014.11.009

Dechent, P., Merboldt, K.-D., & Frahm, J. (2004). Is the human primary motor cortex involved in motor imagery? *Cognitive Brain Research*, *19*(2), 138–144. http://doi.org/10.1016/J.COGBRAINRES.2003.11.012

Dentico, D., Cheung, B. L., Chang, J. Y., Guokas, J., Boly, M., Tononi, G., & Van Veen, B. (2014). Reversal of cortical information flow during visual imagery as compared to visual perception. *NeuroImage*, *100*, 237–243. http://doi.org/10.1016/j.neuroimage.2014.05.081

D'Esposito, M., Detre, J. A., Aguirre, G. K., Stallcup, M., Alsop, D. C., Tippet, L. J., & Farah, M. J. (1997). A functional MRI study of mental image generation. *Neuropsychologia*, *35*(5), 725–30. Retrieved from http://www.ncbi.nlm.nih.gov/pubmed/9153035

Dijkstra, N., Zeidman, P., Ondobaka, S., Van Gerven, M. A. J., & Friston, K. (2017). Distinct top-down and bottom-up brain connectivity during visual perception and imagery. *Scientific Reports*, *7*(1), 1–9. http://doi.org/10.1038/s41598-017-05888-8

Dijkstra, N., Bosch, S., & van Gerven, M. A. J. (2017). Vividness of visual imagery depends on the neural overlap with perception in visual areas. *Journal of Neuroscience*, *37*(5), 1367–1373. http://doi.org/10.1523/JNEUROSCI.3022-16.2016

Diller, L., Weinberg, J., Gordon, W., & Goodkin, R. (1974). Studies in cognition and rehabilitation in hemiplegia. *Rehabilitation Monograph*, *50*.

Dubois, J., de Berker, A. O., & Tsao, D. Y. (2015). Single-unit recordings in the macaque face patch system reveal limitations of fMRI MVPA. *Journal of Neuroscience*, *35*(6), 2791–2802. http://doi.org/10.1523/JNEUROSCI.4037-14.2015

Eickhoff, S. B., Paus, T., Caspers, S., Grosbras, M.-H., Evans, A. C., Zilles, K., & Amunts, K. (2007). Assignment of functional activations to probabilistic cytoarchitectonic areas revisited. *NeuroImage*, *36*(3), 511–521. http://doi.org/10.1016/j.neuroimage.2007.03.060

Engel, S., Glover, G. H., & Wandell, B. A. (1997). Retinotopic organization in human visual cortex and the spatial precision of functional MRI. *Cerebral Cortex*, *7*(2), 181–192. http://doi.org/10.1093/cercor/7.2.181

Epstein, R., Harris, A., Stanley, D., & Kanwisher, N. (1999). The Parahippocampal Place Area. *Neuron*, *23*(1), 115–125. http://doi.org/10.1016/S0896-6273(00)80758-8

Etzel, J. A., Zacks, J. M., & Braver, T. S. (2013). Searchlight analysis: Promise, pitfalls, and potential. *NeuroImage*, *78*, 261–269. http://doi.org/10.1016/j.neuroimage.2013.03.041

Farah, M. J. (1988). Is visual imagery really visual? Overlooked evidence from neuropsychology. *Psychological Review*, *95*(3), 307–317. http://doi.org/10.1037/0033-295X.95.3.307

Farah, M. J. (1984). The neurological basis of mental imagery: A componential analysis. *Cognition*, *18*(1–3), 245–272. http://doi.org/10.1016/0010-0277(84)90026-X

Folstein, M. F., Folstein, S. E., & McHugh, P. R. (1975). Mini-mental state: A practical method for grading the cognitive state of patients for the clinician. *Journal of Psychiatric Research*, *12*(3), 189–98.

Formisano, E., Linden, D. E. J., Di Salle, F., Trojano, L., Esposito, F., Sack, A. T., … Goebel, R. (2002). Tracking the mind's image in the brain I: Time-resolved fMRI during visuospatial mental imagery. *Neuron*, *35*(1), 185–194. http://doi.org/10.1016/S0896-6273(02)00747-X

Fulford, J., Milton, F., Salas, D., Smith, A., Simler, A., Winlove, C., & Zeman, A. (2018). The neural correlates of visual imagery vividness – An fMRI study and literature review. *Cortex*, *105*, 26–40. http://doi.org/10.1016/j.cortex.2017.09.014

Ganis, G., Thompson, W. L., & Kosslyn, S. M. (2004). Brain areas underlying visual mental imagery and visual perception: An fMRI study. *Cognitive Brain Research*, *20*(2), 226–241. http://doi.org/10.1016/j.cogbrainres.2004.02.012

Gauthier, L., Dehaut, F., & Joanette, Y. (1989). The Bells Test: A quantitative and qualitative test for visual neglect. *International Journal of Clinical Neuropsychology*, *11*(2), 49–54.

Gbadamosi, J., & Zangemeister, W. H. (2001). Visual imagery in hemianopic patients. *Journal of Cognitive Neuroscience*, *13*(7), 855–866. http://doi.org/10.1097/JCP.0b013e318283963b

Giorgi, R. G., Woods, R. L., & Peli, E. (2009). Clinical and laboratory evaluation of peripheral prism glasses for hemianopia. *Optometry and Vision Science*, *86*(5), 492–502. http://doi.org/10.1097/OPX.0b013e31819f9e4d

Glover, S., Peter, A. E., Ae, D., Castiello, U., & Rushworth, M. F. S. (2005). Effects of an orientation illusion on motor performance and motor imagery. http://doi.org/10.1007/s00221-005-2328-4

Goodwin, D. (2014, September 22). Homonymous hemianopia: Challenges and solutions. *Clinical Ophthalmology*. Dove Press. http://doi.org/10.2147/OPTH.S59452

Grefkes, C., & Fink, G. R. (2011). Reorganization of cerebral networks after stroke: new insights from neuroimaging with connectivity approaches. *Brain*, *134*(5), 1264–1276. http://doi.org/10.1093/brain/awr033

Grill-Spector, K. (2003). The neural basis of object perception. *Current Opinion in Neurobiology*, *13*, 159–156. http://doi.org/10.1016/S0959-4388(03)00040-0

Grill-Spector, K., Kourtzi, Z., & Kanwisher, N. (2001). The lateral occipital complex and its role in object recognition. *Vision Research*, *41*(10–11), 1409–1422. http://doi.org/10.1016/S0042-6989(01)00073-6

Grill-Spector, K., Kushnir, T., Edelman, S., Avidan, G., Itzchak, Y., & Malach, R. (1999). Differential processing of objects under various viewing conditions in the human lateral occipital complex. *Neuron*, *24*(1), 187–203. http://doi.org/10.1016/S0896-6273(00)80832-6

Halpern, A. R., Zatorre, R. J., Bouffard, M., & Johnson, J. A. (2004). Behavioral and neural correlates of perceived and imagined musical timbre. *Neuropsychologia*, *42*(9), 1281–1292. http://doi.org/10.1016/j.neuropsychologia.2003.12.017

Hanakawa, T., Dimyan, M. A., & Hallett, M. (2008). Motor planning, imagery, and execution in the distributed motor network: a time-course study with functional MRI. *Cerebral Cortex December*, *18*, 2775–2788. http://doi.org/10.1093/cercor/bhn036

Hardiess, G., Papageorgiou, E., Schiefer, U., & Mallot, H. A. (2010). Functional compensation of visual field deficits in hemianopic patients under the influence of different task demands. *Vision Research*, *50*(12), 1158–1172. http://doi.org/10.1016/j.visres.2010.04.004

Harrington, B. (2004). Inkscape. Retrieved from http://www.inkscape.org

Hassabis, D., Kumaran, D., & Maguire, E. A. (2007). Using imagination to understand the neural basis of episodic memory. *The Journal of Neuroscience : The Official Journal of the Society for Neuroscience*, *27*(52), 14365–74. http://doi.org/10.1523/JNEUROSCI.4549-07.2007

Haxby, J. V. (2001). Distributed and overlapping representations of faces and objects in ventral temporal cortex. *Science*, *293*(5539), 2425–2430. http://doi.org/10.1126/science.1063736

Haxby, J. V, Connolly, A. C., & Guntupalli, J. S. (2014). Decoding neural representational spaces using multivariate pattern analysis. *Annual Review of Neuroscience*, *37*(1), 435–456. http://doi.org/10.1146/annurev-neuro-062012-170325

Haxby, J. V, Grady, C. L., Horwitz, B., Ungerleider, L. G., Mishkin, M., Carson, R. E., … Rapoport, S. I. (1991). Dissociation of object and spatial visual processing pathways in human extrastriate cortex. *Neurobiology*, *88*(March), 1621–1625.

Haxby, J. V, Ungerleider, L. G., Clark, V. P., Schouten, J. L., Hoffman, E. A., & Martin, A. (1999). The effect of face inversion on activity in human neural systems for face and object perception. *Neuron*, *22*, 189–199.

Hayes, J. R. (1973). On the function of visual imagery on elementary mathematics. In *Visual Information Processing* (pp. 177–214). Elsevier. http://doi.org/10.1016/B978-0-12-170150-5.50010-X

He, B. J., Snyder, A. Z., Vincent, J. L., Epstein, A., Shulman, G. L., & Corbetta, M. (2007). Breakdown of functional connectivity in frontoparietal networks underlies behavioral deficits in spatial neglect. *Neuron*, *53*(6), 905–918. http://doi.org/10.1016/j.neuron.2007.02.013

Hubel, D. (1995). *Eye, brain, and vision.* Scientific American library series.

Hume, D. (1739). *A treatise of human nature*. (firs baronet, Sir Lewis Amherst Selby-Bigge & P. H. Nidditch, Eds.), *A Treatise of Human Nature*. Oxford University Press. http://doi.org/10.1080/10848770600668399

Ishai, A. (2002). Visual imagery of famous faces: effects of memory and attention revealed by fMRI. *NeuroImage*, *17*(4), 1729–1741. http://doi.org/10.1006/nimg.2002.1330

Ishai, A., Ungerleider, L. G., & Haxby, J. V. (2000). Distributed neural systems for the generation of visual images. *Neuron*, *28*(3), 979–90. http://doi.org/10.1016/s0896-6273(00)00168-9

Ishiai, S., Furukawa, T., & Tsukagoshi, H. (1987). Eye-fixation patterns in homonymous hemianopia and unilateral spatial neglect. *Neuropsychologia*, *25*(4), 675–679. http://doi.org/10.1016/0028-3932(87)90058-3

Jenkinson, M., & Smith, S. (2001). A global optimisation method for robust affine registration of brain images. *Medical Image Analysis*, *5*(2), 143–56.

Jenkinson, M., Bannister, P., Brady, M., & Smith, S. (2002). Improved optimization for the robust and accurate linear registration and motion correction of brain images. *NeuroImage*, *17*, 825–841. http://doi.org/10.1006/nimg.2002.1132

Johnstone, T., Ores Walsh, K. S., Greischar, L. L., Alexander, A. L., Fox, A. S., Davidson, R. J., & Oakes, T. R. (2006). Motion correction and the use of motion covariates in multiple-subject fMRI analysis. *Human Brain Mapping*, *27*(10), 779–788. http://doi.org/10.1002/hbm.20219

Kanwisher, N., McDermott, J., & Chun, M. M. (1997). The Fusiform Face Frea: A module in human extrastriate cortex specialized for face perception. *The Journal of Neuroscience*, *17*(11), 4302–4311. http://doi.org/10.1109/CDC.2005.1583375

Kastner, S., & Ungerleider, L. G. (2000). Mechanisms of visual attention in the human cortex. *Annual Review of Neuroscience*, *23*(1), 315–341. http://doi.org/10.1146/annurev.neuro.23.1.315

Kitterle, F. L. (1986). Psychophysics of lateral tachistoscopic presentation. *Brain and Cognition*, *5*(2), 131–162. http://doi.org/10.1016/0278-2626(86)90052-7

Klein, I., Dubois, J., Mangin, J. F., Kherif, F., Flandin, G., Poline, J. B., … Le Bihan, D. (2004). Retinotopic organization of visual mental images as revealed by functional magnetic resonance imaging. *Cognitive Brain Research*, *22*(1), 26–31. http://doi.org/10.1016/j.cogbrainres.2004.07.006

Klein, I., Paradis, A.-L., Poline, J.-B., Kosslyn, S. M., & Le Bihan, D. (2000). Transient activity in the human calcarine cortex during visual-mental imagery: An event-related fMRI study. *Journal of Cognitive Neuroscience*, *12*(supplement 2), 15–23. http://doi.org/10.1162/089892900564037

Knauff, M., Kassubek, J., Mulack, T., & Greenlee, M. W. (2000). Cortical activation evoked by visual mental imagery as measured by fMRI. *Neuroreport*, *11*(18), 3957–3962. http://doi.org/10.1097/00001756-200012180-00011

Kosslyn, S. M., Pascual-Leone, a, Felician, O., Camposano, S., Keenan, J. P., Thompson, W. L., … Alpert, N. M. (1999). The role of area 17 in visual imagery: convergent evidence from PET and rTMS. *Science (New York, NY)*, *284*(5411), 167–170. http://doi.org/10.1126/science.284.5411.167

Kosslyn, S. M. (1995). *Image and mind*. Harvard University Press. http://doi.org/10.1017/CBO9780511551277

Kosslyn, S. M. (1981). The medium and the message in mental imagery: A theory. *Psychological Review*, *88*(1), 46–66. http://doi.org/10.1037/0033-295X.88.1.46

Kosslyn, S. M. (2005). Mental images and the Brain. *Cognitive Neuropsychology*, *22*(3–4), 333–347. http://doi.org/10.1080/02643290442000130

Kosslyn, S. M., Alpert, N. M., Thompson, W. L., Maljkovic, V., Weise, S. B., Chabris, C. F., … Buonanno, F. S. (1993). Visual mental imagery activates topographically organized visual cortex: PET investigations. *Journal of Cognitive Neuroscience*, *5*, 263–287. http://doi.org/10.1162/jocn.1993.5.3.263

Kosslyn, S. M., & Ochsner, K. N. (1994). In search of occipital activation during visual mental imagery. *Trends in Neurosciences*, *17*(7), 290–292. http://doi.org/10.1016/0166-2236(94)90059-0

Kosslyn, S. M., & Thompson, W. L. (2003). When is early visual cortex activated during visual mental imagery? *Psychological Bulletin*, *129*(5), 723–746. http://doi.org/10.1037/0033-2909.129.5.723

Kosslyn, S. M., Thompson, W. L., Kim, I. J., Rauch, S. L., & Alpert, N. M. (1996). Individual differences in cerebral blood flow in area 17 predict the time to evaluate visualized letters. *Journal of Cognitive Neuroscience*, *8*(1), 78–82. http://doi.org/10.1162/jocn.1996.8.1.78

Kosslyn, S. M., Thompson, W. L., Klm, I. J., & Alpert, N. M. (1995). Topographical representations of mental images in primary visual cortex. *Nature*, *378*(6556), 496–498. http://doi.org/10.1038/378496a0

Kosslyn, S. M. (1973). Scanning visual images: Some structural implications. *Perception & Psychophysics*, *14*(1), 90–94.

Kourtzi, Z., & Kanwisher, N. (2000). Cortical regions involved in perceiving object shape. *The Journal of Neuroscience : The Official Journal of the Society for Neuroscience*, *20*(9), 3310–8.

Kriegeskorte, N., Goebel, R., & Bandettini, P. (2006). Information-based functional brain mapping. *Proceedings of the National Academy of Sciences of the United States of America*, *103*, 3863–3868. http://doi.org/10.1073/pnas.0600244103

Langheim, F. J. P., Callicott, J. H., Mattay, V. S., Duyn, J. H., & Weinberger, D. R. (2002). Cortical systems associated with covert music rehearsal. http://doi.org/10.1006/nimg.2002.1144

Lee, S., Kravitz, D. J., & Baker, C. I. (2012). Disentangling visual imagery and perception of real-world objects. *NeuroImage*, *59*(4), 4064–4073. http://doi.org/10.1016/j.neuroimage.2011.10.055

Levine, D. N., Warach, J., & Farah, M. (1985). Two visual systems in mental imagery: dissociation of what and where in imagery disorders due to bilateral posterior cerebral lesions. *Neurology*, *35*(7), 1010–8. Retrieved from http://www.ncbi.nlm.nih.gov/pubmed/4010939

Lewis, C. M., Baldassarre, A., Committeri, G., Romani, G. L., & Corbetta, M. (2009). Learning sculpts the spontaneous activity of the resting human brain. *Proceedings of the National Academy of Sciences*, *106*(41), 17558 –17563.

Mangione, C. M., Lee, P. P., Gutierrez, P. R., Spritzer, K., Berry, S., & Hays, R. D. (1960). National Eye institute visual function questionnaire field test investigators. Development of the 25-item national Eye institute visual function questionnaire. *Arch Ophthalmol*, *119*, 1050–1058.

Marks, D. F. (1973). Visual imagery differences in the recall of pictures. *British Journal of Psychology*, *64*(1), 17–24. http://doi.org/10.1111/j.2044-8295.1973.tb01322.x

Marzi, C., Mancini, F., Metitieri, T., & Savazzi, S. (2006). Retinal eccentricity effects on reaction time to imagined stimuli. *Neuropsychologia*, *44*(8), 1489–1495. http://doi.org/10.1016/j.neuropsychologia.2005.11.012

Marzi, C. a., & Di Stefano, M. (1981). Hemiretinal differences in visual perception. *Documenta Ophthalmologica, Proceeding Series*, *30*, 273–278. http://doi.org/10.1371/journal.pone.0094539

Mechelli, a. (2004). Where bottom-up meets top-down: Neuronal interactions during perception and imagery. *Cerebral Cortex*, *14*(11), 1256–1265. http://doi.org/10.1093/cercor/bhh087

Mellet, E., Briscogne, S., Tzourio-Mazoyer, N., Ghaëm, O., Petit, L., Zago, L., … Denis, M. (2000). Neural correlates of topographic mental exploration: the impact of route versus survey perspective learning. *NeuroImage*, *12*(5), 588–600. http://doi.org/10.1006/nimg.2000.0648

Mellet, E., Tzourio, N., Crivello, F., Joliot, M., Denis, M., & Mazoyer, B. (1996). Functional anatomy of spatial mental imagery generated from verbal instructions. *J Neurosci*, *16*(20), 6504–6512. http://doi.org/8815928

Miller, G. A. (2003). The cognitive revolution: a historical perspective. *TRENDS in Cognitive Sciences*, *7*(3), 141–144. http://doi.org/10.1016/S1364-6613(03)00029-9

Misaki, M., Kim, Y., Bandettini, P. A., & Kriegeskorte, N. (2010). Comparison of multivariate classifiers and response normalizations for pattern-information fMRI. *NeuroImage*, *53*(1), 103–118. http://doi.org/10.1016/j.neuroimage.2010.05.051

Monaco, S., Malfatti, G., Pizzato, L., Cattaneo, L., & Turella, L. (2018). Decoding action intention from the activity pattern in the Foveal Cortex. *Journal of Vision*, *18*(10), 72. http://doi.org/10.1167/18.10.72

Moro, V., Berlucchi, G., Lerch, J., Tomaiuolo, F., & Aglioti, S. M. (2008). Selective deficit of mental visual imagery with intact primary visual cortex and visual perception. *Cortex*, *44*(2), 109–118. http://doi.org/10.1016/j.cortex.2006.06.004

Muckli, L., Kohler, A., Kriegeskorte, N., & Singer, W. (2005). Primary visual cortex activity along the apparent-motion trace reflects illusory perception. *PLoS Biology*, *3*(8). http://doi.org/10.1371/journal.pbio.0030265

Muckli, L., & Petro, L. S. (2013). Network interactions: Non-geniculate input to V1. *Current Opinion in Neurobiology*. http://doi.org/10.1016/j.conb.2013.01.020

Naughtin, C. K., Mattingley, J. B., & Dux, P. E. (2016). Distributed and overlapping neural substrates for object individuation and identification in visual short-term memory. *Cerebral Cortex*, *26*(2), 566–575. http://doi.org/10.1093/cercor/bhu212

O'Craven, K. M., & Kanwisher, N. (2000). Mental imagery of faces and places activates corresponding stimulus-specific brain regions. *Journal of Cognitive Neuroscience*, *12*(6), 1013–1023. http://doi.org/10.1162/08989290051137549

Oliva, A., & Torralba, A. (2001). Modeling the shape of the scene: A holistic representation of the spatial envelope. *International Journal of Computer Vision*, *42*(3), 145–175. http://doi.org/10.1023/A:1011139631724

O'Neill, E. C., Connell, P. P., O'Connor, J. C., Brady, J., Reid, I., & Logan, P. (2011). Prism therapy and visual rehabilitation in homonymous visual field loss. *Optometry and Vision Science*, *88*(2), 263–268. http://doi.org/10.1097/OPX.0b013e318205a3b8

Oosterhof, N. N., Connolly, A. C., & Haxby, J. V. (2016). CoSMoMVPA: multi-modal Multivariate Pattern Analysis of neuroimaging data in Matlab/GNU Octave. *Frontiers in Neuroinformatics*, *10*, 27. http://doi.org/10.3389/fninf.2016.00027

Oosterhof, N. N., Tipper, S. P., & Downing, P. E. (2012). Visuo-motor imagery of specific manual actions: A multi-variate pattern analysis fMRI study. http://doi.org/10.1016/j.neuroimage.2012.06.045

Pambakian, A. L. M., Mannan, S. K., & Hodgson, T. L. (2004). Saccadic visual search training: a treatment for patients with homonymous hemianopia. *J Neurol Neurosurg Psychiatry*, *75*, 1443–1448. http://doi.org/10.1136/jnnp.2003.025957

Pambakian, A. L. M., & Kennard, C. (1997). Can visual function be restored in patients with homonymous hemianopia? *British Journal of Ophthalmology*. http://doi.org/10.1136/bjo.81.4.324

Papageorgiou, E., Hardiess, G., Mallot, H. A., & Schiefer, U. (2012). Gaze patterns predicting successful collision avoidance in patients with homonymous visual field defects. *Vision Research*, *65*, 25–37. http://doi.org/10.1016/J.VISRES.2012.06.004

Pearson, J., Naselaris, T., Holmes, E. A., & Kosslyn, S. M. (2015). Mental imagery: functional mechanisms and clinical applications. *Trends in Cognitive Sciences*, *19*(10), 590–602. http://doi.org/10.1016/J.TICS.2015.08.003

Peli, E. (2000). Field expansion for homonymous hemianopia by optically Induced peripheral exotropia. *Optometry and Vision Science*, *77*(9), 453–464.

Perky, C. W. (1910). An experimental study of imagination. *The American Journal of Psychology*, *21*(3), 422. http://doi.org/10.2307/1413350

Petersen, S. E., & Dubis, J. W. (2011). The mixed block/event-related design. *NeuroImage*, *62*(2), 1177-84.

Pouget, M.-C., Lévy-Bencheton, D., Prost, M., Tilikete, C., Husain, M., & Jacquin-Courtois, S. (2012). Acquired visual field defects rehabilitation: Critical review and perspectives. *Annals of Physical and Rehabilitation Medicine*, *55*(1), 53–74. http://doi.org/10.1016/j.rehab.2011.05.006

Pourtois, G., Schwartz, S., Spiridon, M., Martuzzi, R., & Vuilleumier, P. (2009). Object representations for multiple visual categories overlap in lateral occipital and medial fusiform cortex. *Cerebral Cortex*, *19*(8), 1806–1819. http://doi.org/10.1093/cercor/bhn210

Pylyshyn, Z. (2003). Return of the mental image: Are there really pictures in the brain? *Trends in Cognitive Sciences*, *7*(3), 113–118. http://doi.org/10.1016/S1364-6613(03)00003-2

Pylyshyn, Z. W. (2013). The imagery debate: analogue media versus tacit knowledge. *Readings in Cognitive Science: A Perspective from Psychology and Artificial Intelligence*, *88*(1), 600–614. http://doi.org/10.1016/B978-1-4832-1446-7.50051-0

Pylyshyn, Z. W. (1973). What the mind's eye tells the mind's brain: A critique of mental imagery. *Psychological Bulletin*, *80*(1), 1–24. http://doi.org/10.1037/h0034650

Pylyshyn, Z. W. (2002). Mental imagery: In search of a theory. *Behavioral and Brain Sciences*, *25*(02), 157–237. http://doi.org/10.1017/S0140525X02000043

Reddy, L., Tsuchiya, T., & Serre, T. (2011). Reading the mind's eye: decoding category information during mental imagery. *Neuroimage*, *50*(2), 818–825. http://doi.org/10.1016/j.neuroimage.2009.11.084.Reading

Richter, W., Somorjai, R., Summers, R., Jarmasz, M., Menon, R. S., Gati, J. S., … Kim, S.-G. (2000). Motor area activity during mental rotation studied by time-resolved single-trial fMRI. *Journal of Cognitive Neuroscience*, *12*(2), 310–322.

Riddoch, M. J., & Humphreys, G. W. (1987). A case of integrative visual agnosia. *Brain : A Journal of Neurology*, *110 (Pt 6)*, 1431–62.

Riddoch, M. J. (1990). Loss of visual imagery: A generation deficit. *Cognitive Neuropsychology*, *7*(4), 249–273. http://doi.org/10.1080/02643299008253444

Rowe, F. J., Wright, D., Brand, D., Jackson, C., Harrison, S., Maan, T., … Freeman, C. (2013). A prospective profile of visual field loss following stroke: Prevalence, type, rehabilitation, and outcome. *BioMed Research International*, *2013*, 12. http://doi.org/10.1155/2013/719096

Sabel, B., Henrich-Noack, P., Fedorov, A., & Gall, C. (2011). *Vision restoration after brain and retina damage: The "residual vision activation theory"* (Vol. 192). http://doi.org/10.1016/B978-0-444-53355-5.00013-0

Sack, A. T., & Schuhmann, T. (2012). Hemispheric differences within the fronto-parietal network dynamics underlying spatial imagery. *Frontiers in Psychology*, *3*(JUN), 1–10. http://doi.org/10.3389/fpsyg.2012.00214

Sack, A. T., Sperling, J. M., Prvulovic, D., Formisano, E., Goebel, R., Di Salle, F., … Linden, D. E. J. (2002). Tracking the mind's image in the brain II: Transcranial magnetic stimulation reveals parietal asymmetry in visuospatial imagery. *Neuron*, *35*(1), 195–204. http://doi.org/10.1016/S0896-6273(02)00745-6

Sack, A. T., Jacobs, C., De Martino, F., Staeren, N., Goebel, R., & Formisano, E. (2008). Dynamic premotor-to-parietal interactions during spatial imagery. *Journal of Neuroscience*, *28*(34), 8417–8429. http://doi.org/10.1523/JNEUROSCI.2656-08.2008

Schenkenberg, T., Bradford, D. C., & Ajax, E. T. (1980). Line bisection and unilateral visual neglect in patients with neurologic impairment. *Neurology*, *30*(5), 509–17. http://doi.org/10.1212/WNL.30.5.509

Schwarzbach, J. (2011). A simple framework (ASF) for behavioral and neuroimaging experiments based on the psychophysics toolbox for MATLAB. *Behavior Research Methods*, *43*(4), 1194–1201. http://doi.org/10.3758/s13428-011-0106-8

Sereno, M. I., Pitzalis, S., & Martinez, A. (2001). Mapping of contralateral space in retinotopic coordinates by a parietal cortical area in humans. *Science*, *294*(5545), 1350–1354. http://doi.org/10.1126/science.1063695

Shepard, R. N., & Metzler, J. (1971). *Mental Rotation of Three-Dimensional Objects*. *Source: Science, New Series* (Vol. 171).

Shin, L. M., Mcnally, R. J., Kosslyn, S. M., Thompson, W. L., Rauch, S. L., Alpert, N. M., … Pitman, K. (1999). Regional cerebral blood flow during script-driven imagery in childhood sexual abuse-related PTSD: A PET investigation. *Am J Psychiatry*.

Slotnick, S. D., Thompson, W. L., & Kosslyn, S. M. (2005). Visual mental imagery induces retinotopically organized activation of early visual areas. *Cerebral Cortex*, *15*(10), 1570–1583. http://doi.org/10.1093/cercor/bhi035

Smith, F. W., & Goodale, M. A. (2015). Decoding visual object categories in early somatosensory cortex. *Cerebral Cortex*, *25*(4), 1020–1031. http://doi.org/10.1093/cercor/bht292

Snodgrass, J. G., & Vanderwart, M. (1980). A standardized set of 260 pictures: Norms for name agreement, image agreement, familiarity, and visual complexity. *Journal of Experimental Psychology: Human Learning & Memory*, *6*(2), 174–215. http://doi.org/10.1037/0278-7393.6.2.174

Sparing, R., Mottaghy, F. M., Ganis, G., Thompson, W. L., Topper, R., Kosslyn, S. M., & Pascual-Leone, a. (2002). Visual cortex excitability increases during visual mental imagery--a TMS study in healthy human subjects. *Brain Res*, *938*(1–2), 92–7. http://doi.org/10.1016/S0006-8993(02)02478-2

Stokes, M., Thompson, R., Cusack, R., & Duncan, J. (2009). Top-down activation of shape-specific population codes in visual cortex during mental imagery. *Journal of Neuroscience*, *29*(5), 1565–1572. http://doi.org/10.1523/JNEUROSCI.4657-08.2009

Stokes, M., Saraiva, A., Rohenkohl, G., & Nobre, A. C. (2011). Imagery for shapes activates position-invariant representations in human visual cortex. http://doi.org/10.1016/j.neuroimage.2011.02.071

Sulzer, J., Haller, S., Scharnowski, F., Weiskopf, N., Birbaumer, N., Blefari, M. L., … Sitaram, R. (2013). Real-time fMRI neurofeedback: progress and challenges. *NeuroImage*, *76*, 386–99. http://doi.org/10.1016/j.neuroimage.2013.03.033

Thompson, W. L., Kosslyn, S. M., Sukel, K. E., & Alpert, N. M. (2001). Mental imagery of high- and low-resolution gratings activates area 17. *NeuroImage*, *14*(2), 454–464. http://doi.org/10.1006/nimg.2001.0803

Todd, M. T., Nystrom, L. E., & Cohen, J. D. (2013). Confounds in multivariate pattern analysis: Theory and rule representation case study. *NeuroImage*, *77*, 157–165. http://doi.org/10.1016/j.neuroimage.2013.03.039

Trojano, L. (2000). Matching two imagined clocks: the functional anatomy of spatial analysis in the absence of visual stimulation. *Cerebral Cortex*. http://doi.org/10.1093/cercor/10.5.473

Ungerleider, L. G., & Haxby, J. V. (1994). “What” and “where” in the human brain. *Current Opinion in Neurobiology*, *4*(2), 157–65. http://doi.org/10.1007/s00601-015-1027-3

Vetter, P., Smith, F. W., & Muckli, L. (2014). Decoding sound and imagery content in early visual cortex. *Current Biology*, *24*(11), 1256–1262. http://doi.org/10.1016/j.cub.2014.04.020

Vu, H. T. V., Keeffe, J. E., McCarty, C. A., & Taylor, H. R. (2005). Impact of unilateral and bilateral vision loss on quality of life. *British Journal of Ophthalmology*. http://doi.org/10.1136/bjo.2004.047498

Ward, J. (2015). *The student’s guide to cognitive neuroscience*. Psychology Press. http://doi.org/10.4324/9781315742397

Winlove, C. I. P., Milton, F., Ranson, J., Fulford, J., MacKisack, M., Macpherson, F., & Zeman, A. (2018). The neural correlates of visual imagery: A co-ordinate-based meta-analysis. *Cortex, 105: 4-25*. http://doi.org/10.1016/j.cortex.2017.12.014

Wojciulik, E., & Kanwisher, N. (1999). The Generality of Parietal Involvement in Visual Attention. *Neuron*, *23*, 747–764. http://doi.org/10.1111/j.1365-2559.1987.tb01859.x

Worsley, K. J., Marrett, S., Neelin, P., Vandal, A. C., Friston, K. J., & Evans, A. C. (1996). A unified statistical approach for determining significant signals in images of cerebral activation. *Human Brain Mapping*, *4*(1), 58–73. http://doi.org/10.1002/(SICI)1097-0193(1996)4:1<58::AID-HBM4>3.0.CO;2-O

Yeatman, J. D., Rauschecker, A. M., & Wandell, B. A. (2013). Anatomy of the visual word form area: Adjacent cortical circuits and long-range white matter connections. *Brain and Language*, *125*, 146–155. http://doi.org/10.1016/j.bandl.2012.04.010

Yomogida, Y., Sugiura, M., Watanabe, J., Akitsuki, Y., Sassa, Y., Sato, T., … Kawashima, R. (2004). Mental visual synthesis is originated in the fronto-temporal network of the left hemisphere. *Cerebral Cortex*, *14*(12), 1376–1383. http://doi.org/10.1093/cercor/bhh098

Zatorre, R. J., & Halpern, A. R. (2005). Mental concerts: musical imagery and auditory cortex. *Neuron*, *47*, 9–12. http://doi.org/10.1016/j.neuron.2005.06.013

Zihl, J. (1995). Eye movement patterns in hemianopic dyslexia. *Brain*, *118*(4), 891–912. http://doi.org/10.1093/brain/118.4.891